Market and Control Mechanisms Enabling Flexible Service Provision by Grid-Edge Resources within End-to-End Power Systems

Final Project Report

M-40

Power Systems Engineering Research Center
Empowering Minds to Engineer
the Future Electric Energy System

Market and Control Mechanisms Enabling Flexible Service Provision by Grid-Edge Resources within End-to-End Power Systems

Final Project Report

Project Team
Leigh Tesfatsion, Project Leader
Zhaoyu Wang
Iowa State University

Subhonmesh Bose
University of Illinois at Urbana-Champaign

Graduate Students
Swathi Battula
Rui Cheng
Iowa State University

Khaled Alshehri
Mariola Ndrio
Anna Winnicki
University of Illinois at Urbana-Champaign

PSERC Publication 21-12

October 2021

For information about this project, contact:

Leigh Tesfatsion
Iowa State University
Department of Economics
260 Heady Hall
Ames, Iowa 50011-1054
Phone: 515-294-6740
Email: tesfatsi@iastate.edu

Power Systems Engineering Research Center

The Power Systems Engineering Research Center (PSERC) is a multi-university Center conducting research on challenges facing the electric power industry and educating the next generation of power engineers. More information about PSERC can be found at the Center's website: http://www.pserc.org.

For additional information, contact:

Power Systems Engineering Research Center
Arizona State University
527 Engineering Research Center
Tempe, Arizona 85287-5706
Phone: 480-965-1643
Fax: 480-727-2052

Notice Concerning Copyright Material

Acknowledgements

The authors wish to extend sincere thanks to our industry team advisors for their thoughtful questions, advice, and support: L. Kristov (Formerly with CAISO), H. Liu (CAISO), Y. Chen (MISO), J. Harrison (MISO), A. Korad (MISO), K. Swenson (MISO), J. Tong (PJM), H. Scribner (SPP), H. Li (Hitachi), K. Cheung (GE), G. Gu (GE), E. Ela (EPRI), E. Farantatos (EPRI), R. Hytowitz (EPRI), N. Singhal (EPRI), and D. Krishnamurthy (NREL).

Executive Summary

Modern electric power systems need new economic and control mechanisms to facilitate the provision of flexible ancillary services. This need arises in great part from an increasing reliance on renewable energy resources, which in turn has increased the uncertainty and volatility of net load, i.e., load net of non-dispatchable generation. In response to this need, our project has pursued four challenging objectives: (i) develop scalable transactive energy designs for power systems that enable the harnessing of flexible ancillary services from locally-controlled grid-edge resources in return for appropriate compensation; (ii) analytically establish the optimality properties of these designs; (iii) develop a software platform modeling the dynamic operations of a transmission system linked with a distribution system; and (iv) use this platform to test design performance.

Part I: Transactive Energy System Designs Managed by Independent Distribution System Operators

Part I studies the conceptual modeling of an *Independent Distribution System Operator (IDSO)* at the interface of a transmission system and a single linked distribution system. The IDSO functions in the transmission system as a wholesale power market participant. The IDSO functions in the distribution system as a power manager for households that own conventional electrical devices plus price-sensitive electrical HVAC systems. The IDSO's goal is to align household goals/constraints with distribution reliability constraints while respecting household privacy.

The IDSO manages household power requirements by means of a *Transactive Energy System (TES)* design. A *TES design* is a collection of economic and control mechanisms that permits the dynamic balancing of demand and supply across an entire electrical infrastructure, using value as the key operational parameter. Two distinct IDSO-managed TES designs have been developed:

- **TD1: Bid-based TES design.** The retail price signals communicated by the IDSO to households for each *Operating Period (OP)* are determined based on the IDSO's system goals and constraints plus bids submitted by the households to the IDSO in advance of OP. *Bids* are either demands for power purchase as a function of charged price or offers for the sale of ancillary service (power absorption) as a function of received price. The IDSO submits aggregated forms of these household bids into an RTO/ISO-managed day-ahead market. If cleared, these bids can affect future wholesale power outputs and locational marginal prices.

- **TD2: Consensus-based TES design.** The retail price signals communicated by the IDSO to households for each operating period OP are determined by a multi-round negotiation process N(OP) conducted in advance of OP instead of a bidding process. At the start of N(OP) each household h communicates to the IDSO a slider-knob control setting on its household thermostat that lies between 0 ("Benefit") and 1 ("Cost"). The closeness of this setting to 0 indicates the degree to which h prefers to emphasize benefit relative to cost during OP. Also, the IDSO sets initial price-to-go sequences for OP based on the *Locational Marginal Prices (LMPs)* determined in a wholesale real-time market for OP. In each subsequent N(OP) round, the IDSO communicates a household-specific price-to-go sequence to each household h for the N sub-periods constituting OP; and the real/reactive power sequences that h communicates back to the IDSO for these N sub-periods are h's optimal response to this price-to-go sequence.

N(OP) terminates either when household responses satisfy all distribution network reliability constraints for OP or a stopping rule is activated.

To permit testing of TD1 and TD2 within an *Integrated Transmission and Distribution (ITD)* system, we developed a co-simulated software platform called the **ITD TES Platform**. The major research outcomes for Part I of this project are as follows:

- **TD1:** Using dynamic programming principles, the optimal state-conditioned form of a household's bid functions for power usage demand and ancillary service (power absorption) supply are analytically derived for an operating period OP partitioned into N successive decision sub-periods. Test cases conducted for TD1 using a 123-bus distribution grid populated by 927 households demonstrate: If N=1 and the bid process is appropriately configured for communication delays and wholesale power market timing, the IDSO can achieve system objectives for OP (e.g., peak load reduction, load matching). Also, if the IDSO participates in the day-ahead market not only as a procurer of power for household usage but also as a provider of ancillary service in the form of power absorption secured from households in return for appropriate compensation, the latter additional household revenue stream can increase household net benefits.

- **TD2:** A complete analytical model is formulated for a distribution system with an unbalanced radial distribution network populated by households whose power requirements are managed by an IDSO using TD2. The negotiation process N(OP) for each operating period OP is implemented by a newly formulated dual decomposition algorithm. The convergence and optimality properties of N(OP) are analytically established. Test cases are conducted for TD2 for twenty-four successive hours of a simulated day D for a 123-bus unbalanced distribution system populated by 345 households. For each simulated hour OP, the negotiation process N(OP) converges in less than 500s (8.4min). Moreover, the real and reactive power outcomes resulting under N(OP) closely approximate the real and reactive power outcomes obtained for OP as the solution to a benchmark centralized optimization problem that makes full use of household private information.

Planned next steps for continuation of our Part I research are as follows:

- Sensitivity of TD1/TD2 performance to changes in the number N of OP decision sub-intervals.
- Extend TD1/TD2 to permit mixes of grid-edge resources that include distributed generation.
- Use the ITD TES Platform to conduct more comprehensive performance testing of TD1/TD2.
- For TD2, consider more sophisticated forms of dual decomposition algorithms, such as Alternating Direction Method of Multipliers (ADMM) algorithms, to achieve improved optimality and convergence properties for the negotiation process N(OP).
- Develop and test TES designs for ITD systems with high penetrations of renewable energy at the transmission level, and with distributed generation that includes wind and/or solar power.
- Develop and test TES designs for ITD systems with *multiple* linked distribution systems.

Part II: Analysis of Market Structures to Harness Flexibilities of Distributed Energy Resources (DERs)

It is widely recognized that the energy and power capacities of individual DERs are too small to provide meaningful services to the grid. The story is quite different with coordinated control of these DERs. A variety of regulatory structures have been proposed for DER coordination. Part II of this final report presents analysis on specific aspects of two such designs proposed in the literature. The first design considers the efficiency impacts of a profit-motivated retail aggregator who harnesses the supply capacities of a collection of prosumers and offers it to the wholesale market. The second model focuses on a bid/offer based retail market design that is administered by a *Distribution System Operator (DSO).* Here, the focus is on the analysis of pricing mechanisms that are suitable for a retail market over the distribution grid. The key findings are as follows:

- An intermediary is necessary to represent the collection of DERs in RTO/ISO-managed wholesale markets since the RTO/ISO seldom has visibility into the low and medium voltage distribution grids. If the intermediary is profit-motivated, then its strategic incentive can have significant impacts on the overall market efficiency. Specifically, the flexibility offered by DERs should ideally improve overall market efficiency. The incentive of the aggregator is such that its presence reduces that attainable efficiency. Thus, one should carefully consider who can and should fulfill the role of this intermediary, as well as the rules of the road determining how this intermediation is to proceed. The results of our Part II analysis underscore the value of regulatory oversight in emerging business models for DER participation.

- Many have advocated the design of a retail market for the distribution grid, very much along the lines of wholesale market design. Such a design must account for unique features of the distribution grid, prescribe a format for bids and offers from market participants and define meaningful settlements. This study characterizes market-relevant properties of a specific pricing mechanism that defines settlements for both real and reactive powers in the distribution grid. This mechanism “convexifies” the nonconvex power flow equations in the distribution grid through its convex relaxation. This relaxation-based *Distributed Locational Marginal Pricing (DLMP)* scheme is shown to possess the favorable properties exhibited by LMP in wholesale markets. Augmenting this scheme with a suitable bid/offer format will complete the design of a retail market mechanism.

Planned next steps for continuation of our Part II research are as follows:

- Propose and evaluate the design of a retail market mechanism (bid/offer format and pricing) combining prior work on non-networked scalar parameterized two-sided market design and convex relaxation-based pricing over a distribution network.
- Create a simulation platform with DER owner-operators as agents and test viable DER coordination strategies, where agents learn to bid/offer in a retail market environment.
- Use the simulation platform to understand the impacts of for-profit DER aggregators versus a possibly independent distribution system operator (DSO) on overall market efficiency. With such a setup, we also want to consider how such a mechanism impacts equity and fairness among customers with possibly different capabilities to afford and operating DERs at different locations within the distribution system.

Project Website: http://www2.econ.iastate.edu/tesfatsi/ITDProjectHome.htm

Project Publications:

[1] L. Tesfatsion, *A New Swing-Contract Design for Wholesale Power Markets*, 20 chpts, 288pp., John Wiley & Sons, Inc. (IEEE Press Series), Hoboken, NJ, USA, 2021.

[2] S. Battula, L. Tesfatsion, Z. Wang, "A Customer-Centric Approach to Bid-Based Transactive Energy System Design," *IEEE Transactions on Smart Grid,* Vol. 11, No. 6, pp. 4996-5008, 2020.

[3] S. Battula, L. Tesfatsion, T.E. McDermott, "An ERCOT Test System for Market Design Studies," *Applied Energy,* Vol. 275, 115182, October 2020.

[4] H.T. Nguyen, S. Battula, R.R. Takkala, Z. Wang, L. Tesfatsion (2019), "An Integrated Transmission and Distribution Test System for Evaluation of Transactive Energy Designs," *Applied Energy,* Vol. 240, pp. 666-679, April 2019.

[5] S. Ma, Z. Wang, L. Tesfatsion, "Swing Contracts with Dynamic Reserves for Flexible Service Management," *IEEE Trans. on Power Systems,* Vol. 34, No. 5, pp. 4024-4037, 2019.

[6] R. Cehng, l. Tesfatsion, Z. Wang, "A Multiperiod Consensus-Based Transactive Energy System for Unbalanced Distribution Networks," WP #21005, ISU Digital Repository, Iowa State University, Ames, IA, April, 30pp, 2021. (under journal review)

[7] L. Tesfatsion, S. Battula, "Analytical SCUC/SCED Optimization Formulation for AMES V5.0," WP#20014, ISU Digital Repository, Aug 2020.

[8] L. Tesfatsion, S. Battula, "Notes on the GridLAB-D Household ETP Model," ITD TES Platform Documentation, WP #19001, ISU Digital Repository, July 2020.

[9] K. Alshehri, M. Ndrio, S. Bose, T. Basar, "Quantifying Market Efficiency Impacts of Aggregated Distributed Energy Resources," *IEEE Trans. on Power Systems*, Vol. 35, No. 5, pp. 4067-4077, 2020.

[10] M. Ndrio, K. Alshehri, S. Bose, "A Scalar-Parameterized Mechanism for Two-Sided Markets," *Proceedings of the IFAC World Congress, 2020*.

[11] A. Winnicki, M. Ndrio, S. Bose, "On Convex Relaxation-Based Distribution Locational Marginal Prices," *Proceedings of Innovative Smart Grid Technologies (ISGT),* 2020.

[12] A. Winnicki, M. Ndrio, S. Bose, "Convex Relaxation Based Locational Marginal Prices for Electricity Markets," 2020. https://arxiv.org/abs/1910.10673

[13] S. Bose, D.H. Nguyen, H. Liu, Y. Guo, T.T. Doan, and C.L. Beck, "Distributed Grid Optimization via Distributed Dual Subgradient Methods with Averaging," 2021. https://arxiv.org/abs/2107.07061

Open-Source Software Releases:

[14] S. Battula, L. Tesfatsion, *AMES V5.0: GitHub Code/Data Repository*, 2020: https://github.com/ames-market/AMES-V5.0

[15] S. Battula, L. Tesfatsion, T.E. McDermott, *ERCOT Test System: GitHub Code/Data Repository*, 2020: https://github.com/ITDProject/ERCOTTestSystem

[16] S. Battula, L. Tesfatsion, *ITD Project/Household Formulation: GitHub Code/Data Repository*, 2020: https://github.com/ITDProject/HouseholdFormulationRepository

[17] S. Battula, L. Tesfatsion, *ITD TES Platform: GitHub Code/Data Repository*, 2021: https://github.com/ITDProject/ITDTESPlatform

Student Theses:

[18] Swathi Battula, “Transactive Energy System Design for Integrated Transmission and Distribution Systems,” *Ph.D. Thesis*, Department of Electrical & Computer Engineering, Iowa State University, February 2021.

[19] Rui Cheng, “Multiperiod Consensus-Based Transactive Energy System Designs for Unbalanced Distribution Systems,” *expected Ph.D. thesis title*, Department of Electrical & Computer Engineering, Iowa State University. Expected graduation date: May 2024.

[20] Khaled Alshehri, “Game-Theoretic Analysis of Deregulated Electricity Markets: From Retail to Wholesale,” *Ph.D. thesis*, Depart. Elect. & Comp. Eng., UIUC, November 2019.

[21] Mariola Ndrio, “Design and Analysis of Competitive Electricity Markets,” *Ph.D. Thesis*, Department of Elect. and Computer Eng., U. of Illinois Urbana-Champaign, January 2021.

[22] Anna Winnicki, “Convex Relaxation Based Locational Marginal Prices for Electricity Markets,” *M.S. Thesis*, Dept. of Electrical & Computer Engineering. UIUC, July 2020.

Part I

Transactive Energy System Designs Managed by Independent Distribution System Operators

Leigh Tesfatsion
Zhaoyu Wang
Swathi Battula, Graduate Student
Rui Cheng, Graduate Student

Iowa State University

For information about this project, contact

Leigh Tesfatsion
Iowa State University
Department of Economics
260 Heady Hall
Ames, Iowa 50011-1054
Phone: 515-294-6740
Email: tesfatsi@iastate.edu

Power Systems Engineering Research Center

The Power Systems Engineering Research Center (PSERC) is a multi-university Center conducting research on challenges facing the electric power industry and educating the next generation of power engineers. More information about PSERC can be found at the Center's website: http://www.pserc.org.

For additional information, contact:

Power Systems Engineering Research Center
Arizona State University
527 Engineering Research Center
Tempe, Arizona 85287-5706
Phone: 480-965-1643
Fax: 480-727-2052

Table of Contents

List of Figures

List of Tables

Nomenclature

Nomenclature for Section 1

D	Generic symbol for a day
DAM	Day-ahead market
DAM(T)	Day-ahead market for operating period T
ERCOT	Electric Reliability Council of Texas
FNCS	Framework for network co-simulation
GER	Grid-edge resource
GERA	Grid-edge resource aggregator
H	Generic symbol for an operating hour
HVAC	Heating, ventilation, and air conditioning
IDSO	Independent distribution system operator
ISO	Independent system operator
ITD	Integrated transmission and distribution
ITSO	Independent transmission system operator
JReLM	Java reinforcement learning module
kWh	Kilowatt hour
LAH(T)	Look-ahead horizon for operating period T
LISA	Local intelligent software agent
LMP	Locational marginal price
LSE	Load-serving entity
M(T)	Market held in advance of operating period T
MWh	Megawatt hour
PSERC	Power Systems Energy Research Center

RTM Real-time market

RTM(T) Real-time market for operating period T

RTO Regional transmission organization

SCED Security-constrained economic dispatch

SCUC Security-constrained unit commitment

T Generic symbol for an operating period

T-D Transmission-distribution

TES Transactive energy system

Nomenclature for Section 2

A. Acronyms, Parameters, and Other Exogenous Terms

$\overline{\boldsymbol{A}}$ Graph-based incidence matrix (p.u.) for the unbalanced radial network

b^* Linkage bus, i.e., the transmission grid bus at which the radial network links to the transmission network

$\boldsymbol{B}$ Diagonal matrix with DDA step-sizes along its diagonal

BP(*j*) Bus immediately preceding bus *j* along radial network, for all j ∈ $\mathcal{N}$

Bus 0 Radial network head bus, which is also the linkage bus b^*

c_ψ Conversion factor (utils/(^oF)^2) between comfort and inside air temperature for customer ψ

d Number *NK* of sub-periods times number *NH* of households

$\boldsymbol{D}_r$ Block diagonal matrix (p.u.) of line segment resistances

$\boldsymbol{D}_x$ Block diagonal matrix (p.u.) of line segment reactances

DDA Dual decomposition algorithm for implementation of N(OP)

DER Distributed energy resource

DSO Distribution system operator

$\boldsymbol{H}_{\boldsymbol{\psi}}(\mathcal{K})$	TCL power-ratio matrix for customer ψ during $\mathcal{K}$
$I_{\max}$	Maximum permitted number of negotiation process iterations
ISO	Independent system operator
$l_j = (i, j)$	Line segment connecting buses *i* and *j* with *i* = BP(*j*) and $j \in \mathcal{N}$
LAH(OP)	Look-ahead horizon for RTM(OP)
LMP	Locational marginal price
$\text{LMP}(b^*, t)$	RTM LMP (cents/kWh) at linkage bus b^* for sub-period *t*
LMP($\mathcal{K}$)	Vector of LMPs (cents/kWh) determined in RTM(OP) for $\mathcal{K}$
m	Number ([1+6N]·*NK*) of explicit Primal Problem constraints
$\bar{M}$	Graph-based incidence matrix (p.u.) for the balanced radial network
N	Number of non-head buses for the radial network
NH	Number of households $\psi \in \Psi$
NK	Number of sub-periods t forming a partition of operating period OP
N(OP)	Negotiation process for OP
N_{ψ}^{ph}	Flag for phase $\phi \in \{a, b, c\}$ of the 1-phase line connecting customer ψ to a distribution network bus
OP	Operating period
$\bar{P}$	Upper limit for peak demand (p.u.)
$\text{PF}_{\psi}(t)$	Power factor (unit free) for the TCL device of customer ψ during sub-period *t*
$p_{\psi}^{\max}$	Maximum real power level (p.u.) for customer ψ 's TCL devices
$p_{\psi}^{\text{non}}(t)$	Non-TCL real power usage (p.u.) of customer ψ at start of sub-period *t*
$\mathcal{P}_{\psi}^{\text{non}}(\mathcal{K})$	Non-TCL real power sequence (p.u.) of customer ψ for $\mathcal{K}$
$q_{\psi}^{\text{non}}(t)$	Non-TCL reactive power usage (p.u.) of customer ψ at start of sub-period *t*

$Q_{\psi}^{\text{non}}(\mathcal{K})$ Non-TCL reactive power sequence (p.u.) of customer ψ for $\mathcal{K}$

R_{ij}, X_{ij} 3-phase resistance and reactance matrices (p.u.) for line segment (i, j)

$\overline{\boldsymbol{R}}_{ij}, \overline{\boldsymbol{X}}_{ij}$ 3-phase resistance and reactance matrices (p.u.) for line segment (i, j) after transformation

RTM(OP) Real-time market for OP

RTO Regional transmission operator

S_{base} Base apparent power (kVA)

SCED(OP) Security-constrained economic dispatch for OP

TB_{ψ} Inside air temperature (^{o}F) at which customer ψ achieves max comfort (bliss)

TES Transactive energy system

TCL Thermostatically-controlled load

$T_{\psi}(0)$ Inside air temperature (^{o}F) for customer ψ at the start of OP

$T_{o}(t)$ Ambient outside air temperature (^{o}F) at the start of sub-period *t*

$u_{\psi}^{\max}$ Customer ψ's maximum attainable thermal comfort (utils)

V_{base} Base voltage (kV)

$\boldsymbol{v_0}(t)$ 3-phase squared voltage magnitudes (p.u.) at the head bus 0 during sub-period *t*

$v^{\text{non}}(t)$ 3-phase squared voltage magnitudes (p.u.) at all non-head buses for sub-period *t*, assuming no TCL

$v_{min}(t), v_{max}(t)$ Lower and upper bounds (p.u.) for 3-phase squared voltage magnitudes during sub-period *t*

α_{ψ}^{H} System inertia temperature parameter (unit-free) for customer ψ

α_{ψ}^{P} Temperature parameter $(^{o}F/\text{kWh})$ for customer ψ

$\beta_1, \beta_2, \beta_3$ Step sizes (unit-free) for the dual decomposition algorithm DDA

$\triangle\, t$ Length (h) of each sub-period *t*

$\eta_{\psi}(t)$ Ratio (unit free) of TCL reactive power to TCL real power for customer ψ during sub-period *t*

γ_{ψ} Benefit/cost slider-knob control setting (unit free) communicated by customer ψ to the DSO for OP

μ_{ψ} Customer ψ 's marginal utility of money (utils/cent) for OP

ϕ Circuit phase of a line segment l_j, or of a 1-phase line connecting a household to a bus

$\psi = (u, \phi, i)$ Designator for a customer with structural and preference attributes *u* located on a phase ϕ line connected to bus *i*

B. Sets and Sequences

$\mathcal{K} = (1, \dots, NK)$ Sequence of sub-periods *t* that partition operating period OP

$\mathcal{L}$ Set of all N distinct line segments (i, j) connecting adjacent buses *i* and *j* in $\{0\} \cup \mathcal{N}$

$\mathcal{N} = \{1, \dots, N\}$ Index set for all non-head buses of the radial network

$\mathcal{N}_j$ Index set for all buses located strictly after bus *j* along the radial network, $0 \leq j \leq N$

$\mathcal{P}(\mathcal{K})$ Set of customer TCL power usage sequences during $\mathcal{K}$

$\mathcal{P}(\pi(\mathcal{K}))$ Set of customer TCL power usage sequences during $\mathcal{K}$, given $\pi(\mathcal{K})$

$\mathcal{U}_{i,\phi}$ Set of attributes u such that $(\mathrm{u}, \phi, \mathrm{i})$ denotes a customer $\psi \in \Psi$

$\mathcal{X}_{\psi}(\mathcal{K})$ Set of customer ψ constraints for $\mathcal{K}$

$\pi(\mathcal{K})$ Set of customer price-to-go sequences for $\mathcal{K}$

Ψ Set of all customers ψ

C. Functions and Variables

f_{ψ} Power-factor function for price-sensitive demands communicated by customer ψ to the DSO for OP

$L(x, \lambda)$ Lagrangian Function for the DSO's centralized optimization problem

$NetBen_{\psi}$ Customer ψ 's net benefit function (utils) for OP

$P_{ij}(t), Q_{ij}(t)$ 3-phase real & reactive power flows (p.u.) over line segment (i, j) during *t*

$P(t), Q(t)$ 3-phase real & reactive power flows (p.u.) over all line segments during sub-period *t*

$p_i(t), q_i(t)$ 3-phase real & reactive power (p.u.) at bus *i* during sub-period *t*

$p(t), q(t)$ 3-phase real & reactive power (p.u.) at all non-head buses during sub-period *t*

$p_\psi(t), q_\psi(t)$ TCL real & reactive power usage (p.u.) of customer ψ during sub-period *t*

$\mathcal{P}_\psi(\mathcal{K})$ TCL real power usage sequence (p.u.) of customer ψ for $\mathcal{K}$

$\mathcal{Q}_\psi(\mathcal{K})$ TCL reactive power usage sequence (p.u.) of customer ψ for $\mathcal{K}$

$T_\psi\big(p_\psi(t), t\big)$ Inside air temperature $({}^oF)$ of customer ψ 's home at the end of sub-period *t*, given $\mathrm{p}_\psi(\mathrm{t})$

$u_\psi\big(p_\psi(t), t\big)$ Comfort (utils) attained by customer ψ during sub-period *t*, given $p_\psi(t)$

$U_\psi\left(\mathcal{P}_\psi(\mathcal{K})\right)$ Total comfort (utils) attained by customer ψ during OP, given $\mathcal{P}_\psi(\mathcal{K})$.

$v\big(t, p_\Psi(t)\big)$ 3-phase squared voltage magnitudes (p.u.) at all non-head buses for sub-period *t*

$v_i\big(t, p_\Psi(t)\big)$ 3-phase squared voltage magnitudes (p.u.) at bus *i* for sub-period *t*

λ Dual variables (utils/p.u.) for all network reliability constraints for $\mathcal{K}$

$\lambda_{\bar{P}}(t)$ Dual variable (utils/p.u.) associated with demand limit for sub-period *t*

$\lambda_{\bar{P}}(\mathcal{K})$ Dual variables (utils/p.u.) associated with demand limits for $\mathcal{K}$

$\lambda_{v_{\max}}(t)$ Dual variables (utils/p.u.) associated with upper voltage limits for sub-period *t*

$\Lambda_{v_{\max}}(\mathcal{K})$ Dual variable matrix associated with upper voltage limits for $\mathcal{K}$

$\boldsymbol{\lambda}_{v_{\min}}(t)$ Dual variables (utils/p.u.) associated with lower voltage limits for sub-period *t*

$\boldsymbol{\Lambda}_{v_{\min}}(\mathcal{K})$ Dual variable matrix associated with lower voltage limits for $\mathcal{K}$

$\pi_\psi(t)$ Retail price (cents/kWh) for customer ψ 's price-sensitive demand for sub-period *t*

$\pi_\psi(\mathcal{K})$ Price-to-go sequence (cents/kWh) for customer ψ during $\mathcal{K}$

1. A Bid-Based Transactive Energy System Design Managed by an Independent System Operator[1]

1.1 Introduction

The growing participation of photovoltaic solar and wind power facilities in modern electric power systems at both the transmission and distribution levels is increasing the uncertainty and volatility of *net load*, i.e., load net of non-dispatchable power. This is hindering the ability of RTOs/ISOs to forecast future net loads, hence their ability to maintain an efficient balancing of net load in real-time operations.

In response to these concerns, RTOs/ISOs and power system researchers are exploring market-based initiatives to facilitate the provision of flexible reserve (e.g., flexible net load balancing services), especially flexible reserve harnessed from distribution system resources. Implementation of these initiatives implies tighter two-way connections between transmission and distribution system operations.

Three major premises motivating our research have therefore been as follows:

- To ensure efficient and reliable operation of future power systems, researchers need to consider with care *integrated transmission and distribution (ITD)* operations over time.
- Researchers need to develop scalable market-based approaches that permit the efficient procurement of flexible reserve from ITD system resources as the number of these resources continues to increase.
- To evaluate the technical and financial feasibility of these approaches in advance of implementation, researchers need software platforms that permit ITD systems to be modeled and studied as coherent dynamic systems with grid sizes ranging from small to realistically large, and with an appropriate degree of operational verisimilitude.

The research reported in Section 1 of Part I studies the ability of *Independent Distribution System Operators (IDSOs),* operating as linkage entities at T-D interfaces, to participate in RTO/ISO-managed wholesale power markets as suppliers of reserve procured from collections of distribution system resources. This research thus addresses issues raised by FERC Order 2222 [1].[2]

More precisely, an IDSO-managed *Transactive Energy System (TES)* design is formulated that permits an IDSO to participate in an RTO/ISO-managed wholesale power market as a supplier of reserve procured from distribution system resources by means of a bidding process. In addition, new types of swing contracts are formulated to facilitate the IDSO's wholesale power market participation. Together, these design elements constitute a scalable market-based approach facilitating reserve procurement from a fuller range of resources.

[1] The research reported in Section 1 of Part I is a continuation of research initiated under award DE-OE 000089 (PI: Zhaoyu Wang, Co-PI: Leigh Tesfatsion; GRA Swathi Battula) from the U.S. DOE Office of Energy (OE), with period of performance 01/01/2017-12/31/2019.

[2] FERC Order 2222 establishes rules governing the participation of distribution system resource aggregators in wholesale power markets. However, it neither requires nor advocates that this participation be restricted to IDSOs.

The efficacy of this approach is investigated by conceptual analyses supported by test cases. The test case simulations are carried out by means of a newly developed co-simulation software platform, called *the ITD TES Platform V2.0*, that permits comprehensive performance testing of TES designs implemented within ITD systems. The *Electric Reliability Council of Texas (ERCOT)* energy region is used as the empirical anchor for the transmission component of this platform.

Detailed accounts of this work are provided in a book [2], four refereed journal articles [3-6], and a PhD thesis [7]. The key components of the platform have been released as open source software at GitHub repositories [8-11] together with supporting documentation [12-13].

1.2 Objectives

The research reported in Section 1 of Part I studies the ability of an IDSO to offer into an RTO/ISO-managed wholesale power market the availability and real-time deployment of flexible reserve in the form of dispatchable power-paths.[3] This reserve is to be harnessed from *grid-edge resources (GERs)*[4] in aggregated form by an appropriately formulated *bid-based TES design*.[5] The objective is to facilitate robust management of risks and uncertainties for ITD systems; see Fig. 1.1.

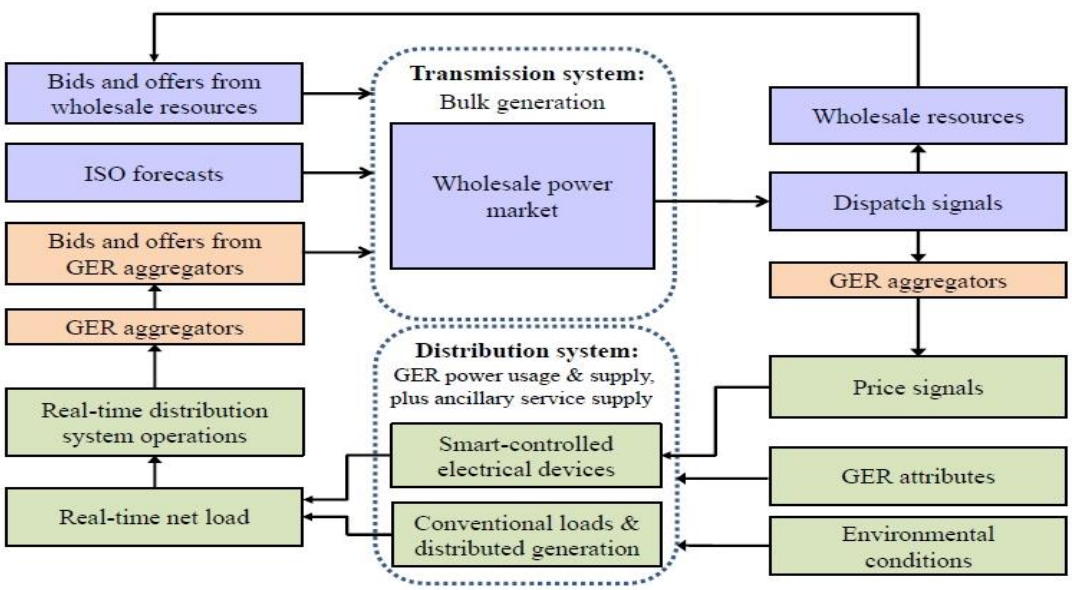

Fig. 1.1: Illustration of an ITD system with GER aggregators operating as T-D linkage entities.

The four specific objectives guiding the research reported in Section 1 of Part I are as follows:

---

[3] As defined in [2] a *power-path* for an operating period T is a flow of power injections and/or withdrawals occurring at a single grid location during T.

[4] For the purposes of this project, a *GER* is defined to be any power resource with a direct point of connection to a distribution grid. Examples include households, commercial businesses, small-scale wind and solar farms, storage entities, and directly connected individual devices. In [3] we propose and illustrate a method for classifying GERs into representative types based on their power-relevant attributes.

[5] For the purposes of this project, a *bid-based TES design* is defined to be a collection of economic and control mechanisms that facilitates net load balancing across an entire distribution system via bid-based transactions, consistent with the maintenance of reliable distribution system operations. For simplicity of exposition, the term "bid" is used broadly to refer to power demands, power supplies, and/or ancillary service supplies.

- **Objective-1:** Develop a bid-based TES design that permits an IDSO to function in a distribution system as a GER aggregator, able to extract dependable flexible reserve (dispatchable power-paths) from GERs in return for appropriate compensation.
- **Objective-2:** Develop swing-contract formulations that permit this IDSO to offer flexible reserve (dispatchable power-paths) into an ISO-managed wholesale power market with appropriate separate compensation for reserve availability and real-time reserve deployment.
- **Objective-3:** Develop a software platform permitting performance evaluation of bid-based TES designs for ITD systems via systematic computational experiments.
- **Objective-4:** Use this platform to evaluate the effects of our Objective-1 and Objective-2 innovations on the overall reliability and efficiency of ITD system operations.

1.3 Technical Approach

1.3.1 Overview

To accomplish the four specific project objectives outlined in Section 1.2, we have developed a scalable framework for an ITD system that permits IDSOs to function as linkage entities at T-D system interfaces. This framework consists of a hierarchical structuring of localized two-way communication links between entities at different system levels.

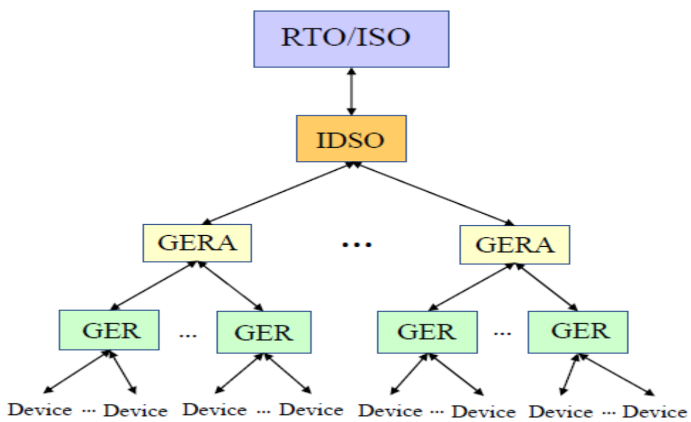

Fig. 1.2: A scalable framework supporting IDSOs as linkage entities at T-D interfaces.

As depicted in Fig. 1.2, our framework models an RTO/ISO-managed transmission system linked to an IDSO-managed distribution system populated by GERs. The IDSO has a fiduciary responsibility to ensure the welfare of its managed GERs, subject to the maintenance of distribution system reliability, where welfare is measured as *net benefit* (i.e., benefit minus cost). The IDSO thus seeks to align GER goals/constraints with distribution system reliability constraints in a manner that respects GER privacy.

The IDSO is in two-way communication with one or more GER aggregators[6] tasked with handling power usage demand, power supply, and/or ancillary service supply for each GER. Finally, each GER manages the operations of one or more behind-the-meter electrical devices.

A key envisioned use of this framework is the support of IDSO-managed bid-based TES designs. A *TES design* is a collection of economic and control mechanisms permitting the dynamic balancing of power demands and supplies across an entire electrical infrastructure, using value as the key operational parameter. A *bid-based* TES design is a TES design for which valuations are based explicitly on purchase and sale reservation values[7] expressed through bids.

1.3.2 Communication Network for Proposed Scalable Framework

Communication among the participants in the scalable framework depicted in Fig. 1.2 is managed by a network of *Local Intelligent Software Agents (LISAs)*. As depicted in Fig. 1.3, the LISAs operating at the edge of the distribution grid, referred to as *Edge* LISAs, constitute the lowest layer in this communication network. Each Edge LISA is associated with a particular GER that owns an array of electrical devices. Some of these devices have conventional controllers responsive only to local state conditions, and some have smart controllers able to send and/or respond to power price signals. The network can also include one or more *Interior* LISAs operating at interior layers of the network. Finally, the IDSO constitutes the *Top* LISA in this network.

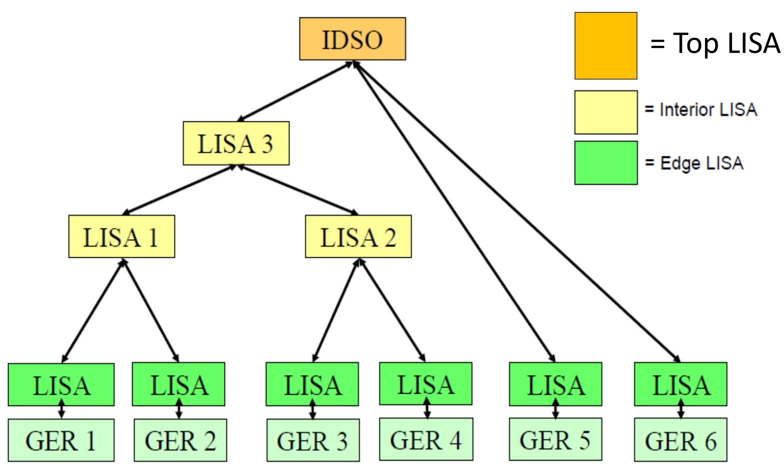

Fig. 1.3: A LISA communication network for an IDSO-managed distribution system.

Each Edge LISA constructs bid functions for its associated GER that reflect the GER's current willingness and ability to buy power, sell power, or sell ancillary service as a function of price, conditional on the GER’s local state conditions. Thus, each Edge LISA functions as a device aggregator for its associated GER.

---

[6] A *GER aggregator* is any entity that manages power usage demand, power supply, and/or ancillary service supply for a collection of GERs.

[7] A *purchase reservation value* for a quantity amount q at a particular time t is defined to be a buyer's maximum willingness to pay for q at time t. A *sale reservation value* for a quantity amount q at a particular time t is defined to be the minimum payment that a seller is willing to receive for the sale of q at time t. .

Each Edge LISA communicates its constructed bid functions to a LISA in the next-higher layer of the network, either an Interior LISA or the IDSO itself. Each Interior LISA aggregates all bids it receives from lower-layer LISAs into a vector of aggregated bid functions, which it communicates to a LISA in a next-higher layer. Thus, Interior LISAs function in the network as GER aggregators.

1.3.3 Five-Step TES Design: General Formulation

Our proposed *Five-Step TES Design* is an IDSO-managed bid-based TES design for GER participants. The design is implemented by means of a two-layer LISA communication network; see the illustrative two-layer network depicted in Fig. 1.4.

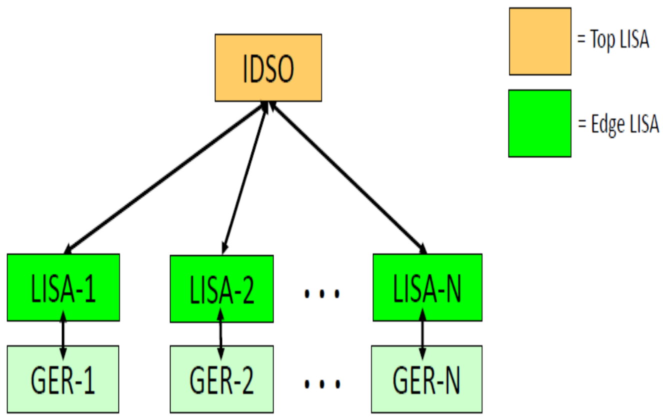

Fig. 1.4: Two-layer LISA communication network support for the Five-Step TES Design.

The types of structural and preference attributes assumed to characterize each GER participant in the Five-Step TES design are depicted in Fig. 1.5.

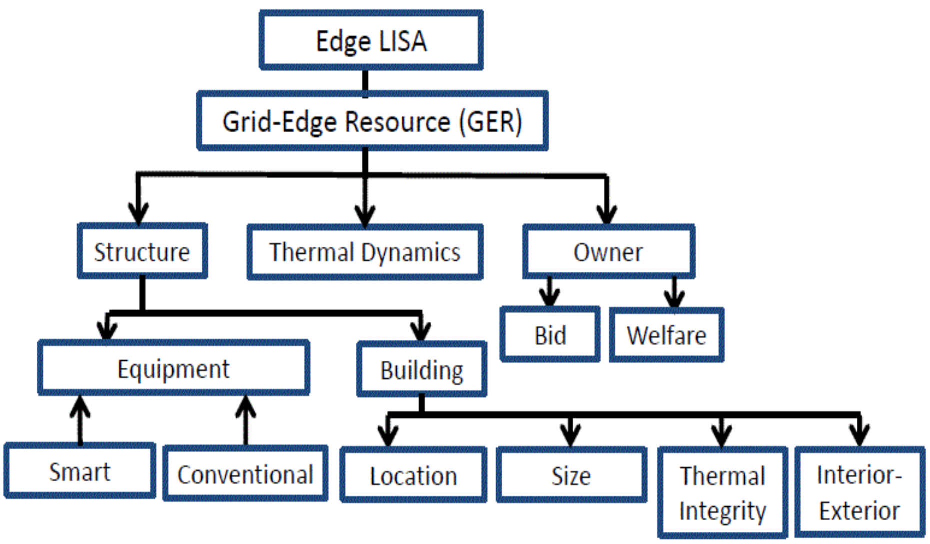

Fig. 1.5: Common types of attributes characterizing GER participants in the Five-Step TES Design. Down-arrows denote "has a" relations and up-arrows denote "is a" relations.

The IDSO's goal is to use the Five-Step TES Design to maximize the net benefit of the participant GERs, subject to distribution system reliability constraints, and in a manner that respects GER privacy. The five steps comprising each iteration of the Five-Step TES Design are as follows:

Step 1: The Edge LISA for each GER R collects data on R and each smart device v(R) owned by R at a *data check rate* and uses these data to form state-conditioned bid functions $Bid_v(R)$. Each $Bid_v(R)$ expresses either a demand function for power usage by device v(R), a supply function for power generation by device v(R), or a supply function for ancillary service provision by device v(R).

Step 2: The Edge LISA for each GER R uses the device bid functions $Bid_v(R)$ to form a state-conditioned vector **Bid**(R) consisting of one or more aggregate device bid functions, which it communicates to the IDSO at a *bid refresh rate*.

Step 3: The IDSO combines its latest received GER bid vectors **Bid**(R) into a vector **AggBid** of one or more aggregate bid functions at an *aggregate bid refresh rate*.

Step 4: The IDSO uses **AggBid** to determine price signals that it communicates back to the Edge LISAs at a *price signal rate.*

Step 5 (Control Step): The Edge LISA for each GER R inserts its latest received price signals into its latest refreshed state-conditioned device bid functions $Bid_v(R)$ at a *power control rate*, which triggers a power response from each smart device v(R).

The five time-rates characterizing the Five-Step TES Design are a critical aspect of this design, affecting both its feasibility and its efficiency. An illustrative timing implementation is depicted in Fig. 1.6 for the special case in which each of these five time-rates has a common value 1/Δt.

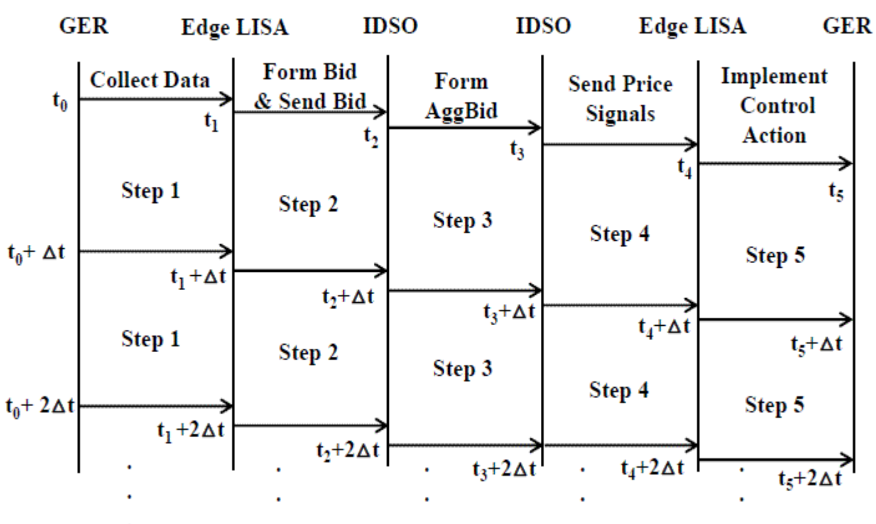

Fig. 1.6: Illustration of staggered timing implementation for the Five-Step TES Design.

1.3.4 Coordination of the Five-Step TES Design with Wholesale Power Market Operations at the Transmission Level

We have developed a co-simulated software platform, referred to as the ITD TES Platform V2.0, to implement ITD test-case studies of the Five-Step TES Design. In each of these test-case studies, we implement the five steps of the Five-Step TES Design in an iterative manner that permits coordination of the design with the operations of a typical U.S. RTO/ISO-managed *Day-Ahead Market (DAM)* and *Real-Time Market (RTM).*

The independent system operator tasked with the management of the transmission system in our test-case studies is hereafter referred to as an *Independent Transmission System Operator (ITSO)* to distinguish this entity from the IDSO tasked with the management of the distribution system. The ITSO-managed DAM conducted on day D for an operating day D+1 will hereafter be denoted by DAM(D+1). The time interval between the close of DAM(D+1) and the start of day D+1 will be referred to as the *Look-Ahead Horizon for DAM(D+1)*, denoted by LAH(D+1). Similarly, the ITSO-managed RTM conducted on day D for any operating period T during day D will be denoted by RTM(T). The time interval between the close of RTM(T) and the start of T will be referred to as the *Look-Ahead Horizon for RTM(T),* denoted by LAH(T).

The timing of DAM and RTM operations during a typical day D for a future operating period T occurring during day D+1 is illustrated in Fig. 1.7.

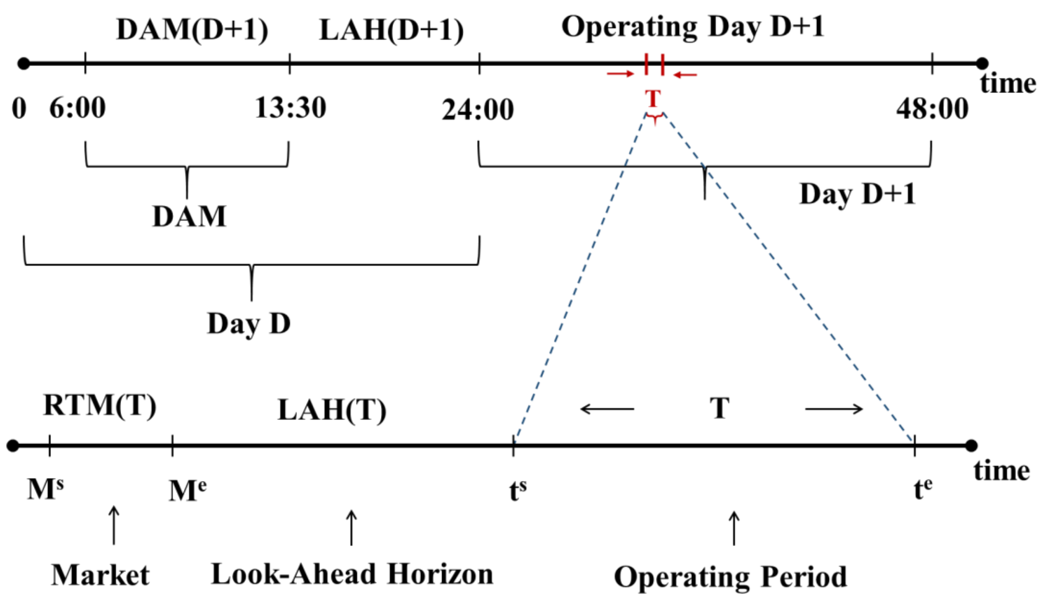

Fig. 1.7: Timing of DAM operations on Day D for a future operating day D+1, and RTM operations on day D+1 for an operating period T during day D+1.

For simplicity of exposition, suppose T coincides with a single control-step (Step 5) for the Five-Step TES Design. The manner in which the five steps of the Five-Step TES Design can then be carried out in relation to the operations of RTM(T), LAH(T), and T is then depicted in Fig. 1.8.

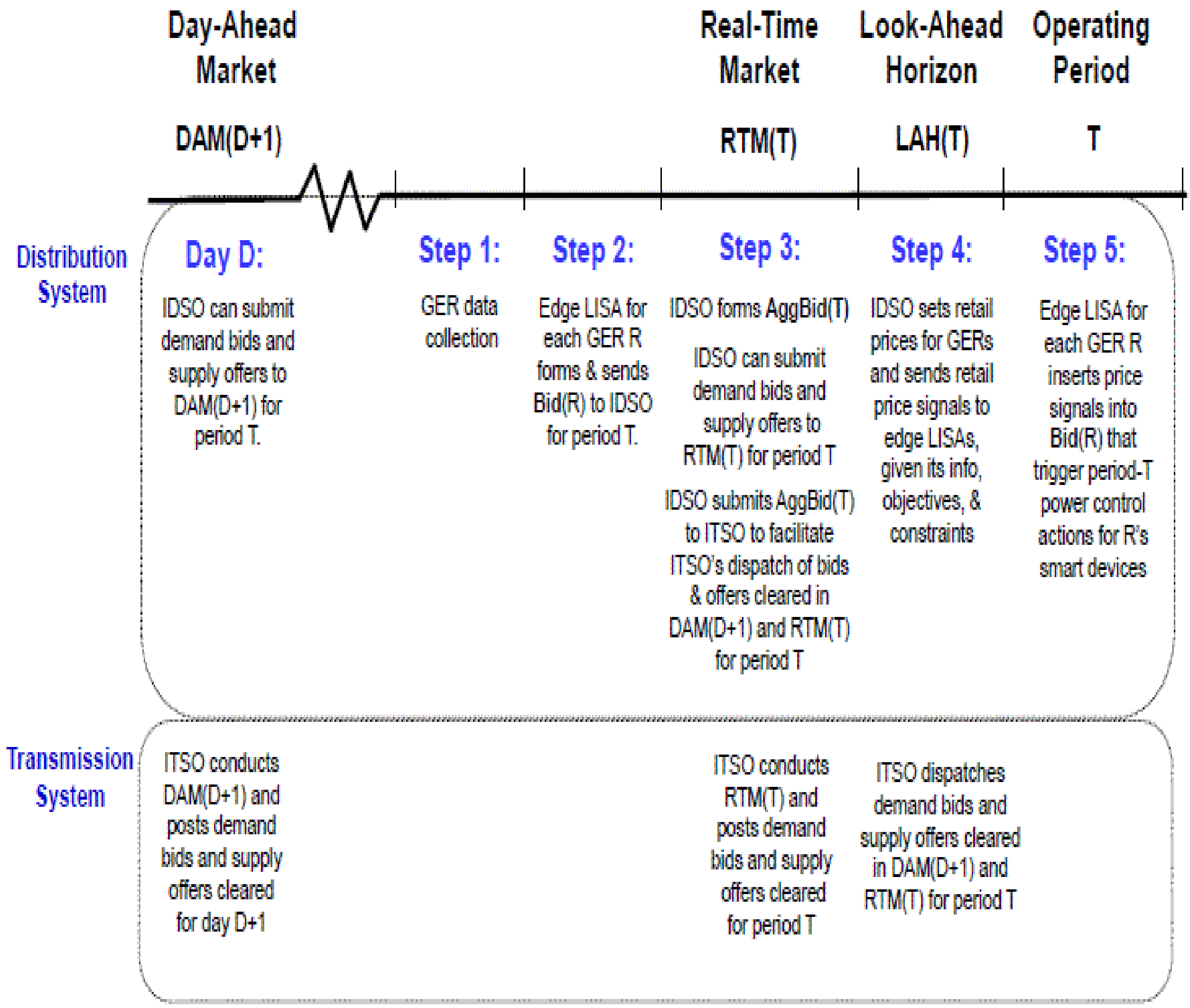

Fig. 1.8: Timing coordination between the Five-Step TES Design for a control-step T during day D+1 and the operations of DAM(D+1) and RTM(T) as depicted in Fig. 7.

1.3.5 General Swing-Contract Formulation for a Dispatchable Power Resource

Given a transmission grid, a *power-path* for this grid corresponding to any time interval T is defined in book [2] to be a flow of power injections and/or withdrawals (MW) occurring at a single grid location during T. An illustrative power-path is depicted in Fig. 1.9.

Let M(T) denote an ITSO-managed wholesale power market for a future operating period T. A general swing contract has been formulated that permits any dispatchable resource to offer into M(T) the availability of collections of feasible dispatchable power-paths for T, as dependable flexible reserve for the support of net load balancing during T. These dispatchable resources can include IDSOs functioning as linkage entities at T-D interfaces that wish to offer reserve into wholesale power markets that has been harnessed from GERs in return for appropriate compensation.

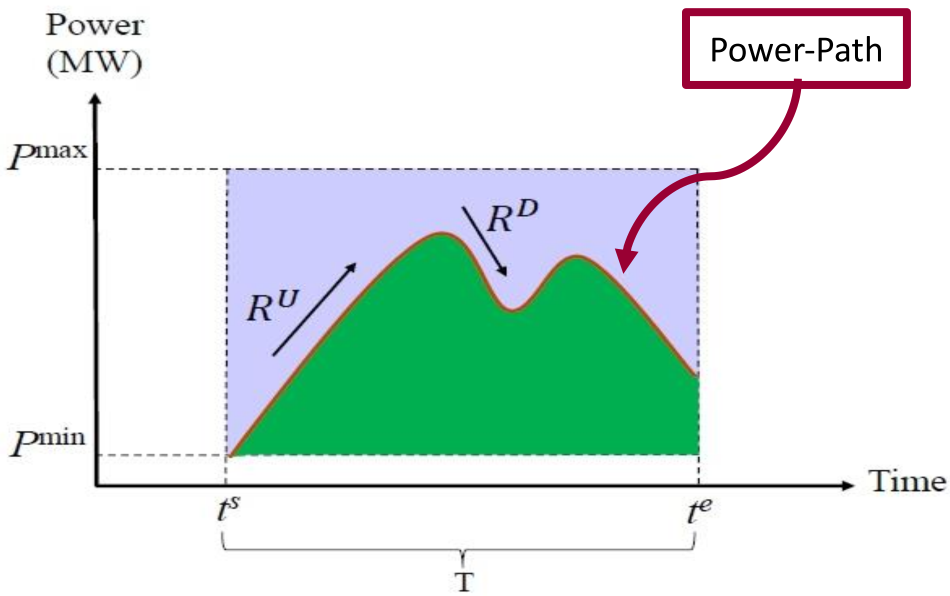

Fig. 1.9: An illustrative power-path for an operating period T.

Specifically, a *swing contract* for a dispatchable resource *m* takes the following general form:

$$\mathrm{SC}_m = \left(\alpha_m, \mathbb{T}_m^{\mathrm{ex}}, \mathbb{PP}_m, \phi_m\right)$$

where the contractual terms included in $\mathrm{SC_m}$, each designated by *m*, are as follows:

- an offer price α_m;
- an exercise set $\mathrm{T_m^{ex}}$ consisting of possible contract exercise times occurring between the end of market M(T) and the start of operating period T;
- a physically characterized set PP_m of power-paths for T, each of which *m* could deliver at a designated grid location during T in response to dispatch signals;
- a performance payment method φ_m.

The offer price α_m permits the dispatchable power resource *m* to ensure coverage ex ante (i.e., prior to operating period T) of all cost that *m* must incur to ensure the period-T *availability* of the power paths in PP_m. Examples of *availability cost* include: capital investment cost; transaction cost (e.g., insurance, licensing); unit commitment cost; and opportunity cost.

The exercise set $\mathrm{T}_m^{\mathrm{ex}}$ determines whether the swing contract is in firm or option form. If the exercise set includes at least one exercise time occurring strictly after the close of market M(T) and before the start of the operating period T, it permits the power resource *m* to offer unit commitment flexibility to the ITSO for operating period T.

The collection PP_m of power-paths permits *m* to offer the availability of power-paths for operating period T with valued attributes that can include both static and dynamic aspects. Examples of *static* aspects include delivery time/place and delivered energy amount (MWh). Examples of *dynamic* aspects include power amplitude range, down/up-time durations, down/up ramp rate limits, power mileage, and power factor (P-Q) relationships.

The performance payment method φ_m permits *m* to ensure coverage ex post (i.e., after operating period T) of any cost that *m* must incur for period-T *performance*, i.e., for the verified dispatched delivery of a power-path in PP_m. Examples of *performance cost* include fuel cost, labor cost, transmission service charges, and equipment wear and tear due to ramping.

Swing contracts are thus two-part pricing contracts permitting dispatchable resources to ensure full cost coverage for verified reserve provision and for verified reserve use in real-time operations, where this reserve (dispatchable power-paths) can take a wide range of forms.

1.3.6 Illustrative Swing Contracts for a Dispatchable Resource

Five swing contract examples with increasing swing (flexibility) in their offered dispatchable power-paths are depicted below. Careful presentations and discussions of these and other forms of swing contracts are provided in book [2, Ch.4].

Figure 1.10 depicts the power requirements for a simple energy-block swing contract submitted by a dispatchable resource *m* into an ITSO-managed market M(T) for a future operating period T. Ensuring the *availability* of the offered energy block ("Dispatch") during T requires *m* to incur *availability cost* for start-up (SU), ramp-up (RU), behind-the-meter power generation (No-Load), ramp-down (RD), and shut-down (SD) before, during, and after T. The *ITSO-dispatched delivery* of this energy block during T requires *m* to incur *performance cost* for dispatched power injection during T.[8]

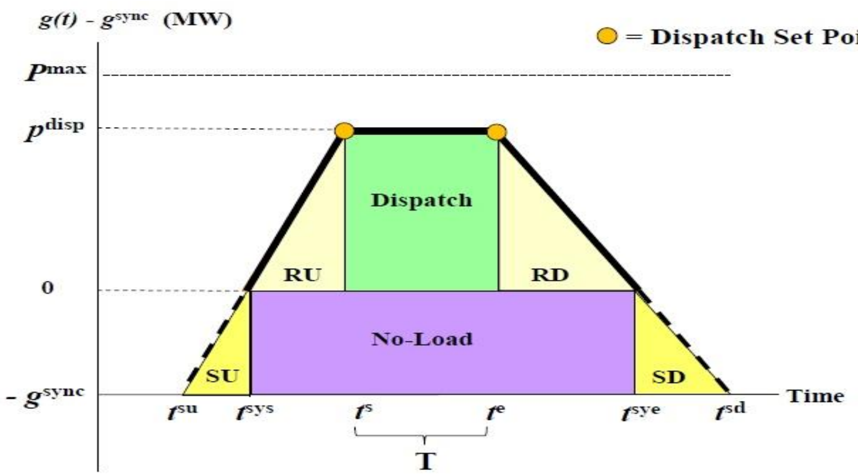

Fig. 1.10: A simple energy-block swing contract.

[8] In this and subsequent swing-contract examples given in Section 1.3.6, no attempt is made to provide a complete description of all availability cost and performance cost that would be associated with this type of swing contract. Rather, illustrations of these two types of costs are given, based on depictions of possible dispatched power-paths.

Figure 1.11 depicts the power requirements resulting from one possible exercise and dispatch of an option swing contract submitted by a dispatchable resource *m* into an ITSO-managed market M(T) for a future operating period T. This option swing contract offers two energy blocks E1 and E2 with specified power levels and durations, supported by an interim ramp-down interval R. Ensuring the *availability* of E1, E2, and R for operating period T requires *m* to incur *availability cost* for start-up (SU), ramp-up (RU), behind-the meter power generation (No-Load), ramp-down (RD), and shut-down (SD) before, during, and after period T. The *dispatched delivery* of E1, E2, and R during T requires *m* to incur *performance cost* for dispatched power injection during T.

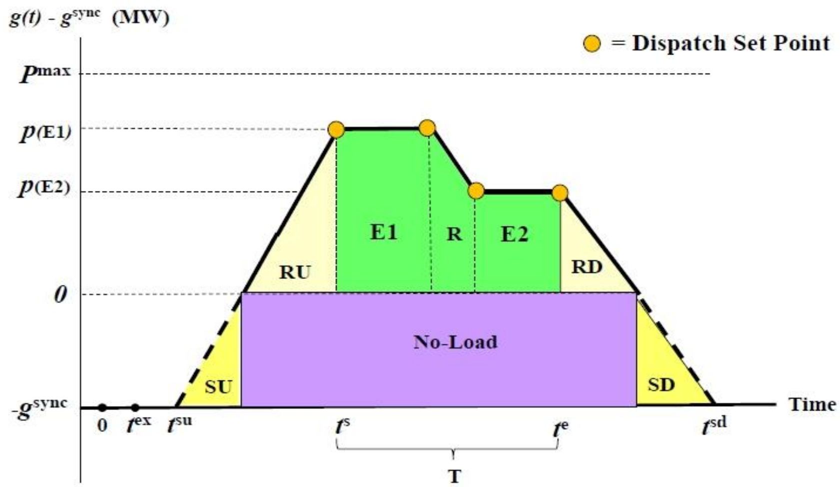

Fig. 1.11: An option swing contract offering two energy blocks with specified power levels and durations, supported by an interim ramp-down interval.

Fig. 1.12 depicts one among many possible power-paths that a generator *m* could be dispatched to deliver during day D+1 if *m*'s swing contract offering multiple energy blocks with multiple possible power levels and durations, supported by multiple possible down/up ramp rates, is cleared by the ITSO in a day-ahead market M(D+1).

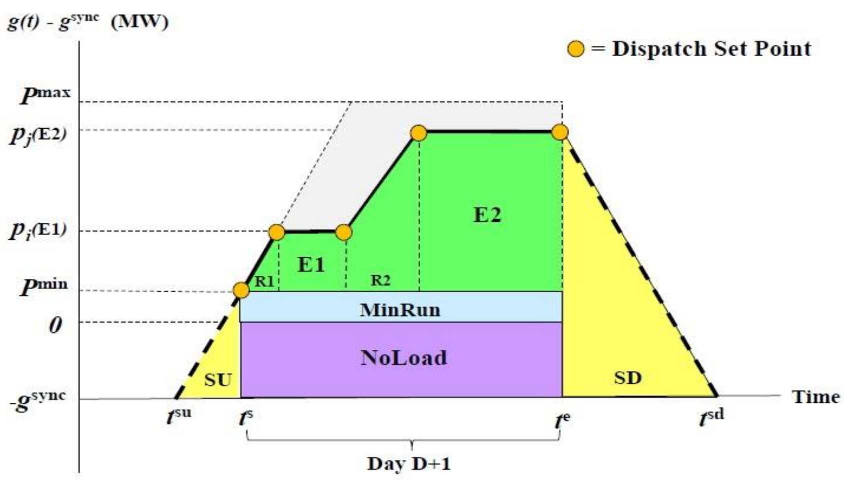

Fig. 1.12: A swing contract offering multiple energy blocks with power/ramp flexibility.

Ensuring the *availability* of multiple energy blocks with power/ramp flexibility for dispatch during day D+1 requires *m* to incur *availability cost* for behind-the-meter power generation (NoLoad), and for minimum sustainable power injection (MinRun) during day D+1. The *ITSO-dispatched delivery* of the depicted energy blocks E1 and E2 with supporting ramp intervals R1 and R2 requires *m* to incur *performance cost* for power start-up (SU) before day D+1, dispatched power injection during day D+1, and power shut-down (SD) immediately after day D+1. Note that SU and SD depend on the exact form of the dispatched power-path.

Fig. 1.13 depicts one among many possible down/up power-paths that an IDSO managing down/up power for a collection of dispatchable GERs by means of a bid-based TES design could be dispatched by the ITSO to deliver during day D+1 if the IDSO's swing contract offering down/up power as ancillary service for the transmission system during day D+1 is cleared by the ITSO in a day-ahead market M(D+1).

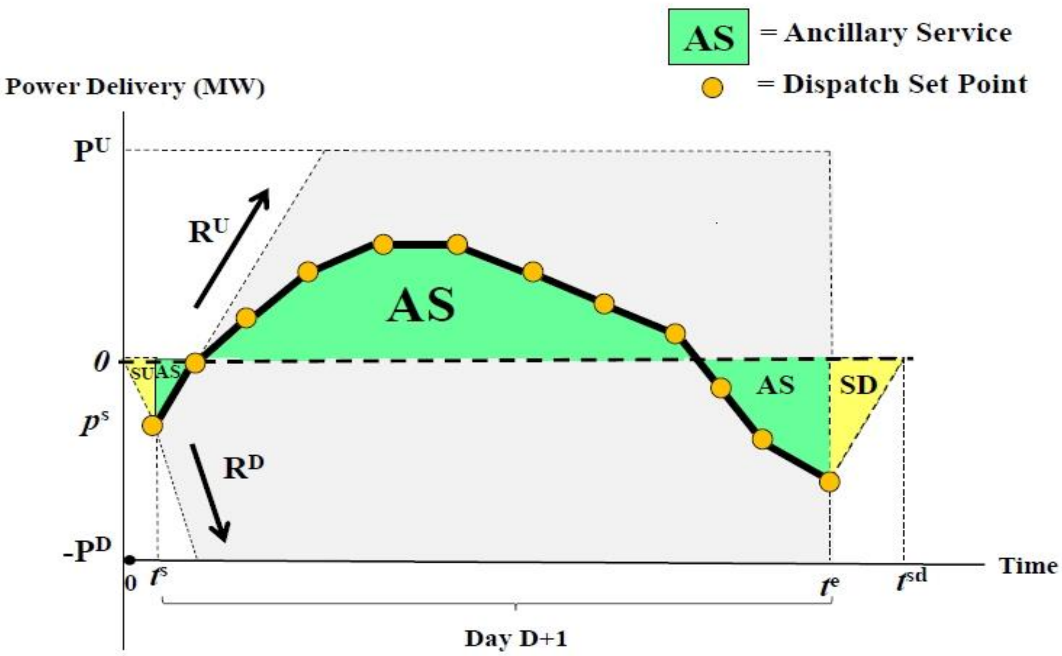

Fig. 1.13: A swing contract offering power-paths with down/up power/ramp flexibility.

Ensuring the *availability* of this down/up power during day D+1 does not incur no-load or minimum-run availability cost, assuming the down/up power is being harnessed from GER devices already in operation. However, the IDSO could incur *availability cost* in the form of lost opportunity cost if the IDSO has an ability to use this down/up power in a next-best opportunity.

In addition, the *ITSO-dispatched delivery* of the depicted dispatched down/up power-path during day D+1 requires the IDSO to incur *performance cost* for down-power (SU) before day D+1, ITSO-dispatched down/up power injection during day D+1, and up-power (SD) after day D+1. This occurs because the IDSO is obligated (through bid contracts) to compensate its managed GERs fully for all down/up power they must provide to meet their dispatch obligations, even if it is only the AS regions that provide valuable ancillary service for transmission level operations.

Finally, suppose a dispatchable battery resource *m* with round-trip efficiency 1.0 will be in a fully charged state at the start of an operating hour H and must be returned to a fully charged state by the end of hour H. Fig. 1.14 depicts one among many possible power-paths that an ITSO could dispatch *m* to deliver during hour H if the ITSO clears *m*'s battery swing contract submitted into an hour-ahead market M(H).

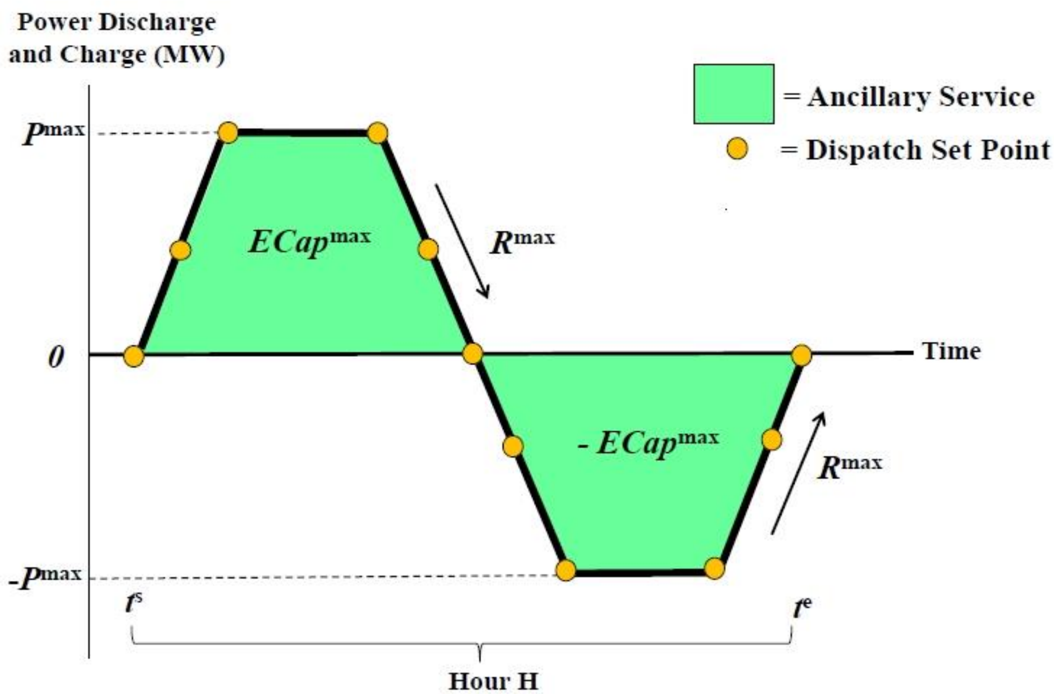

Fig. 1.14: A swing contract offering battery service with down/up power/ramp flexibility.

Ensuring the availability of down-up power during hour H could require *m* to incur *availability cost* in the form of lost opportunity cost, if *m* has a next-best alternative use for its battery services. The *ITSO-dispatched delivery* of the depicted dispatched down/up power-path during hour H requires *m* to incur *performance cost* during H in the form of battery wear-and-tear.

1.4 Test-Case Studies

1.4.1 Overview

ITD test-case studies of the Five-Step TES Design have been conducted for an IDSO-managed 123-bus distribution system populated by a collection of 927 households whose electrical devices require power to operate; see Fig. 1.15.

Households in these test case studies have no distributed generation; rather, all of their power usage must be obtained from a linked transmission system managed by an *Independent Transmission System Operator (ITSO)*. This transmission system is modeled by means of the 8-bus ERCOT Test Case, developed in [4,9]. The resulting ITD feedback loop is depicted in Fig. 1.16.

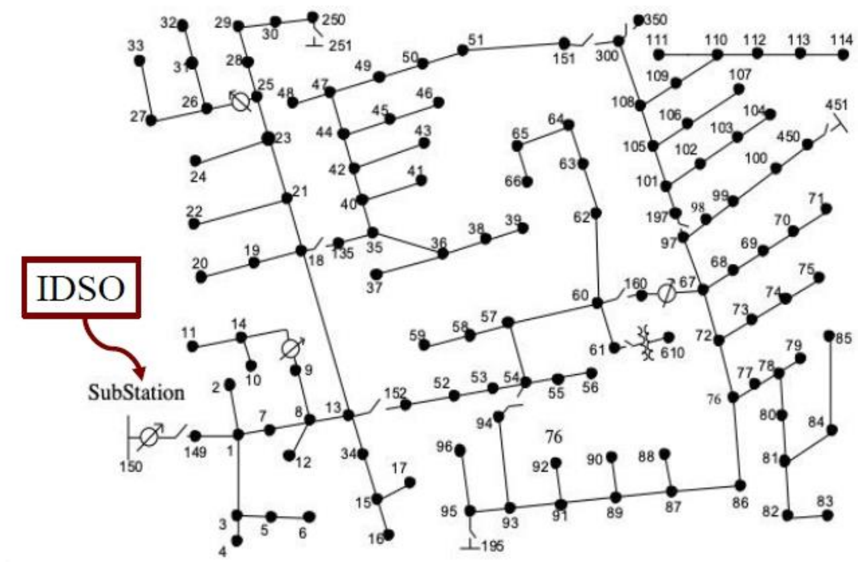

Fig. 1.15: The 123-bus distribution grid for all reported ITD household test cases.

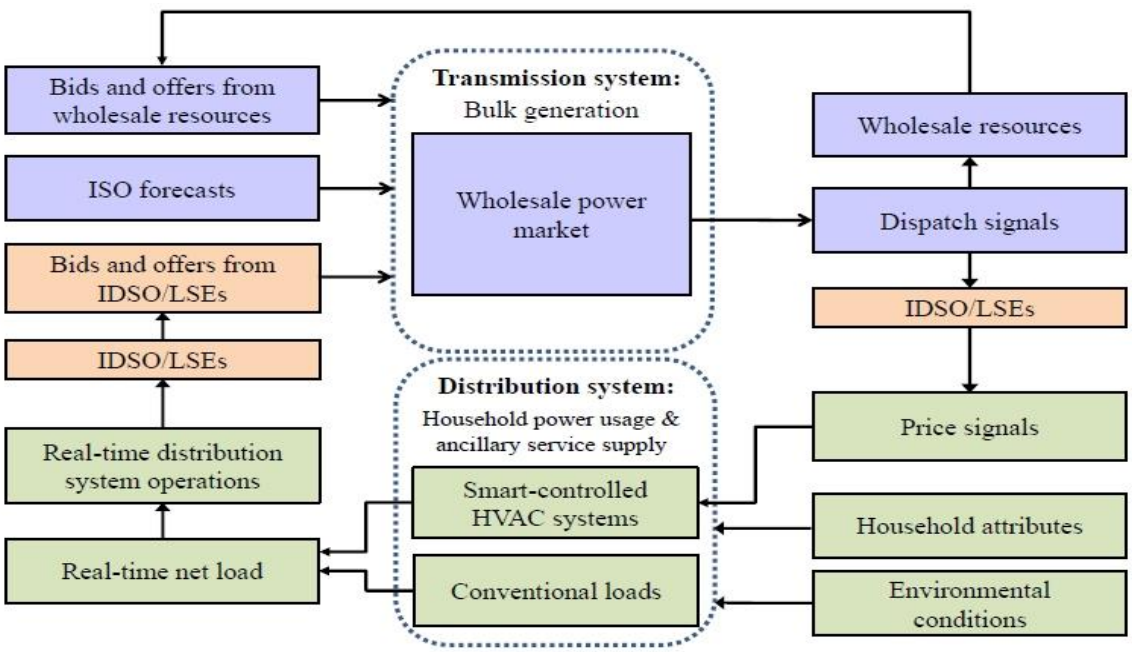

Fig. 1.16: ITD feedback loop for each ITD household test case.

As depicted in Fig. 1.17, each household consists of a resident occupying a house at a particular location subject to external weather conditions. Each household has a smart (price-sensitive) electric *Heating, Ventilation, and Air-Conditioning (HVAC)* system with ON/OFF power settings. This HVAC system consists of a basic HVAC unit operating in parallel with a one-speed fan for air circulation. Each household also has a collection of conventional thermostatically controlled appliances whose load is *fixed*, i.e., not price sensitive.

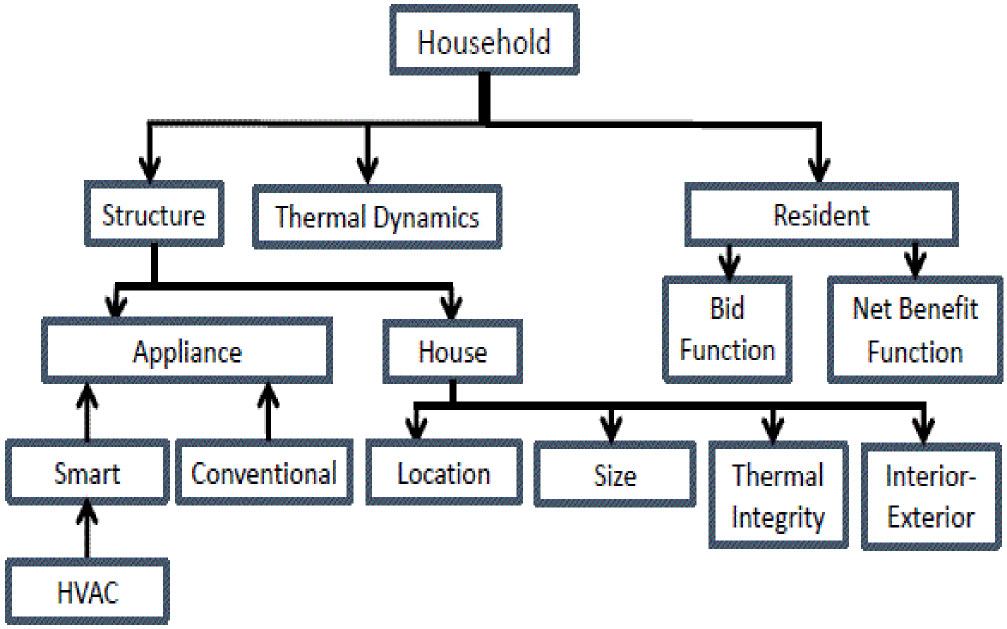

Fig. 1.17: Basic attributes characterizing a household in the ITD household test-case studies. Down-arrows denote "has a" relations and up-arrows denote "is a" relations.

As detailed in our project work [10, 13], the thermal dynamics of each household h are determined by an *Equivalent Thermal Parameter (ETP)* model reflecting h's specific attributes. This ETP model, together with external forcing terms (e.g., weather, network voltage conditions) and h's ON/OFF power control settings for its HVAC system, determines the dynamic change over time of h's inside air temperature and inside mass temperature.

Each household h's general goal is to maximize its *net benefit* over time, measured as thermal comfort minus cost. In pursuit of this goal, h participates in a Five-Step TES design. The Edge LISA for h that manages the daily power operation of h's HVAC system under this design will hereafter be referred to as h's *HVAC controller*. Each HVAC controller for each household h sends bids to the IDSO that express either h's demands for HVAC power usage as a function of required price payment or h's supplies of ancillary service (HVAC power absorption) as a function of offered price compensation, depending on h's current state. In turn, the IDSO sends price signals to h's HVAC controller that determine ON/OFF power control settings for h's HVAC system.

For each household h, the time interval during which an ON/OFF power setting is maintained for h's HVAC system is called a *control-step*. For simplicity of exposition, assume each control-step has the same duration and occurs at the same time for each h. The timeline for each h can thus be divided into common control-steps $n = [n^s, n^e)$ of equal duration. At the start-time n^s for each control-step n, a control signal is transmitted to each h's HVAC controller either to retain or switch its current HVAC ON/OFF control setting. This setting is then maintained for the remainder of control-step n.

The specific goal of each household h at the start-time n^s for each control-step n is to maximize its net benefit over the next N control-steps, where N denotes the household's look-ahead horizon. The net benefit (utils) of each household is calculated as

$$\text{Net Benefit} = \text{Benefit} - \mu\,[\text{Cost}]$$

where Benefit is measured in utils, the coefficient μ (utils/$) denotes the household's benefit-cost trade-off parameter, and Cost is measured in $. Roughly described, μ measures the benefit (utility) that would be attained by the household if its cost were reduced by $1.[9]

As established in [3], the optimal form of state-conditioned bid function for each household h is as depicted in Fig. 1.18. Given this form of bid function, h can communicate to the IDSO its entire state-conditioned bid function at the start of each control-step n by means of two scalar data points: a cut-off price Π^* (either positive or negative); and a forecasted ON HVAC power level P_n^*

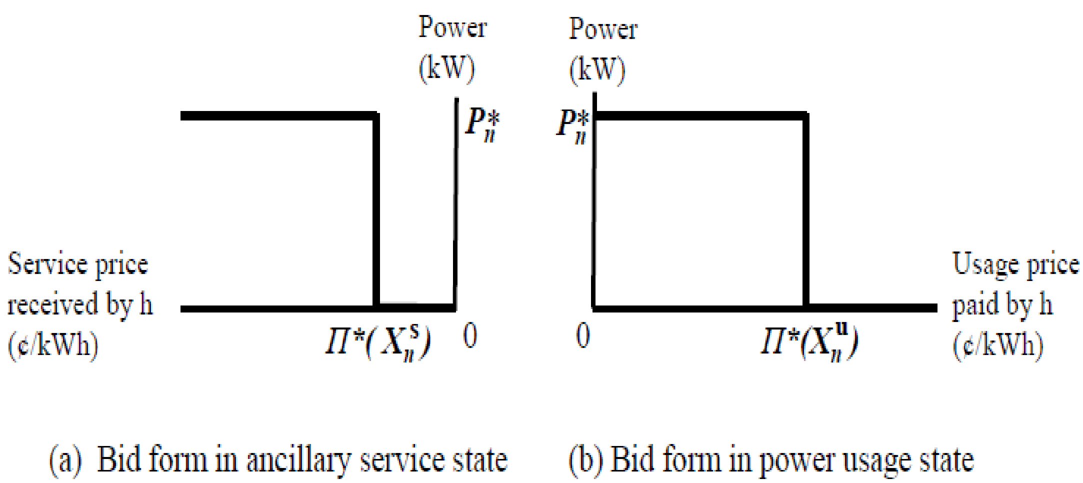

Fig 1.18: Optimal price-sensitive bid form for each household h for each control-step n in (a) an ancillary service provision state and (b) a power usage state. A negative price denotes a price received by household h for provision of ancillary service (power absorption). A positive price denotes a price paid by household h for power usage.

1.4.2 Implementation Details

Each ITD household test case is implemented by means of the ITD TES Platform V2 [11], an agent-based software platform developed as part of our project. A partial agent hierarchy for the ITD TES Platform V2 is depicted in Fig. 1.19.

[9] In economics, the value of μ for a household h -- called the *marginal utility of money* for h – is derived as the dual variable solution for the budget constraint in a budget-constrained utility (benefit) maximization problem for h. The utility function of a household (resident) represents the household's preference order over a given set of bundles containing different amounts of goods and services. This utility function can be analytically expressed (up to a positive transformation) on the basis of the outcomes of bundle choice experiments, assuming the choices expressed by the household in these experiments satisfy various choice axioms.

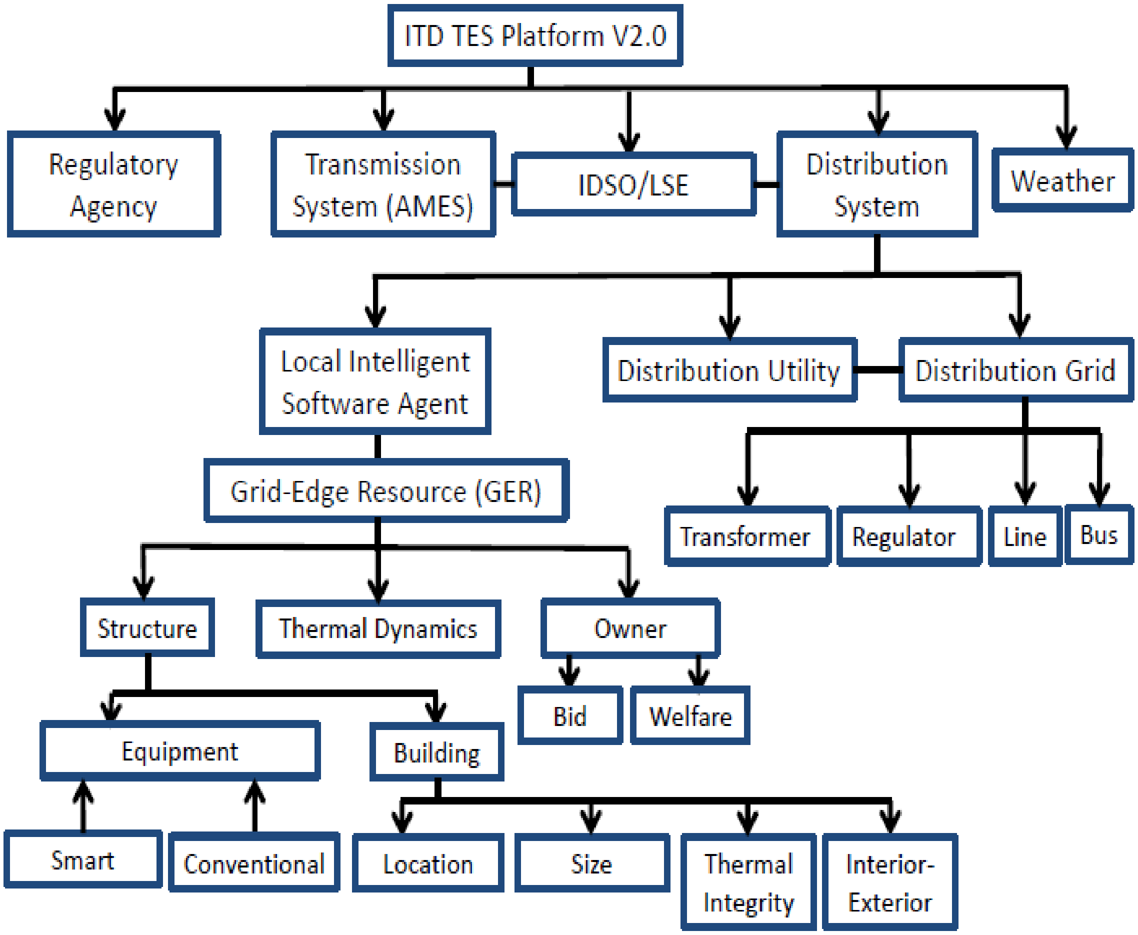

Fig. 1.19: Partial agent hierarchy for the ITD TES Platform V2 [11]. Down-arrows denote "has a" relations and up-arrows denote "is a" relations.

The transmission system component for the ITD TES Platform V2 is implemented by means of Version 5 of AMES (*A*gent-based *M*odeling of *E*lectricity *S*ystems) [8,12]. AMES V5 is an open source agent-based Java/Python platform that permits users to model core institutional and operational aspects of current U.S. RTO/ISO-managed wholesale power markets.

For example, AMES V5 is used in Battula et al. [4] to implement the ERCOT Test System [9], a specialized software platform that permits researchers to model and simulate ERCOT's day-ahead and real-time markets operating over a synthetically constructed ERCOT transmission grid during successive days.

A partial agent hierarchy for AMES V5 is depicted in Fig. 1.20. As indicated, the market participants include: dispatchable generators, non-dispatchable variable energy resources, *Load-Serving Entities (LSEs)*, and an IDSO. The *J*ava *Re*inforcement *L*earning *M*odule (*JReLM*) included within AMES V5 permits any decision-making market participant to be equipped with reinforcement learning capabilities.

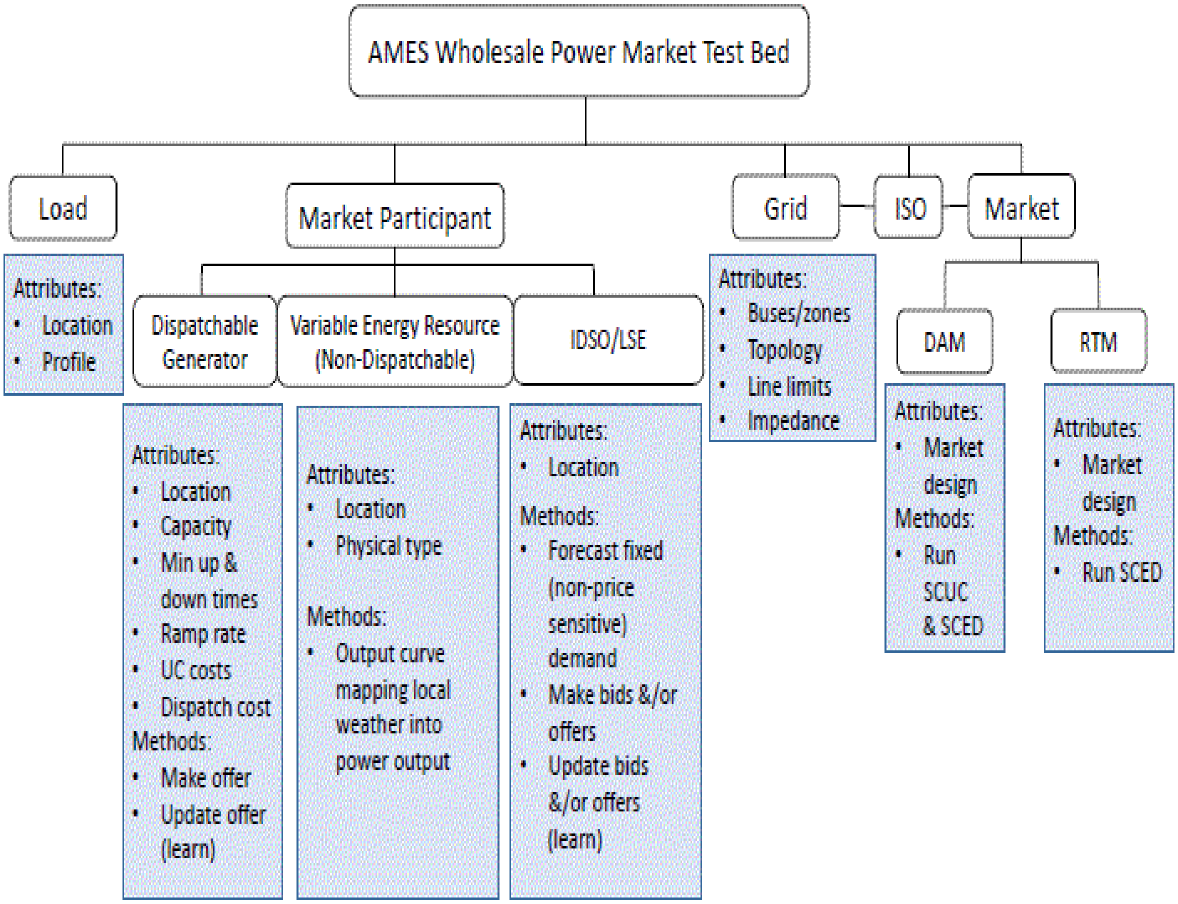

Fig. 1.20: Partial agent hierarchy for AMES V5 [8]. The IDSO agent is an externally modeled agent at a T-D interface that can participate in AMES market operations.

The complete analytical formulation for the SCUC/SCED optimization implemented in AMES V5 is carefully presented in Tesfatsion and Battula [12]. This formulation permits unit commitment costs and dispatch costs for market participants to be incorporated into the objective function whether the supply offers of these participants are in standard or swing-contract form.

The distribution system component for the ITD TES Platform V2 is implemented in part by means of GridLAB-D, a C/C++ platform whose software library permits the modeling and simulation of GERs (business, commercial, and household entities), electrical devices, unbalanced distribution grid operations, and various types of voltage controls. In addition, this distribution system component includes Python agents that we have developed during this project for the modeling and simulation of the IDSO and the Edge LISAs that manage GER power usage.

Finally, the *Framework for Network Co-simulation (FNCS)* – a TCP/IP-based middleware developed by PNNL researchers -- handles data exchange among all software components for the ITD TES Platform V2. For example, FNCS enables the IDSO and LISA agents to engage in two-way communications.

The key software components for the ITD TES Platform V2 are depicted in Fig. 1.21.

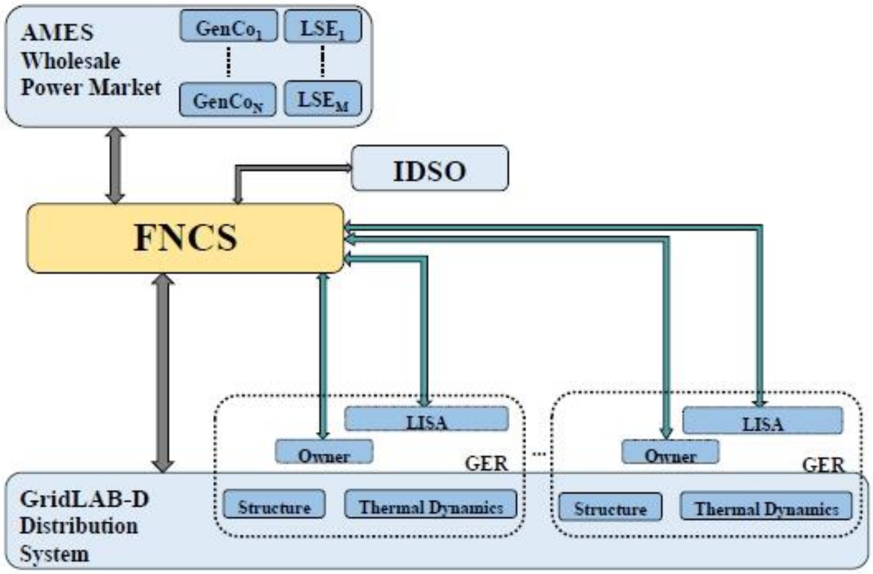

Fig. 1.21: Key software components for the ITD TES Platform V2 [11].

1.4.3 Maintained Assumptions

The transmission system for each ITD Household Test Case discussed in this project report is specified to be an 8-bus version of the ERCOT Test System developed in [4,9], extended to include an IDSO operating as the sole T-D linkage agent at a designated transmission grid bus B* called the *linkage bus*. Thus, no LSEs operate at B* as aggregators of distribution system loads whose intermediary activities could conflict with the fiduciary goals of the IDSO.

As depicted in Fig. 1.15, the distribution system for each test case is the standard IEEE 123-bus distribution system with three modifications. First, all GERs take the form of households; specifically, 927 households are distributed across the 123 buses in proportion to the original loads, which are then omitted. Second, the distribution grid is connected to the transmission system at a substation linked to the transmission grid bus B*; all wholesale power is supplied to the distribution system through this T-D interface. Third, the distribution system is managed by an IDSO operating at this T-D interface.

The IDSO manages the power demands and ancillary service supplies of each household h by means of the following *Household Five-Step TES Design* characterized by five time-rates:

Step 1: The HVAC controller for each household h collects data on h at a d*ata check rate* and uses these data to form a state-conditioned bid function Bid(h) for h's HVAC system. The bid function Bid(h) expresses either a demand function for HVAC power usage or a supply function for the HVAC provision of ancillary service (power absorption).

Step 2: The HVAC controller for each household h communicates Bid(h) to the IDSO at a *bid refresh rate*.

Step 3: The IDSO combines its latest received household bid functions Bid(h) into a vector **AggBid** of aggregate bid functions at an *aggregate bid refresh rate*.

Step 4: The IDSO uses **AggBid** to determine price signals that it communicates back to the household HVAC controllers at a *price signal rate*.

Step 5 [Control-Step]: The HVAC controller for each household h inserts its latest received price signal into its latest refreshed bid function Bid(h) at a *power control rate*, which triggers an ON/OFF power control action for h's HVAC system.

The five time-rates for the Household Five-Step TES Design are set to $1/\Delta t$ with a common time-step Δt = 300s. Let the time-delay between Step *j* and Step *j+1* in any given iteration of the five steps be denoted by ε_j for j=1, … , 5, where "Step 6"' is equated with "Step 1"' in the subsequent iteration. The time delays ε_j are commonly set for the ITD Household Test Cases so that their summation does not exceed Δt . Finally, let $t_j = t_{j-1} + \varepsilon_j$ for j = 1, … , 5. The iterated staggered implementation of Steps 1-5 for the Household Five-Step TES Design is then as depicted in Fig. 1.22.

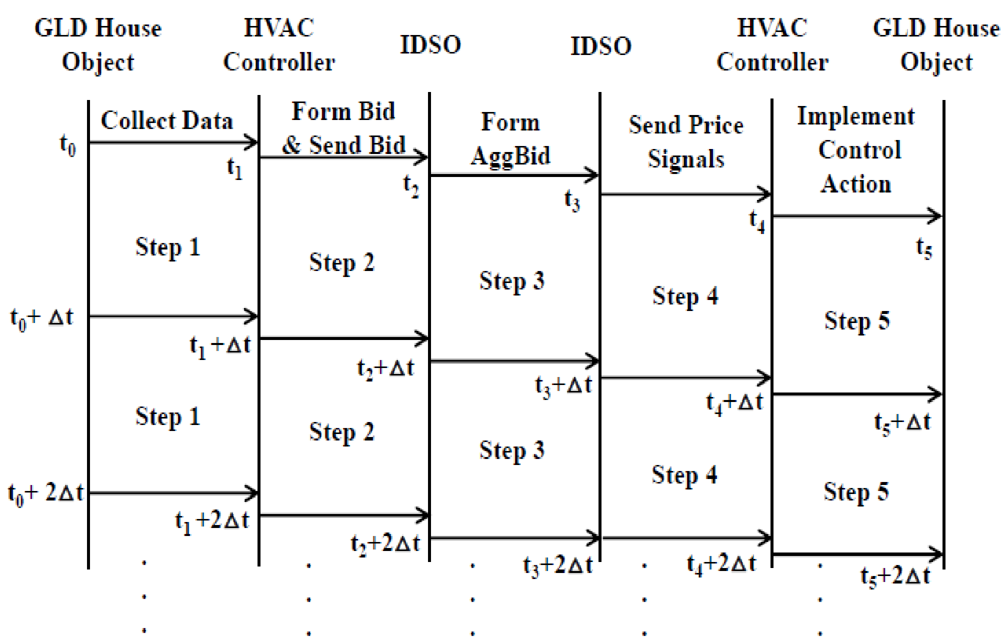

Fig. 1.22: Staggered implementation of the five steps comprising the Household Five-Step TES Design for the ITD household test cases.

Finally, households are classified into representative types based on *structure quality*: "Low," "Medium," or "High." As carefully explained in Battula et al. [3], each of these structure quality types is determined by correlated parameter settings for the appliance and house structural attributes depicted in Fig. 1.17. For example, a household with a "Low" structure quality type has an HVAC system with a low performance rating and a house that is small in size with poor thermal insulation.

1.4.4 Development of the 8-Bus ERCOT Test Case Used as the Transmission Component for ITD Household Test Cases

As part of this project we have developed the ERCOT Test System, a computational platform modeling the ISO-managed wholesale power market operations of the *Electric Reliability Council of Texas (ERCOT)*. As detailed in [4, Sections II-III], the ERCOT Test System captures key features of current ERCOT *Day-Ahead Market (DAM)* and *Real-Time Market (RTM)* operations, with congestion managed by *Locational Marginal Pricing (LMP)*. These markets are simulated over successive days of operation, with continual updating of system conditions.

The market component of the ERCOT Test System is implemented by means of AMES V5 [8,12], an open-source computational framework that captures salient operational aspects of U.S. RTO/ISO-managed wholesale power markets; see Fig. 1.20. The ERCOT Test System implements actual ERCOT DAM/RTM timing configurations as default settings. However, users are able to adjust these default settings to suit their research purposes.

The grid (bus/line) construction methods comprising the grid component of the ERCOT Test System are carefully explained in [4, Section IV]. These methods, adapted from work by Tom Overbye and his collaborators [14], make use of a clustering algorithm and a Delaunay Triangulation process as well as historical ERCOT generation and load data. These grid construction methods are used in [4, Section V] to construct a relatively small 8-bus ERCOT test grid suitable for exploratory studies of transactive market mechanisms. This 8-bus ERCOT test grid is depicted in Figs. 1.23 and 1.24.

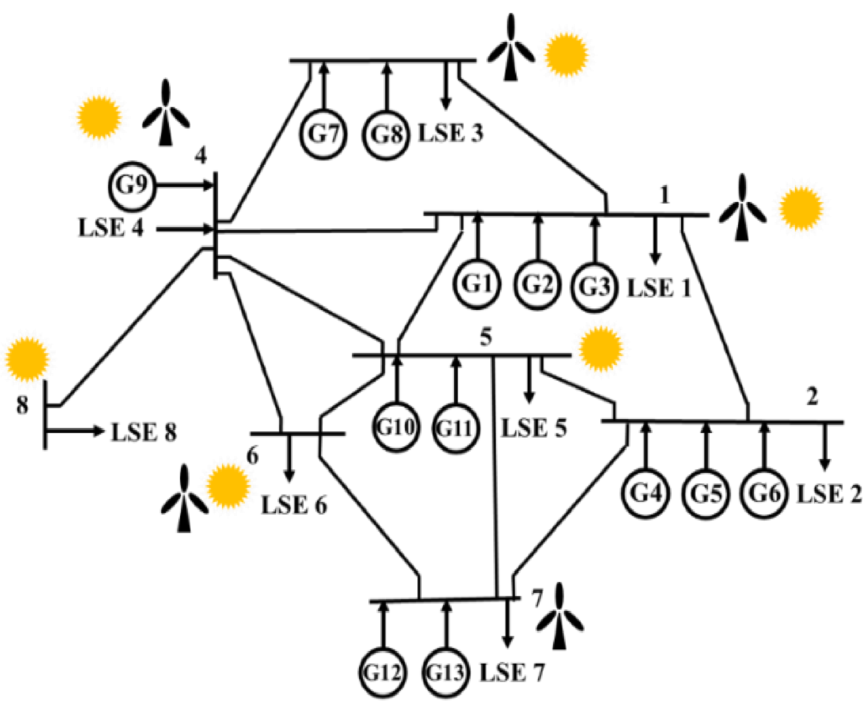

Fig. 1.23: Schematic depiction of the 8-Bus ERCOT test grid consisting of 345-kV lines with distributed wind, solar, and thermal generation.

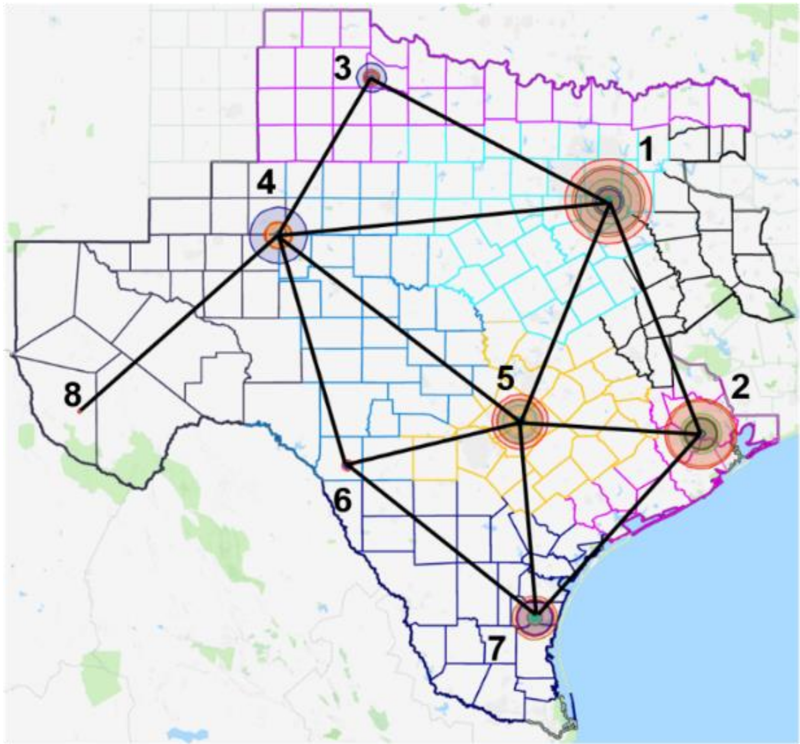

Fig. 1.24: The 8-bus ERCOT test grid superimposed on the ERCOT energy region.

The 8-bus ERCOT test grid is extended in [4, Sections VI-VII] to a complete 8-bus ERCOT Test Case. This test case illustrates the ability of the ERCOT Test System to model ERCOT day-ahead and real-time markets operating over a high-voltage transmission grid during successive days with continually updated system operating conditions. As established in [1, Ch. 16], the AMES V5 SCUC/SCED formulation implemented by the ERCOT 8-bus test case permits dispatchable resources to submit supply offers either in standard ERCOT form or in swing-contract form.

The 8-bus ERCOT Test Case is used to implement transmission operations for the ITD household test cases described below in Section 1.4.6. For each of these test cases the distribution grid is linked to bus 2 of the 8-bus ERCOT test grid depicted in Fig. 1.23. Thus, bus 2 constitutes the linkage bus B* for these test cases. All power requirements for distribution system households are managed by an IDSO operating at this linkage bus B*; thus, no LSEs operate at B*.

Finally, in each ITD household test case the transmission system is assumed to be large relative to the distribution system, implying that distribution loads have only a negligible impact on DAM and RTM locational marginal prices.

1.4.5 Classification of ITD Household Test Cases: TC1 vs. TC2

As indicated in Table 1.1, we have developed two types of ITD Household Test Cases to explore the performance of the IDSO-managed Five-Step TES design within an ITD system. These two types of test cases, called TC1 and TC2, postulate different roles for the IDSO in wholesale power market operations. Sections 1.4.7 and 1.4.8 report illustrative outcomes for TC1 and TC2.

Table 1.1: Two basic types of ITD Household Test Cases used to explore the performance of the Five-Step TES Design implemented within an ITD system.

Test Case	Household Role	IDSO Role	Household Mix of Appliances
TC1	Each household submits a state conditioned price-sensitive bid to the IDSO expressing either HVAC demand for power usage or HVAC supply of ancillary service (power absorption) .	The IDSO submits a fixed demand bid into each day-D DAM as its forecasted total household power usage for day D+1. In real-time operations on each day D+1, the IDSO sets prices for household price-sensitive bids to meet IDSO system goals and constraints.	Each household has conventional (fixed load) appliances plus a smart (price-sensitive) HVAC system
TC2	Same as TC1	The IDSO submits a fixed demand bid into each day-D DAM as its forecasted total household power usage for day D+1. The IDSO also submits ancillary service offer(s) into each day-D DAM for supply of ancillary services during day D+1. In real-time operations on each day D+1, the IDSO sets prices for household price-sensitive bids to meet IDSO system goals and constraints, conditional on the IDSO's obligation to satisfy any ITSO-instructed dispatch set points for ancillary service resulting from DAM-cleared IDSO ancillary service offers.	Same as TC1

1.4.6 Illustrative Test-Case Outcomes for TC1

This section reports illustrative TC1 outcomes for ITD Household Test Cases whose key features have been carefully described in Sections 1.4.1 – 1.4.5. A more detailed discussion of these TC1 outcomes can be found in Battula et al. [3].

The TC1 net benefit outcomes reported below are average net benefit attained by households for a particular operating day D, calculated as follows:

- Avg Cost ($/day) = (Total electricity cost incurred by all households on day D) divided by (Total number of households)

- Avg Benefit (utils/day) = (Total thermal comfort attained by all households on day D) divided by (Total number of households)

- Avg Net Benefit (utils/day) =
  Avg Comfort (utils/day) - [μ (utils/$) • Avg Electricity Cost ($/day)]

Bid Function Comparisons

The basic issue examined in the bid-function comparison test cases is whether household net benefit (comfort minus cost) increases when a household switches from the use of the heuristically motivated bid function developed by Nguyen et al. [5] to the optimal bid function developed by Battula et al. [3] whose general structural form is depicted in Fig. 1.18.

The heuristic bid function developed by Nguyen et al. [5] for a household h specifies cut-off prices for ancillary service provision and power usage that vary in direct proportion to the deviation between h's bliss (maximum comfort) temperature TB and the inside air temperature of h's house.

The outcomes reported in Fig. 1.25 for this test case show that the optimal bid function developed in [3] results in higher net benefit for all tested values of the household marginal-utility-of-money parameter μ. This net benefit improvement is larger for larger μ values. Moreover, this same pattern holds across all three tested settings for household structure quality.

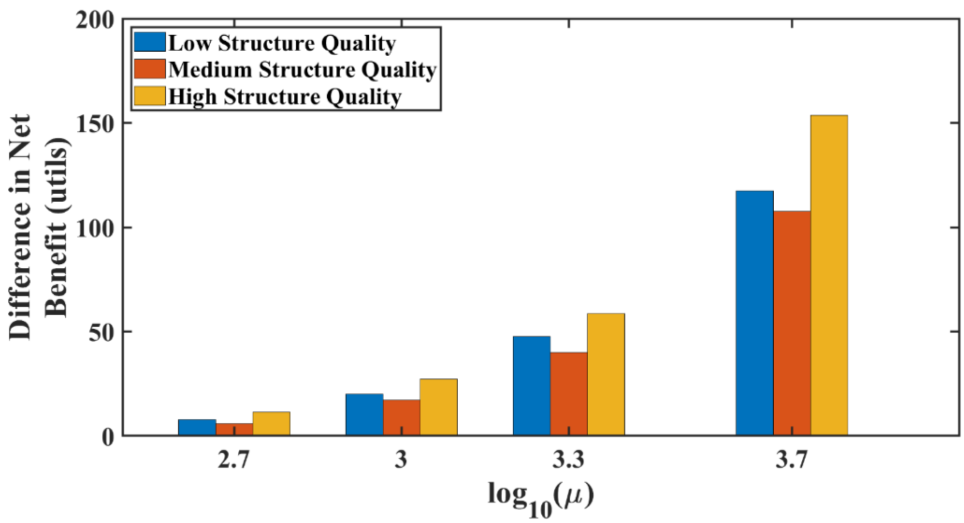

Fig. 1.25: Increase in net benefit resulting when a household switches from the heuristic bid function developed in [5] to the optimal bid function developed in [3], under varied settings for household marginal utility of money μ (utils/$) and household structure quality type.

IDSO Peak-Load Reduction Capabilities

The basic issue considered in the peak-load reduction test cases is as follows: Can the IDSO use retail price signals to achieve target peak-load reductions? The key finding is that the IDSO can indeed achieve target peak-load reductions through appropriate retail price signals; but the mix of household structural quality types strongly affects the required form of these signals.

The IDSO on day D forecasts household peak load for day D+1. The IDSO uses this forecast to determine a target peak load for day D+1, given by forecasted peak load reduced by a designated percentage. During day D+1 the IDSO then uses latest refreshed household bids to send an appropriate sequence of retail price signals to households to maintain total household load at or below this target peak-load level.

Figs. 1.26-1.28 report the IDSO's ability to achieve a 0.5MW peak-load reduction by means of retail prices communicated to households with optimally formulated bid functions. These retail prices take either a flat-rate form (10₵/kWh) or a peak-load pricing form. All households have the same structure quality type, either all Low, all Medium, or all High.

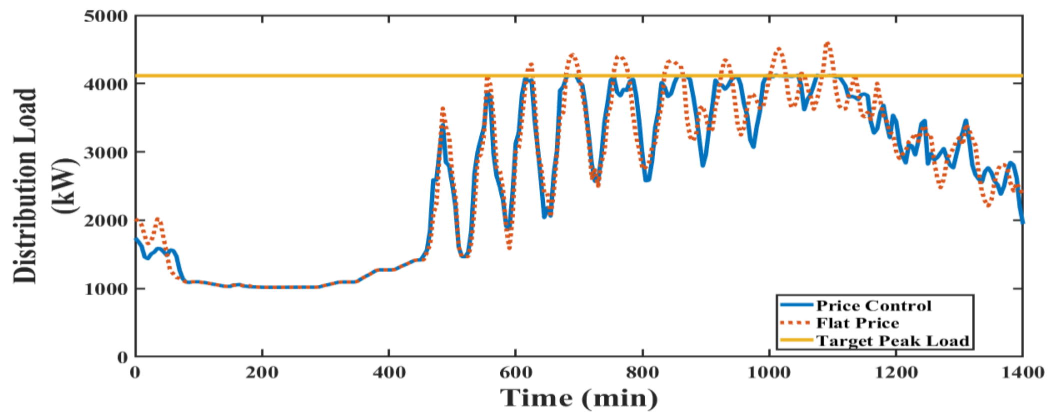

Fig. 1.26: *Low Structure Quality Type (SQT) Case:* Load outcomes on day D+1 when the IDSO controls retail prices to achieve a 0.5MW target peak load reduction and all households have Low SQT.

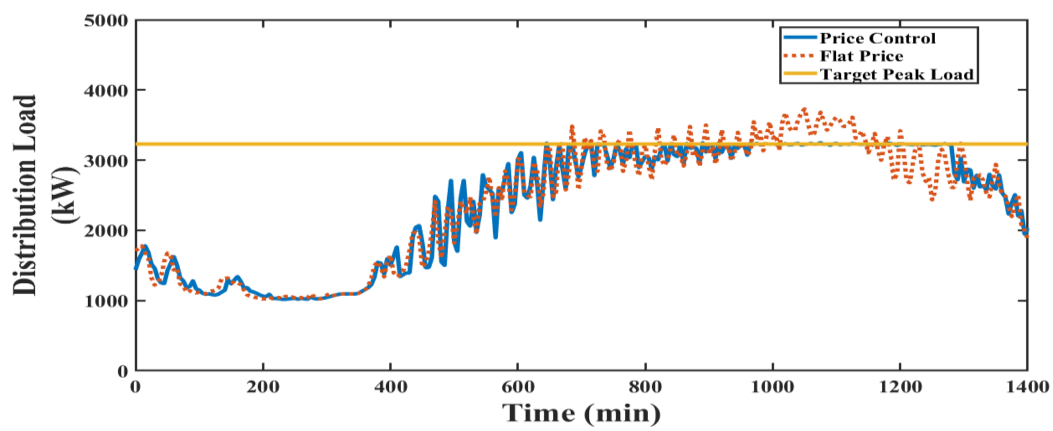

Fig. 1.27: *Medium Structure Quality Type (SQT) Case:* Load outcomes on day D+1 when the IDSO controls retail prices to achieve a 0.5MW target peak load reduction and all households have Medium SQT.

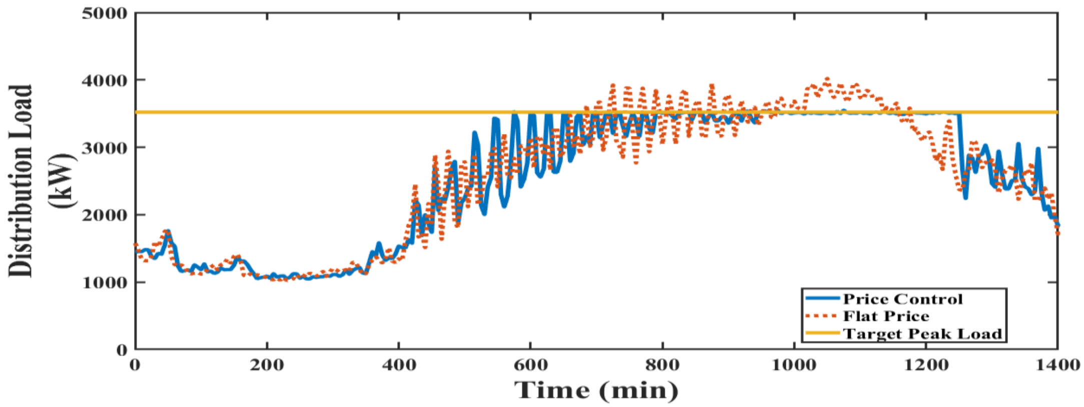

Fig. 1.28: *High Structure Quality Type (SQT) Case*: Load outcomes on day D+1 when the IDSO controls retail prices to achieve a 0.5MW target peak load reduction and all households have High SQT.

Fig. 1.29 reports the peak-load retail prices required to achieve a targeted 0.5MW peak-load reduction when households have all Low, all Medium, or all High structure quality types. The substantial differences in retail prices observed for these three test cases indicate that household structure quality should be given careful consideration in any peak-load reduction effort.

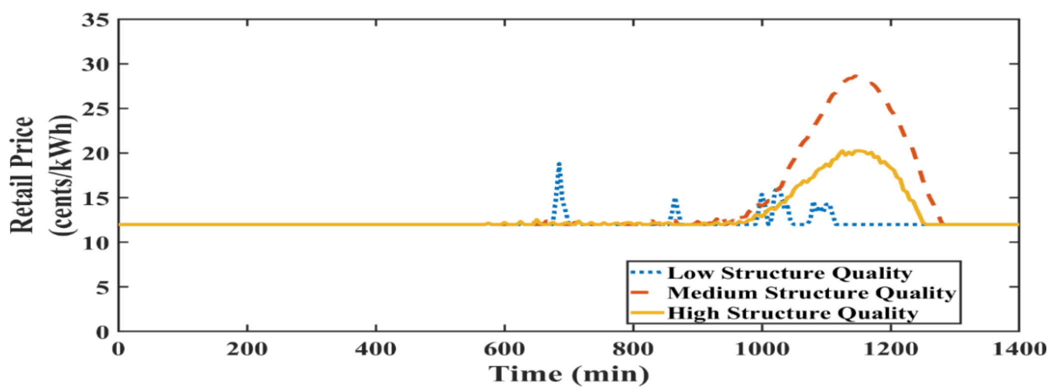

Fig. 1.29: IDSO-controlled retail price signals used by the IDSO on day D+1 to achieve a 0.5MW target peak load reduction under three different household structure quality type treatments: all Low; all Medium; or all High.

IDSO Load-Matching Capabilities

The next basic issue explored is as follows: Can the IDSO use retail price signals to ensure total realized household load matches a target load profile? The key finding is that the IDSO can indeed achieve target load matching. However, to do so the IDSO is sometimes forced to purchase ancillary service from households in an ancillary service state, where this ancillary service takes the form of price-dispatchable power absorption.

As for the peak-load reduction test cases, the IDSO manages a Household Five-Step TES design for a 123-bus distribution grid populated by 927 households. The IDSO is located at a substation that connects the distribution grid to a transmission grid at transmission bus 1, the linkage bus B*; and all wholesale power supplied to the distribution system passes through this substation.

The IDSO participates in an ISO-managed DAM operating over the transmission grid. On each day D the IDSO submits a fixed demand bid into the DAM consisting of a forecasted 24-hour household load profile for day D+1. On day D+1, to avoid triggering uncertain (hence risky) RTM price adjustments, the IDSO attempts to ensure that actual household load does not deviate from the fixed demand bid it submitted into the DAM on day D.

Fig. 1.30 reports load-matching outcomes for an illustrative case in which the distribution grid is populated with a random mix of households with Low, Medium, and High structure quality types. Specifically, the structure quality type of each household connected at each distribution grid bus is configured to be Low, Medium, or High with corresponding probabilities (1/3, 1/3, 1/3). As seen in Fig. 1.30, the IDSO is successfully able to use retail price signals on day D+1 to match household load to the load profile it submitted to the day-D DAM as its fixed demand bid.

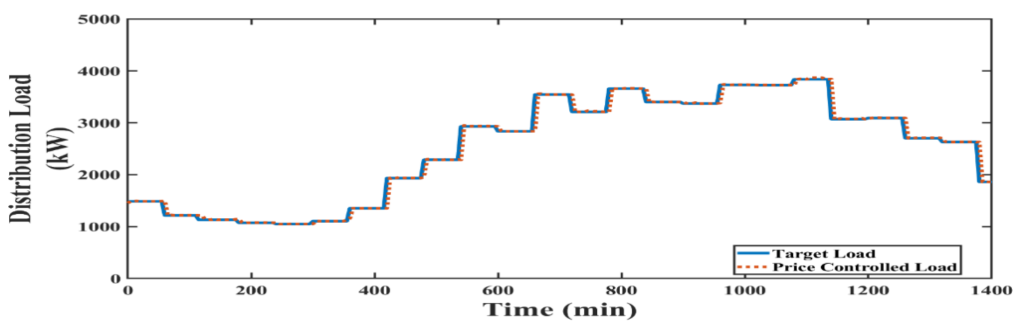

Fig. 1.30: IDSO's ability to use retail price signals to match total household load on day D+1 to a target load profile, given by the IDSO's fixed demand bid submitted into the DAM on day D.

The retail price signals used by the IDSO to achieve the good load matching depicted in Fig. 1.30 are shown in Fig. 1.31. Note all retail price signals are positive. This indicates that only households in a power usage state are receiving these price signals, which indicate how much each household must pay for its demanded power usage.

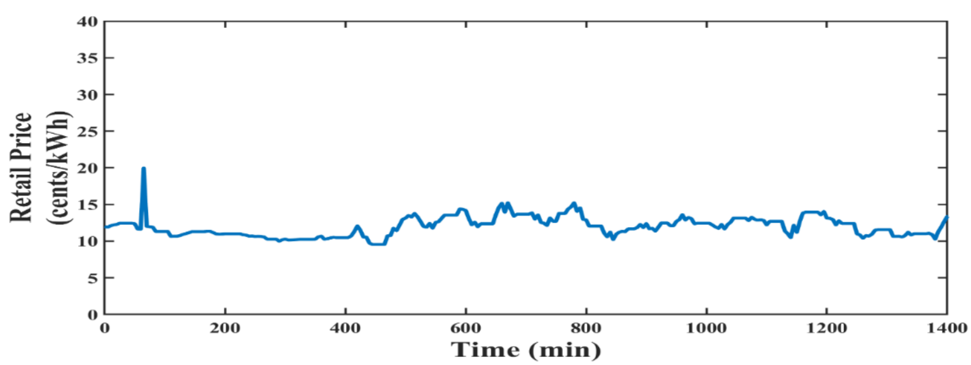

Fig. 1.31: The retail price signals sent by the IDSO on day D+1 to households in a power usage state to match total household load to the IDSO's day-D DAM fixed demand bid, depicted as the target load profile in Fig. 1.30.

As a second load-matching test case, suppose the IDSO instead submits into the day-D DAM the fixed demand bid (load profile) depicted in Fig. 1.32. Once again, as seen, the IDSO is successfully able to use retail price signals on day D+1 to match total household load to this target load profile.

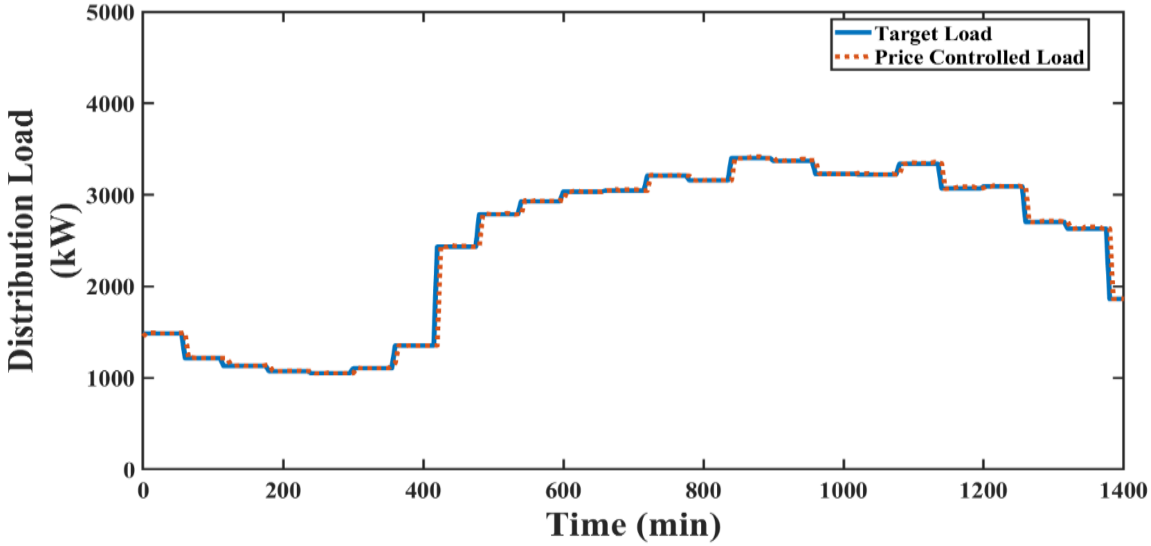

Fig. 1.32: The IDSO's ability to use retail price signals to match total household load on day D+1 to a different target load profile, i.e., a different fixed demand bid submitted into the day-D DAM.

The retail price signals used by the IDSO to accomplish the good load matching depicted in Fig. 1.32 are shown in Fig. 1.33. In contrast to the earlier load-matching test case, it is seen that the IDSO must now purchase ancillary service from households in an ancillary service state in order to achieve its load-matching goal, where this ancillary service takes the form of price-dispatchable power absorption.

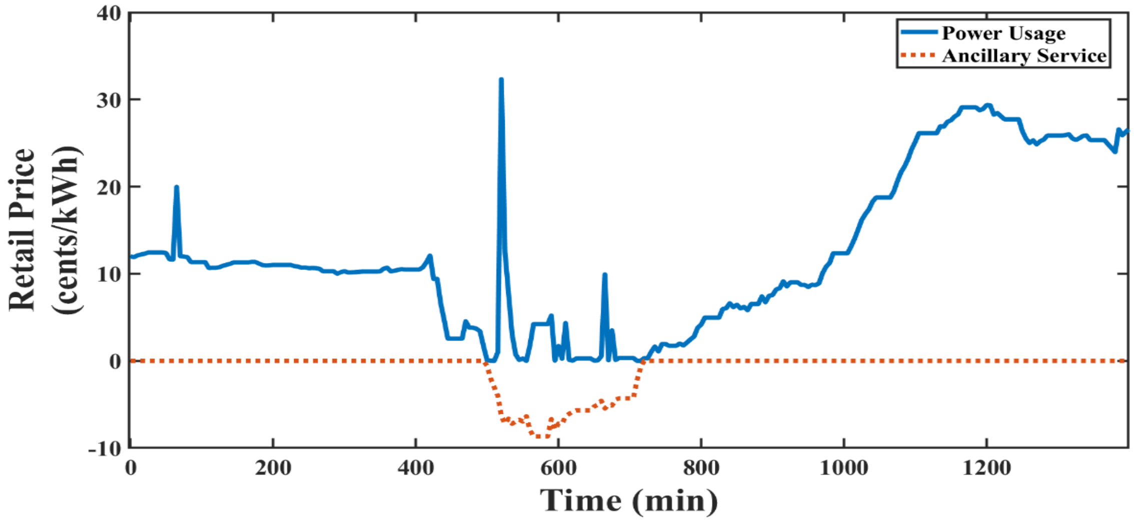

Fig. 1.33: The positive and negative retail price signals communicated by the IDSO to households on day D+1 to match total household load to the target load profile in Fig. 1.32.

Specifically, the target load profile depicted in Fig. 1.32 sharply increases starting around hour H7 (minute 420) on day D+1. To match actual load to this upward shift in targeted load, the IDSO sends *positive* retail price signals to households in a power usage state to induce their maximum power usage; but the IDSO also sends *negative* retail price signals to households in an ancillary service provision state to procure power absorption.

Recall the magnitude of a *negative* retail price signal denotes the price a household in an ancillary service state will *receive* in compensation for any supplied ancillary service (power absorption).

However, in attempting to interpret more fully the retail price movements depicted in Fig. 1.33, it is essential to keep in mind they arise from a complicated underlying causal process.

Specifically, they depend on dynamic nonlinear interactions among external forcing terms (e.g., grid voltage and weather conditions), house and appliance attributes, resident net benefit and bid functions, thermal dynamic relationships, IDSO system goals and constraints, and past price-induced HVAC ON/OFF control actions. For example, the rising retail prices observed subsequent to hour H12 (minute 720) in Fig. 1.33 reflect the IDSO's need to reduce household power usage demand down to the IDSO's target load levels, given all that has gone before.

1.4.7 Illustrative Test-Case Outcomes for TC2

Overview

As explained in Table 1.1 in Section 1.4.5, the key distinction between test cases of types TC1 and TC2 is the role of the IDSO in the wholesale power market. For TC1, the IDSO is a passive procurer of wholesale power. In contrast, for TC2 the IDSO also actively competes for the provision of ancillary services as support services for wholesale power market operations.

This section reports illustrative outcomes for test cases of type TC2.[10] The basic issue addressed is whether the IDSO can use swing contracts to facilitate its participation in a DAM as an ancillary service provider. These ancillary services are harnessed from the households participating in an IDSO-managed Five-Step TES Design in return for appropriate compensation. Thus, the IDSO's participation in the DAM as an ancillary service provider can create additional revenue streams for these households.

As explained in Section 1.4.4, the modeling of DAM and RTM operations for these TC2 test cases is based on ERCOT's two-settlement system. The specific ERCOT market timings used to implement DAM and RTM operations for three successive simulated days D1, D2, and D3 are shown in Fig. 1.34.

[10] The TC2 outcomes reported in this section are part of the project work reported in detail in the PhD thesis [7] of our project GRA Swathi Battula. Technical TC2 outcome details are omitted here for ease of exposition.

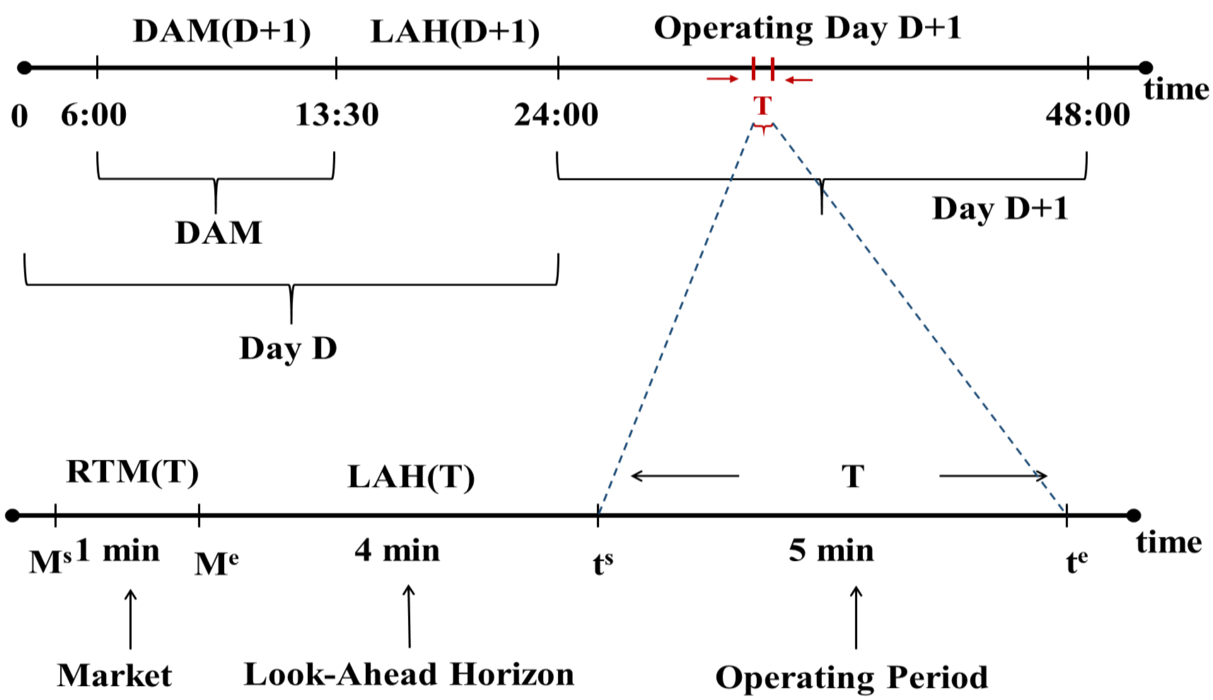

Fig. 1.34: Specific ERCOT market timings used to implement DAM and RTM operations for three successive simulated days D1, D2, and D3

Table 1.2: Nomenclature table.

Term	Description
Acronyms:	
FD	Subscript indicating fixed demand for power
SD	Subscript indicating price-sensitive demand for power
TD	Subscript indicating total demand for power
Functions & Variables:	
$P_{FD}^{DA}(B*, H, D+1)$	Power level (MW) submitted by the IDSO into the day-D DAM as its fixed (non-price-sensitive) demand for power at the linkage bus B* during hour H of day D+1
$PAvg_{FD}(B*, H, D-1)$	Average household fixed (non-price-sensitive) power usage (MW) realized at the linkage bus B* during hour H of day D-1
$PAvg_{SD}(B*, H, D-1)$	Average household price-sensitive power usage (MW) realized at the linkage bus B* during hour H of day D-1
$PAvg_{TD}(B*, H, D-1)$	Average household total power usage (MW) realized at the linkage bus B* during hour H of day D-1

IDSO participation in the DAM: Fixed Demand Bid

On each simulated day D, the IDSO submits into the day-D DAM a set of 24 hourly fixed (non-price-sensitive) demand bids for household power usage during day D+1. These hourly fixed demand bids are determined as follows.

On each day D, the IDSO calculates average household total power usage (MW) realized at the linkage bus B* during each hour H of the previous day D-1, denoted by $PAvg_{TD}(B*, H, D-1)$ for H = 1, …, 24. The IDSO then submits these hourly power usage calculations into the day-D DAM as its hourly fixed demand bids at bus B* for day D+1. Formally:

$$P_{FD}^{DA}(B*, H, D+1) \;=\; PAvg_{TD}(B*, H, D-1)\,,\;\; \forall H \in \{1, 2, \ldots, 24\} \qquad (1)$$

IDSO Participation in the DAM: Swing-Contract Offer

On each day D, the IDSO submits into the day-D DAM an ancillary service offer in firm swing-contract form for each hour H = $[t^s(H), t^e(H))$ of day D+1. The offered ancillary service is a constant power injection level to be maintained during hour H, where this level is to be selected from a specified power level set P= $[P^{min}, P^{max}]$. The specific form of this swing contract for each hour H of day D+1 is as follows:

$$SC = (\;\alpha, PP(H), \varphi(H)\;) \qquad (2)$$

where:

α = SC offer price = 0

PP(H) = Set of dispatchable power-paths for hour H = $(B^*, t^s(H), t^e(H), P\;)$

B* = Power-path delivery location (linkage bus)

$t^s(H)$ = Start-time of each offered power-path

$t^e(H)$ = End-time of each offered power-path

P = Power level set = $[P^{min}, P^{max}]$ = [0MW, 0.5MW]

φ(H) = Performance payment method for hour H: namely, if the ITSO signals the IDSO to maintain a power injection level p ϵ P at bus B* during hour H, the IDSO is to be compensated in accordance with the *average* RTM LMP ($/MWh) determined during hour H for the linkage bus B* .

Suppose the ITSO clears the swing contract (2) in the day-D DAM and ultimately signals the IDSO to maintain a power injection level p ϵ P at bus B* during hour H. The IDSO must be able to fulfill these dispatch instructions by means of a corresponding reduction in the amount of household power usage scheduled at bus B* during hour H in accordance with the fixed demand bid (1) that the IDSO has submitted to the day-D DAM.

Input Net Load Data for Simulations

The DAM ITSO-forecasted and realized net load profiles for three successive days used as inputs for the TC2 test cases are displayed in Figs. 1.35 and 1.36.

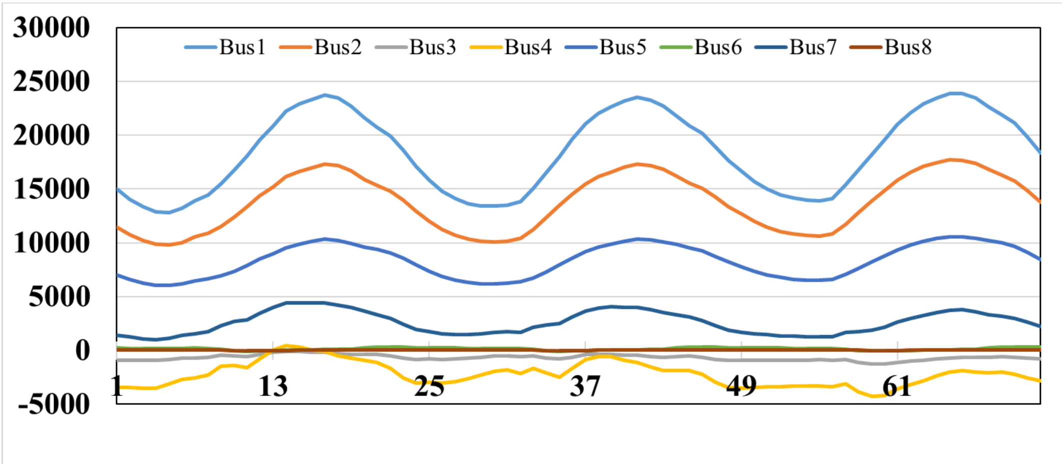

Fig. 1.35: Day-ahead forecasted hourly net load for three consecutive simulated days.

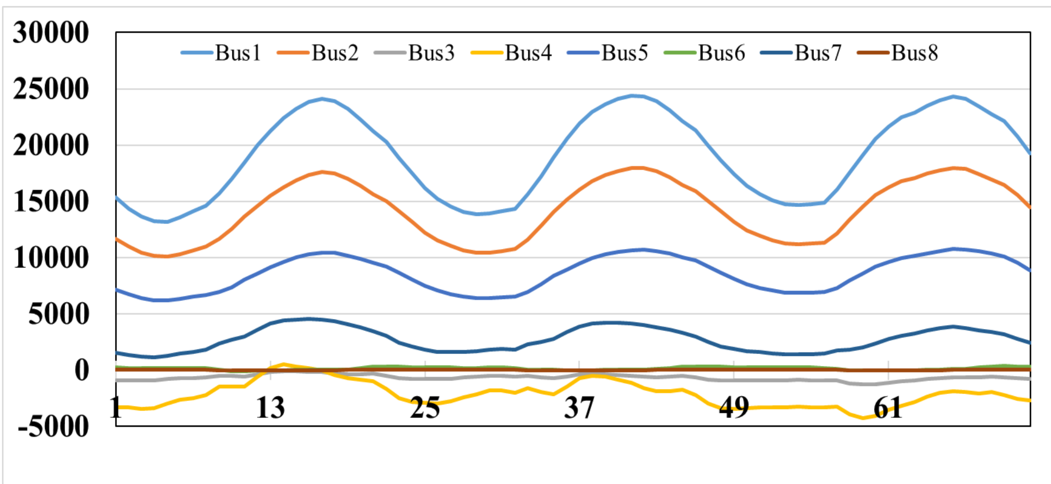

Fig. 1.36: Realized hourly net load for three consecutive simulated days.

Benefit, Cost, and Net Benefit Assessments

To preserve its independent status, the IDSO must allocate back to the households all costs and revenues arising from its ITD system operations.

Let ElectricityCost(H,D+1) ($) denote the total cost charged to the IDSO by the ITSO for its day-D DAM power procurement for hour H of day D+1. Also, let ASRev(H,D+1) ($) denote the total revenue earned by the IDSO from its day-D DAM offer of ancillary services for hour H of day D+1. Finally, let a superscript h denote the particular allocation of this cost or revenue to a household h.

The total benefit, total cost, and total net benefit attained by a household h for hour H of day D+1, each commensurately measured in utils, can then be expressed as follows:

$$\text{Benefit}^h(\text{H,D+1}) \;=\; \text{Comfort}^h(\text{H,D+1}) \;+\; \mu^h\,[\text{ASRev}^h(\text{H,D+1})]$$

$$\text{Cost}^h(\text{H,D+1}) \;=\; \mu^h\,[\text{ElectricityCost}^h(\text{H,D+1})]$$

$$\text{NetBenefit}^h(\text{H,D+1}) \;=\; \text{Benefit}^h(\text{H,D+1}) \;-\; \text{Cost}^h(\text{H,D+1})]$$

where

$$\mu^h \text{ (utils/\$)} \;=\; \text{Marginal utility of money for household h}$$

Benefit, Cost, and Net Benefit Outcome Comparisons

Fig. 1.37 compares, in normalized form, the average benefit, cost, and net benefit attained by a household on simulated day 3 for the TC2 test case in comparison with a corresponding TC1 test case with a more passive type of IDSO that does not make DAM ancillary service offers.

More precisely, for both test cases the IDSO submits a fixed demand bid into the day-2 DAM for the servicing of HVAC and non-HVAC power usage during each hour H of day 3. However, in the TC2 test case the IDSO also submits a swing contract into the day-2 DAM that offers ancillary service during each hour H of day 3. This ancillary service consists of a range of price-dispatchable power injection levels that the IDSO can harness from households as compensated reductions in their DAM-scheduled power usage at the linkage bus B*.

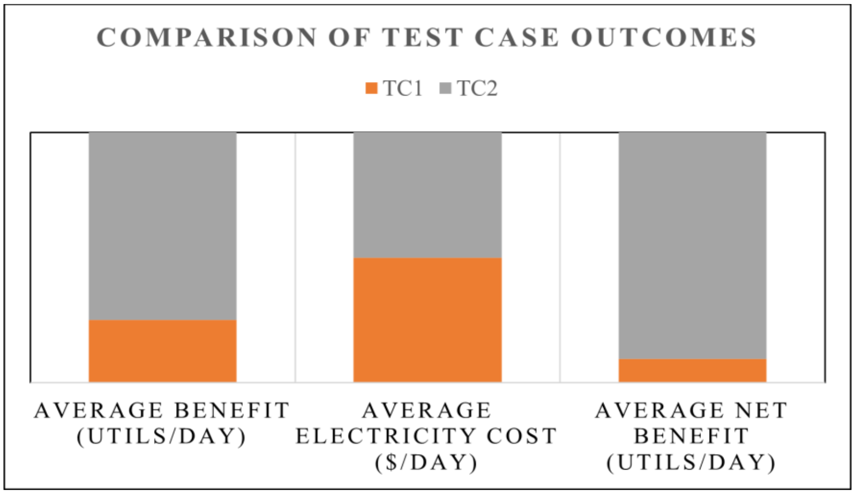

Fig. 1.37: Comparison of TC1 and TC2 outcomes (in normalized form) for household average benefit, average cost, and average net benefit. Under TC2 the IDSO submits swing contracts into the DAM offering next-day ancillary services, harnessed from its managed households.

As seen in Fig. 1.37, the switch from the relatively passive IDSO in TC1 to the *more active* IDSO in TC2 results in an *increase* in household average net benefit.

More precisely, the ability of the IDSO in TC2 to submit a swing-contract offer into the day-D DAM for ancillary services harnessed from its managed households results in an additional revenue stream for households. The households can experience lower comfort levels under TC2 since households are now offering to turn their HVAC systems OFF for sufficiently high compensation even if their comfort net of electricity cost would be higher if their HVAC systems were maintained or switched to ON. However, the additional benefit attained by households from the compensatory revenue they receive from ancillary service provision -- plus their lower electricity cost during ancillary service provision hours -- offsets these lower comfort levels, thus permitting households to attain higher average net benefit levels.

1.5 Conclusions and Future Research

The objective of the research reported in Section 1 of Part I has been to investigate the ability of IDSOs, functioning as linkage agents for ITD systems, to facilitate the flexible availability and use of reserve in support of ITD system operations by means of a bid-based TES design.

In accordance with this objective, we have developed a new type of IDSO-managed bid-based TES design for distribution system operations, called the Five-Step TES Design. In addition, we have developed new types of swing contracts permitting the IDSO to participate in transmission system operations as a provider of reserve harnessed from GERs by means of this design. Together, these design elements constitute a scalable market-based approach facilitating efficient reserve procurement for ITD system operations from a fuller range of power resources. The efficacy of our approach has been demonstrated by detailed conceptual analyses and test case simulations.

With regard to conceptual analyses, we have contributed five important developments for TES design. First, we have developed an optimal bid form for thermostatically-controlled devices (e.g., electric HVAC systems) owned by GERs that permits the GER owners to submit demand bids for power usage and/or supply offers for ancillary service provision (power absorption), depending on their local state. Second, we have developed a method to classify and model "representative" GERs based on their structural and preference attributes. Third, we have developed an IDSO-managed Five-Step TES design that permits an IDSO to manage GER power usage demands and ancillary service supplies. Fourth, we have demonstrated how the Five-Step TES Design can be coordinated with wholesale power market operations. Fifth, we have developed new types of swing contracts that facilitate the participation of the IDSO in these wholesale power markets as a provider of ancillary services harnessed from its managed GERs, thus permitting the IDSO to create additional revenue streams for these GERs.

To implement our test-case simulations, we have developed a carefully validated computational platform, the ITD TES Platform V2, that models ITD system operations over time. The transmission component for this platform models day-ahead and real-time market operations as currently conducted in U.S. RTO/ISO-managed wholesale power markets. A version of this transmission component that specifically models wholesale power market operations in the ERCOT energy region has been used to implement all test cases for part I.1 of our project.

2. A Consensus-Based TES Design Managed by an Independent DSO

2.1 Introduction

The rapidly growing penetration of distributed energy resources (DERs) poses new challenges for the efficient and reliable management of distribution networks. Researchers and practitioners are exploring a variety of management strategies to meet these challenges.

Transactive energy system (TES) design is an emerging innovative energy management strategy that engages DERs through market interactions. As originally formulated by the GridWise Archi-tecture Council [16], a TES design is a collection of economic and control mechanisms that allows the dynamic balance of power supply and demand across an entire electrical infrastructure using value as the key operational parameter. Typically, valuations for power demands and supplies are expressed by means of purchase and sale prices.

The TES design literature is rapidly expanding. Many different conceptual TES designs are actively under investigation. These designs range from peer-to-peer TES designs based on bilateral customer transactions to TES designs for which customer power requirements are centrally managed by some form of Distribution System Operator (DSO). In addition, researchers have developed software platforms for Integrated Transmission and Distribution (ITD) systems that permit the study of interactions between TES design operations at the distribution level and wholesale power market operations at the transmission level.

Nevertheless, to date, most TES design studies do not carefully take into account network power flow constraints for the empirically relevant case of *unbalanced* distribution networks. Consequently, the studied TES designs cannot ensure the reliable operation of these networks. For example, Nguyen et al. [5] show how voltage violations can arise for an unbalanced distribution network operating under PowerMatcher [17], a well-known TES design that does not explicitly consider the need to satisfy distribution network reliability constraints.

A second TES design issue is that attention is typically focused on the sequential determination of single-period decisions, with no consideration of possible future effects. This single-period focus does not permit decision makers to take into account cross-period correlations among their successive decisions.

A third TES design issue is the desirability of aligning customer goals and constraints with distribution network goals and constraints by means of a decentralized communication process that ensures customer privacy as well as network reliability.[1] To date, the precise form of decentralization that

[1] The study of institutions mapping private activities into social outcomes by means of decentralized communication

would be needed to achieve this multi-faceted objective for unbalanced distribution networks has not been extensively investigated.

The present study proposes a multiperiod consensus-based TES design that addresses all three of these issues. This TES design can be used by an independent[2] DSO to manage the daily power requirements of customers populating an unbalanced distribution network.

The TES design is *consensus-based* in that retail prices for each operating period OP are determined by means of a negotiation process between the DSO and the customers that preserves customer privacy. The TES design is *multiperiod* in that each operating period OP, of arbitrary duration, is assumed to be partitioned into finitely many successive sub-periods; and the negotiation process for OP results in the joint determination of retail prices and customer real and reactive power usage levels for each of these sub-periods.

The retail prices for price-sensitive demands that result from the negotiation process between the DSO and the customers have an informative structural form. Each of these prices is the summation of an initial price set by the DSO together with customer-specific price deviations entailed by the need (if any) to ensure that network reliability constraints are met.

The remainder of this study is organized as follows. The relation of this study to previous TES design work is discussed in Section 2.2. The key features of the consensus-based TES design are described in Section 2.3.

An illustration of the consensus-based TES design is formulated analytically in Sections 2.4 through 2.7 for the special case of an unbalanced radial distribution network populated by households. A dual decomposition algorithm implementing the negotiation process for this TES design is developed in Section 2.8, and sufficient conditions are established analytically for its convergence to a TES equilibrium ensuring the alignment of DSO and household goals and constraints.

A case study is presented in Section 2.9 to demonstrate the capabilities of the consensus-based TES design. The case study models a DSO-managed unbalanced 123-bus radial distribution network connected to a relatively large transmission network at a single point of connection. The distribution network is populated by household customers with a mixture of thermostatically-controlled load (TCL) and non-TCL, where only TCL is sensitive to price.

Concluding comments are given in Section 2.10. A nomenclature table, plus important technical details regarding unbalanced distribution network modeling, dual decomposition, and proposition proofs, are provided in [15].

processes is referred to as *mechanism design* in the economics literature; see [18, 19].

[2] The qualifier *independent* means that the DSO has no financial or ownership stake in the operations of the distribution network.

2.2 Relationship of Current Work to Existing Energy Management Work

As extensively surveyed in [20,21], current energy management strategies can roughly be classified into four categories: top-down switching, centralized optimization; price reaction; and TES design.

A *top-down switching method* for a group of electrical devices, implemented by a utility or other entity, is a method for simultaneously controlling the energy usage of these devices by means of signals that are commonly and simultaneously communicated to each device. Top-down switching methods are easy to implement. However, they cannot fully exploit the response potential of individual electrical devices based on differences in physical attributes and owner preferences.

In contrast, *centralized optimization* [22, 23] for an electrical system is the centrally-managed formulation and solution of system-wide optimizations during successive operating periods. The main advantage of centralized optimization is that the manager has more certain control over system outcomes [24]. However, a major disadvantage is that effective centralized optimization can require the violation of customer privacy. Moreover, centralized optimization can entail large amounts of computation time, hindering scalability. For example, the computations required for centralized optimization become extremely challenging when distribution network power flow is explicitly considered; see [25].

A *price-reaction method* is an energy management method based on one-way communication that uses price signals communicated to customers to modify their energy usage patterns [26,27]. Price-reaction methods are simple to deploy. However, price-reaction methods can result in reliability problems due to the the difficulty of accurately predicting customer responses to price signals. In addition, price-reaction methods can result in divergent price and quantity outcomes over time [28], a well-known issue referred to in the economics literature as “cobweb dynamics.”

A *TES design* is an energy management strategy that uses market mechanisms to ensure the continual balancing of power demands and supplies across an entire electrical infrastructure based on customer purchase and sale valuations [29–31]. For example, *peer-to-peer TES designs* [32] posit direct bilateral transactions among design participants with no central management. In contrast, *centrally-managed bid-based TES designs* posit the existence of a central manager that repeatedly communicates prices to power customers for successive operating periods based on bid functions received from these customers that express their updated power demands, power supplies, and/or ancillary service supplies; see, e.g., [3].

The potential advantages of TES design relative to the previous three energy management approaches include the ability to align distribution network goals and constraints with local customer goals and constraints in a tractable scalable manner while respecting customer privacy. These potential advantages have resulted in rapidly expanding TES research efforts and demonstration projects [33]- [39].

The study by Hu et al. [40] is closest to our study. The authors develop a DSO-managed multiperiod

TES design based on a negotiation process between the DSO and a collection of aggregators managing the charging schedule for electric vehicle (EV) owners. The DSO and aggregators exchange primal and dual variable information in order to determine a retail energy price sequence for EV charging from a single-phase distribution network, where the resulting EV charging schedule can contribute to the support of power balance for a day-ahead market operating over a transmission network connected to the distribution network. The DSO undertakes an optimization to ensure the charging schedule satisfies voltage and peak demand constraints for the distribution network.

Our study differs from Hu et al. [40] in four important regards. First, our proposed TES design is suitable for managing the operations of an *unbalanced* distribution network. Second, our proposed TES design ensures the satisfaction of distribution network constraints without requiring the DSO to solve an optimization problem.

Third, our TES design aligns DSO goals and constraints with customer goals and constraints, where customer goals are explicitly expressed in terms of customer net benefits, and customer constraints are explicitly expressed in terms of customer physical and financial considerations. In contrast, Hu et al. do not consider whether the EV charging schedule determined by their proposed negotiation process is in fact the best possible schedule for EV owners, measured in terms of the goals and constraints of these EV owners.

Fourth, the negotiation process postulated by our TES design for each operating period is based on a more intuitive, readily interpreted exchange of information than in Hu et al. [40]. At the beginning of this negotiation process the DSO is assumed to receive two types of structural information from each customer: namely, power factor rating information for the customer's price-sensitive demand; and a thermostat slider-knob control setting between 0 and 1 indicating the customer's preferred emphasis on power-usage benefit relative to power-usage cost. Given this information, the DSO iteratively communicates retail price-to-go sequences to customers who in turn indicate their power usage responses. This iterative process comes to a halt once the customers' power usage responses satisfy all distribution network constraints.

2.3 The General Consensus-Based TES Design

2.3.1 Design Overview

Retail customer participation in existing U.S. RTO/ISO-managed wholesale power markets is typically handled by some form of intermediary, such as a Qualified Scheduling Entity (QSE) or a Load-Serving Entity (LSE). However, FERC Order 2222 [1] promotes participation by a broader range of distributed resource aggregators.

This study develops a consensus-based TES design managed by a DSO within an integrated transmission and distribution system. This DSO operates as a linkage agent at a transmission grid bus b^* that connects an unbalanced radial distribution network to a relatively large transmission network. The DSO manages the power usage needs for a collection of customers located across the distribution network who have a mix of fixed and price-sensitive demands. The DSO is an independent entity with a fiduciary responsibility for ensuring the welfare of the customers, conditional on the maintenance of distribution network reliability.

Each operating day is partitioned into a finite number of operating periods OP. Prior to each OP, the DSO engages its customers in a negotiation process that results in retail prices for OP. The objective of this negotiation process is to permit customers to select power usage levels for OP that maximize their net benefit, subject to retail prices and local constraints, in a manner that ensures both the reliability of distribution network operations and customer privacy.

The power usage needs of the customers must be met by power procured from the transmission network.[3] The DSO manages this power procurement on behalf of the customers. All DSO net procurement costs are allocated back to customers on the basis of their relative power usage.

2.3.2 Design Timing Relative to Real-Time Market Processes

In advance of each operating period OP, the ISO/RTO conducts a real-time market (RTM) consisting of a security-constrained economic dispatch (SCED) optimization. Hereafter this RTM will be denoted by RTM(OP).

Figure 2.1 depicts the timing of the consensus-based TES design outlined in Section 2.3.1 in relation to RTM(OP). The look-ahead horizon for RTM(OP), denoted by LAH(OP), is the time interval between the close of RTM(OP) and the start of OP. Each operating period OP is assumed to be partitioned into NK sub-periods t. The negotiation process N(OP) between the DSO and its customers to determine retail prices for each sub-period t of OP takes place during LAH(OP).

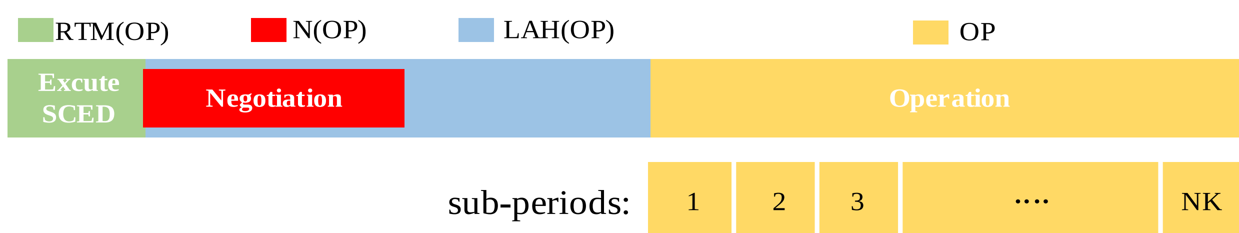

Figure 2.1: Timing of the consensus-based TES design in relation to a standard real-time market RTM(OP) for an operating period OP.

2.3.3 Design Negotiation Process: General Outline

The negotiation process N(OP) for each operating period OP consists of three basic components:

C1. Initialization: At the start of N(OP), the DSO receives from each customer ψ a power-factor

[3] As noted in Sec. 2.1, distributed generation is not considered in this study.

function f_ψ for price-sensitive demand permitting reactive power usage to be determined from real power usage. In addition, the DSO receives from ψ a thermostat slider-knob control setting γ_ψ between 0 ("Benefit") and 1 ("Cost") whose closeness to 0 indicates the degree to which ψ prefers to emphasize the benefit of power usage relative to its cost.[4] The DSO then sets retail prices for all fixed loads during each sub-period t of OP, as well as *initial* retail prices for all price-sensitive demands during each sub-period t of OP, and communicates these prices to its customers.

C2. Adjustment: Upon receipt of prices from the DSO, each customer ψ communicates back to the DSO its optimal price-sensitive real power usage level for each sub-period t of OP. The DSO then determines whether estimated customer real and reactive power usage levels for OP would result in any violation of network reliability constraints. If so, and if the DSO's stopping rule has not been activated, the DSO determines adjusted prices for price-sensitive demands during each sub-period t of OP and communicates these adjusted prices back to its customers to initiate another negotiation round. Otherwise, the DSO terminates the negotiation process.

C3. Stopping Rule: If the negotiation process has not terminated by a designated time prior to the end of LAH(OP), the DSO invokes a standardized procedure to set final prices for customer price-sensitive demands that ensure the reliability of distribution network operations.

2.3.4 Design Negotiation Process: Implementation Details

In greater detail, the implementation of our TES design negotiation process N(OP) for any given operating period OP proceeds as follows:

- At the start of RTM(OP), the ISO/RTO submits a forecast to RTM(OP) for load during OP, including distribution network load at the linkage bus b^*. The ISO/RTO then conducts a SCED optimization for RTM(OP), which determines the locational marginal price LMP(b^*, OP) (cents/kWh) at bus b^* for OP.

- At the close of RTM(OP), i.e., the start of LAH(OP), the ISO/RTO communicates LMP(b^*, OP) to the DSO. The DSO also receives from each customer ψ a power-factor function f_ψ for price-sensitive demand and a slider-knob control setting γ_ψ.

- At the start of N(OP) during LAH(OP), the DSO communicates to each of its customers that LMP(b^*, OP) will be the price it charges for all fixed load during each sub-period t of OP.

- The DSO then conducts a multi-round negotiation with each customer ψ to determine a retail price $\pi_\psi(t)$ for the price-sensitive demand of customer ψ during each sub-period t of OP, $t = 1, \ldots, NK$.

[4] See [15, App. D] for a more detailed constructive definition of γ_ψ.

- At the start of this multi-round negotiation process, the DSO communicates to each customer ψ an *initial retail price-to-go sequence* $\pi^o_\psi(\mathcal{K})$ for price-sensitive demand during OP taking the row-vector form $\pi^o_\psi(\mathcal{K}) = [\pi^o_\psi(1), ..., \pi^o_\psi(NK)]$, where: (i) $\mathcal{K} = (1, \ldots, NK)$ is a partition of OP into sub-periods t; and (ii) $\pi^o_\psi(t)$ = LMP(b^*, OP) for each sub-period t.

- Each customer ψ then communicates back to the DSO its optimal price-sensitive real power usage sequence for OP, conditional on its own local constraints plus the initial retail price-to-go sequence $\pi^o_\psi(\mathcal{K})$ received from the DSO. This permits the DSO to estimate total customer real and reactive power usage sequences for OP.

- The DSO continues to conduct successive negotiation rounds until either its estimated power usage sequences for OP satisfy all network constraints or its stopping rule is activated.

- At the termination of the multi-round negotiation process, each customer ψ implements its optimal real and reactive power usage sequences for OP, conditional on its final received retail price-to-go sequence and its own local constraints.

Important Remark on N(OP) Retail Price Initialization:

In the seven existing U.S. RTO/ISO-managed wholesale power markets, RTM LMPs are measured in $/MWh. Moreover, the prices charged to QSE/LSE intermediaries for the wholesale power usage of their managed customers are typically based on temporal and/or spatial *averages* of RTM LMP realizations in order to mitigate customer exposure to price volatility.

The presumption in this study that the DSO sets initial retail prices for N(OP) equal to RTM LMPs measured in cents/kWh is made purely for ease of exposition. These initial retail prices could instead be set as averages of RTM LMPs measured in $/MWh, in conformity with current practices. This change would not have any substantive effect on reported results.

2.4 TES Design Illustration: Overview

This section illustrates our proposed DSO-managed consensus-based TES design for the special case of an unbalanced radial distribution network populated by households. More precisely, the distribution network consists of a collection of buses connected by multi-phase line segments; and each household is connected to a particular bus by an external 1-phase line; see Fig. 2.2.

The goal of each household ψ is to maximize its own net benefit, subject to retail prices and local constraints. Every household owns a mixture of TCL and non-TCL devices. Each non-TCL device is a fixed-load device, meaning its load is not sensitive to charged prices. In contrast, each TCL device is a smartly controlled device with price-sensitive power usage.

Two important restrictions are imposed on household loads for the TES design illustration. First, in the absence of all household TCL, household non-TCL satisfies all network reliability constraints.

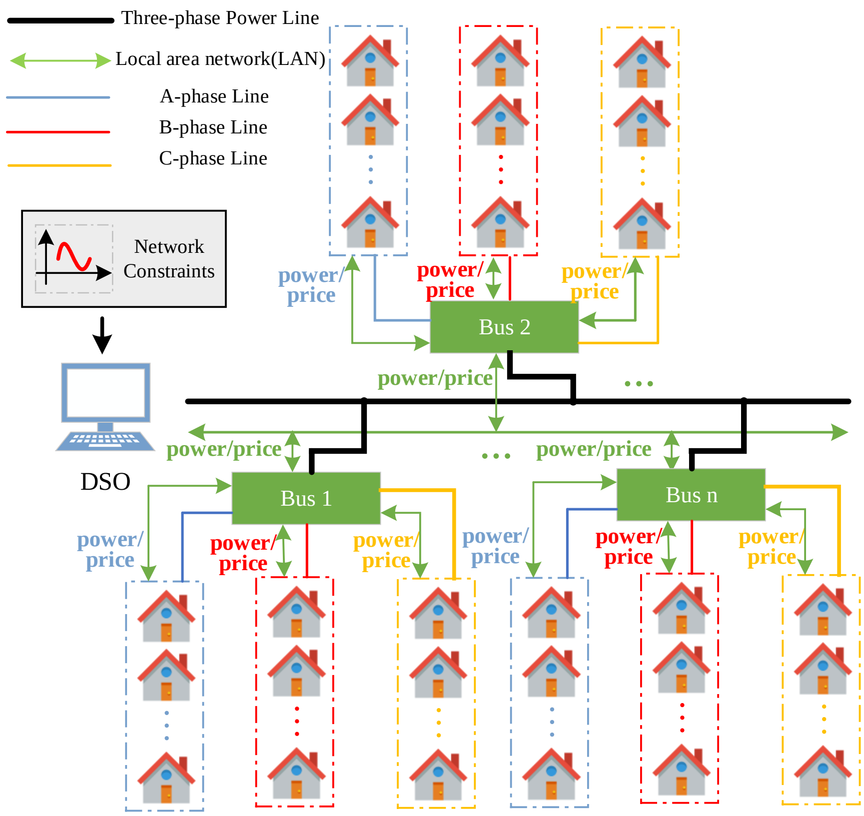

Figure 2.2: General features of the household TES design illustration.

Second, the price-sensitive TCL of each household reduces to zero at a finite sufficiently-high TCL price; and these sufficiently-high TCL prices are known to the DSO based on historical experience.

Household load for each operating period OP must be serviced by power obtained from a transmission network connected to the distribution network at a linkage bus b^*. ISO-forecasted power deliveries to households during OP are pre-scheduled in RTM(OP), an ISO-managed RTM operating over the transmission network. The rules governing the operations of RTM(OP) are based on the rules governing RTM operations in the U.S. ERCOT energy region [4, 41].

Household power usage for each operating period OP is managed by means of the DSO-managed consensus-based TES design outlined in Section 2.3. The DSO tasked with managing this TES design conducts a negotiation process N(OP) with households during the look-ahead horizon LAH(OP) for RTM(OP). As depicted in Fig.2.3, this negotiation process N(OP) consists of the following three components:

C1. Initialization: The DSO receives from each household ψ a power-factor function f_ψ for price-sensitive demand and a slider-knob control setting γ_ψ. The DSO sets the non-TCL retail price for all households during OP equal to LMP(b^*, OP), the LMP determined in RTM(OP) for the linkage bus b^*. The DSO also initially sets the TCL retail price for all households during OP equal to LMP(b^*,OP). The DSO then ensures these non-TCL and TCL retail prices are signaled to the households. Finally, the DSO sets a maximum permitted number I_{max} of iterations for N(OP) that ensures N(OP) will come to a close prior to the end of LAH(OP).

C2. Adjustment: Each household adjusts its real TCL power usage for OP to maximize its net benefit, conditional on local constraints and its latest received TCL price-to-go sequence for OP. The resulting household real TCL power usage schedules are communicated to the DSO, which permits the DSO to estimate total real and reactive power schedules for OP. If these schedules result in violations of network reliability constraints, the DSO updates the household TCL price-to-go sequences and communicates these updated sequences back to the households.

C3. Stopping Rule: The negotiation process continues until either there are no network reliability constraint violations or the number of iterations reaches I_{max}, whichever comes first. If violations remain after I_{max} is reached, the DSO sets final household TCL prices for OP to levels that are sufficiently high to reduce household TCL to zero.

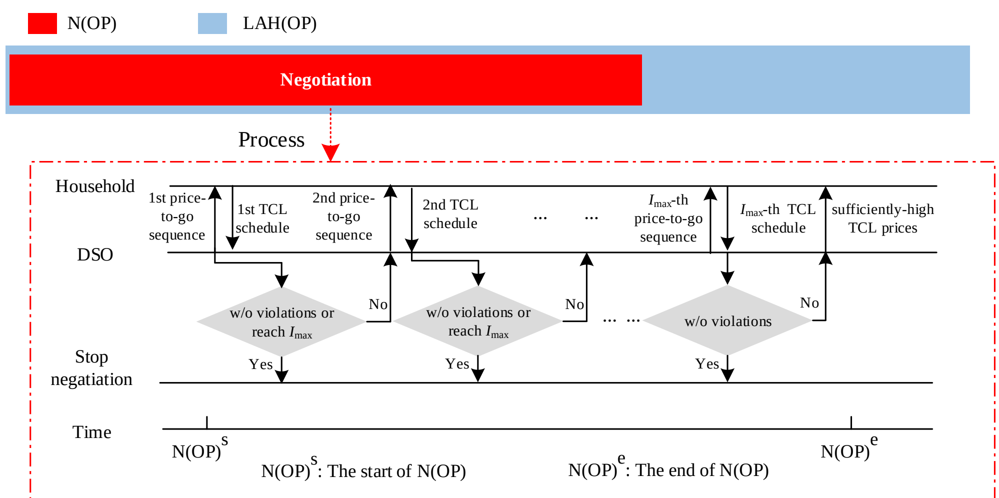

Figure 2.3: Negotiation Process N(OP) for the household TES design illustration.

2.5 TES Design Illustration: Network Model

2.5.1 Radial network model for a distribution system

Consider a radial network with N+1 buses. Let $\{0\}\bigcup\mathcal{N}$ denote the index set for these buses, where $\mathcal{N} = \{1,2,...,N\}$. As shown in Fig. 2.4, bus 0 is the head bus of the radial network. In addition, bus 0 is the *linkage bus* b^* at which the distribution network connects to the transmission network.

By definition of a radial network, each bus located on a radial network can have at most one bus that is an immediate predecessor, measured relative to the feeder head. For each bus $j \in \mathcal{N}$, let $BP(j) \in \{0\}\bigcup\mathcal{N}$ denote the bus that immediately precedes bus j along the radial network headed

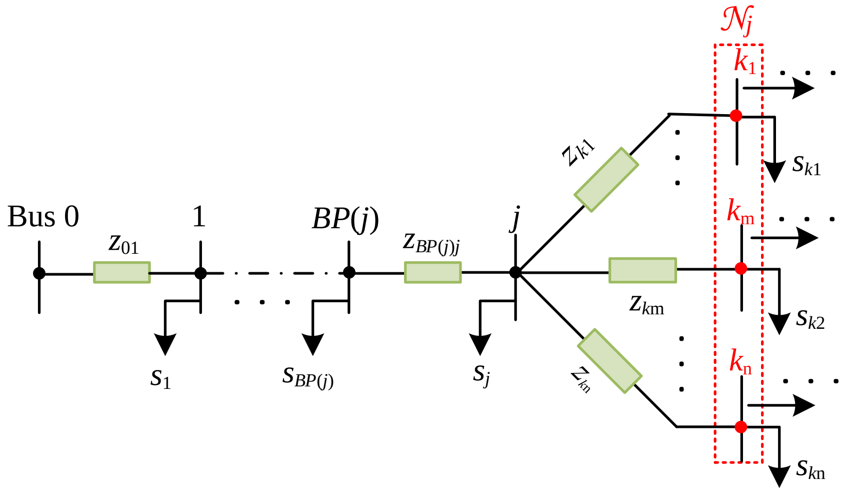

Figure 2.4: The radial network for the household TES design illustration from the vantage point of bus j.

by bus 0. Thus, as seen in Fig. 2.4, the distance between bus $BP(j)$ and bus 0 is strictly smaller than the distance between bus j and bus 0.

Also, let $\mathcal{N}_j$ denote the set of all buses located strictly after bus j along the radial network. For example, in Fig. 2.4, the depicted buses $k_1, k_2, \ldots, k_n$ comprise all buses that strictly follow bus j. Thus, $\mathcal{N}_j = \{k_1, k_2, \ldots, k_n\}$ for this case.

Finally, the edge set for any radial network with $N+1$ buses consists of N distinct *line segments* connecting pairs of adjacent buses along the radial network. More precisely, this edge set is given by $\mathcal{L} = \{\ell_j = (i, j) | i = BP(j), j \in \mathcal{N}\}$, i.e., the collection of all line segments connecting bus $BP(j)$ to bus j for each $j \in \mathcal{N}$. For an unbalanced radial network, each line segment can consist of single-phase, two-phase, or three-phase circuits. Hereafter, such line segments are simply referred to as 1-phase, 2-phase, and 3-phase line segments, respectively.

2.5.2 Single-phase radial network

Consider a radial network consisting of 1-phase line segments with a common phase. For each bus $i \in \{0\} \bigcup \mathcal{N}$, let $V_i(t)$ denote its voltage magnitude, let $v_i(t) = |V_i(t)|^2$ denote its squared voltage magnitude, and let $p_i(t)$ and $q_i(t)$ denote its active and reactive bus load, all measured per unit (p.u.). Also, for each line segment $(i, j) \in \mathcal{L}$, let $z_{ij} = r_{ij} + jx_{ij}$ denote its line impedance, and let $P_{ij}(t)$ and $Q_{ij}(t)$ denote the real and reactive power flow from bus i to j, respectively, all measured per unit (p.u.).

The following *Linearized Distribution Flow (LinDistFlow)* equations,[5] adapted from [42] and [43],

[5] The derivation of the LinDisFlow power flow equations assumes that the power loss on each radial network line

model the single-phase radial network power flow. For all $(i,j) \in \mathcal{L}$,

$$P_{ij}(t) = \sum_{k \in \mathcal{N}_j} P_{jk}(t) + p_j(t) \tag{2.1a}$$

$$Q_{ij}(t) = \sum_{k \in \mathcal{N}_j} Q_{jk}(t) + q_j(t) \tag{2.1b}$$

$$v_i(t) = v_j(t) + 2 \cdot \left(P_{ij}(t) r_{ij} + Q_{ij}(t) x_{ij}\right) \tag{2.1c}$$

2.5.3 Extension to an unbalanced radial network

Section 2.5.2 focuses on the case of a single-phase radial distribution network. However, distribution networks are typically unbalanced as well as radial, with multi-phase line segments. The common form of a 3-phase line segment for a radial distribution network is shown in Fig.2.5.

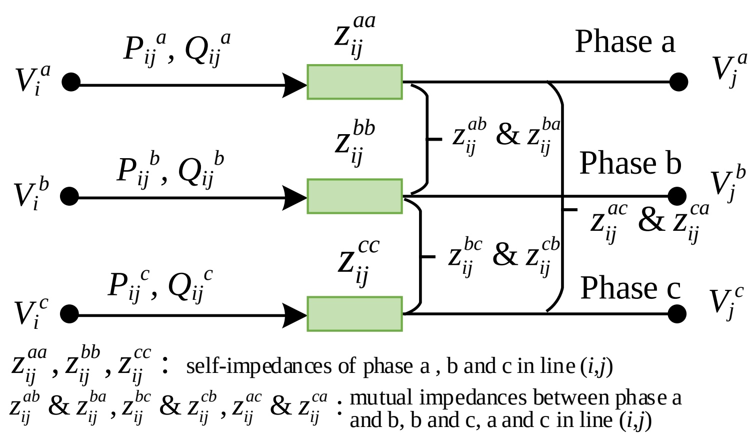

Figure 2.5: Depiction of a 3-phase line segment in a radial network.

Thus, making use of previous work [25], [44], [45], this section extends the LinDistFlow power flow equations (2.1a)-(2.1c) to handle the case of an unbalanced radial distribution network. More precisely, as will be seen below, this extended model assumes: (i) unbalanced phases $\{a,b,c\}$ for which the successive phase differences are given by $\frac{2}{3}\pi$; and (ii) voltage magnitudes across phases are approximately the same. This results in approximately balanced 3-phase voltages. Without loss of generality,[6] each line segment in the network edge set $\mathcal{L}$ is assumed to be a 3-phase line segment.

The following column vectors and matrices are used to depict squared 3-phase voltage magnitudes, bus active and reactive loads, real and reactive power flows over line segments, and line segment

segment is negligible relative to the power flow on this line segment.

[6] As discussed and illustrated in [15, App. B] , any k-phase line segment in the network edge set $\mathcal{L}$ with $k < 3$ can be represented as a 3-phase line segment by introducing an appropriate number of additional "virtual" circuits for this line segment with "virtual" phases whose self-impedance and mutual impedance are set to zero. The introduction of these virtual elements does not affect the resulting power flow solutions.

impedance values for this unbalanced radial network, all measured per unit (p.u.): For $(i,j) \in \mathcal{L}$,

$$
\begin{aligned}
\boldsymbol{v}_i(t) &= [v_i^a(t), v_i^b(t), v_i^c(t)]^T \\
\boldsymbol{p}_i(t) &= [p_i^a(t), p_i^b(t), p_i^c(t)]^T \\
\boldsymbol{q}_i(t) &= [q_i^a(t), q_i^b(t), q_i^c(t)]^T \\
\boldsymbol{P}_{ij}(t) &= [P_{ij}^a(t), P_{ij}^b(t), P_{ij}^c(t)]^T \\
\boldsymbol{Q}_{ij}(t) &= [Q_{ij}^a(t), Q_{ij}^b(t), Q_{ij}^c(t)]^T \\
\boldsymbol{Z}_{ij} = \boldsymbol{R}_{ij} + j\boldsymbol{X}_{ij} &= \begin{bmatrix} z_{ij}^{aa} & z_{ij}^{ab} & z_{ij}^{ac} \\ z_{ij}^{ba} & z_{ij}^{bb} & z_{ij}^{bc} \\ z_{ij}^{ca} & z_{ij}^{cb} & z_{ij}^{cc} \end{bmatrix}
\end{aligned}
$$

where $\boldsymbol{Z}_{ij} \in \mathbb{C}^{3\times 3}$ is a symmetric matrix.

Using this notation, the extended LinDistFlow model equations can be expressed as follows. For all $(i,j) \in \mathcal{L}$,

$$\boldsymbol{P}_{ij}(t) = \sum_{k \in \mathcal{N}_j} \boldsymbol{P}_{jk}(t) + \boldsymbol{p}_j(t) \tag{2.2a}$$

$$\boldsymbol{Q}_{ij}(t) = \sum_{k \in \mathcal{N}_j} \boldsymbol{Q}_{jk}(t) + \boldsymbol{q}_j(t) \tag{2.2b}$$

$$\boldsymbol{v}_i(t) = \boldsymbol{v}_j(t) + 2(\bar{\boldsymbol{R}}_{ij}\boldsymbol{P}_{ij}(t) + \bar{\boldsymbol{X}}_{ij}\boldsymbol{Q}_{ij}(t)) \tag{2.2c}$$

where

$$
\begin{aligned}
\boldsymbol{a} &= [1, e^{-\mathrm{j}2\pi/3}, e^{\mathrm{j}2\pi/3}]^T \\
\bar{\boldsymbol{R}}_{ij} &= Re(\boldsymbol{a}\boldsymbol{a}^H) \odot \boldsymbol{R}_{ij} + Im(\boldsymbol{a}\boldsymbol{a}^H) \odot \boldsymbol{X}_{ij} \\
\bar{\boldsymbol{X}}_{ij} &= Re(\boldsymbol{a}\boldsymbol{a}^H) \odot \boldsymbol{X}_{ij} - Im(\boldsymbol{a}\boldsymbol{a}^H) \odot \boldsymbol{R}_{ij}
\end{aligned}
$$

$\odot$ denotes element-wise multiplication

$\boldsymbol{a}^H$ denotes the conjugate transpose of $\boldsymbol{a}$

2.5.4 Representation of Unbalanced Radial Networks

Consider, first, the standard matrix representation $\bar{\boldsymbol{M}} = [\boldsymbol{m}_0, \boldsymbol{M}^T]^T \in \mathbb{R}^{(N+1)\times N}$ for the incidence matrix of a single-phase radial network. The rows of this matrix correspond to the buses i in the bus set $\{0\} \bigcup \mathcal{N}$, ordered from lowest to highest i value. The columns of this matrix correspond to the line segments ℓ_j in the edge-set $\mathcal{L}$, ordered from lowest to highest j value. The entries of the matrix indicate, for each bus and line segment, whether or not the bus is a "from" node or a "to" node for this line segment.

More precisely, the incidence matrix $\bar{\boldsymbol{M}}$ with an entry 1 for each "from" node and -1 for each "to" node takes the following form:

$$\bar{\boldsymbol{M}} = \begin{bmatrix} \mathbb{J}(0,\ell_1) & \mathbb{J}(0,\ell_2) & \dots & \mathbb{J}(0,\ell_N) \\ \mathbb{J}(1,\ell_1) & \mathbb{J}(1,\ell_2) & \dots & \mathbb{J}(1,\ell_N) \\ \vdots & \vdots & \ddots & \vdots \\ \mathbb{J}(N,\ell_1) & \mathbb{J}(N,\ell_2) & \dots & \mathbb{J}(N,\ell_N) \end{bmatrix} \tag{2.4}$$

where $\mathbb{J}(\cdot)$ is an indicator function defined as

$$\mathbb{J}(i,\ell_j) = \begin{cases} 1 & \text{if } i = BP(j) \\ -1 & \text{if } i = j \\ 0 & \text{otherwise} \end{cases}$$

The first row $\boldsymbol{m}_0^T$ of the matrix $\bar{\boldsymbol{M}}$ represents the connection structure between bus 0 and the line segments in $\mathcal{L}$; the remaining submatrix, denoted by $\boldsymbol{M}$, represents the connection structure between the remaining buses and the line segments in $\mathcal{L}$. Since $\boldsymbol{M}$ is a square matrix with full rank [46], it is an invertible matrix. A numerical example illustrating the construction of $\bar{\boldsymbol{M}}$ for a single-phase radial network is given in [15, App. C].

Next consider, instead, an unbalanced radial network with a bus set $\{0\}\bigcup\mathcal{N}$ and edge set $\mathcal{L}$ for which each line segment $\ell_j \in \mathcal{L}$ is a 3-phase line.[7] An extended incidence matrix $\bar{\boldsymbol{A}} = [\boldsymbol{A}_0, \boldsymbol{A}^T]^T \in \mathbb{R}^{3(N+1)\times 3N}$ for this unbalanced radial network is constructed as follows:

$$\bar{\boldsymbol{A}} = \bar{\boldsymbol{M}} \otimes \boldsymbol{I}_3 = \begin{bmatrix} \mathbb{J}(0,\ell_1)\boldsymbol{I}_3 & \mathbb{J}(0,\ell_2)\boldsymbol{I}_3 & \dots & \mathbb{J}(0,\ell_N)\boldsymbol{I}_3 \\ \mathbb{J}(1,\ell_1)\boldsymbol{I}_3 & \mathbb{J}(1,\ell_2)\boldsymbol{I}_3 & \dots & \mathbb{J}(1,\ell_N)\boldsymbol{I}_3 \\ \vdots & \vdots & \ddots & \vdots \\ \mathbb{J}(N,\ell_1)\boldsymbol{I}_3 & \mathbb{J}(N,\ell_2)\boldsymbol{I}_3 & \dots & \mathbb{J}(N,\ell_N)\boldsymbol{I}_3 \end{bmatrix} \tag{2.5}$$

where

$$\begin{aligned} \boldsymbol{I}_3 &= 3\times 3 \text{ identity matrix;} \\ \otimes &= \text{Kronecker product operation.} \end{aligned}$$

In (2.5), the term $\mathbb{J}(i,\ell_j)\boldsymbol{I}_3 \in \mathbb{R}^{3\times 3}$ represents the 3-phase connection structure between bus i and line segment ℓ_j. The submatrix $\boldsymbol{A}_0^T \in \mathbb{R}^{3\times 3N}$ represents the 3-phase connection structure between the feeder head bus 0 and each of the line segments in $\mathcal{L}$. Finally, the submatrix $\boldsymbol{A} \in \mathbb{R}^{3N\times 3N}$

[7] As previously noted in footnote 6, for the purposes of the current study any unbalanced radial network whose edges consist of a mix of 1-phase, 2-phase, and 3-phase line segments can equivalently be represented as an unbalanced radial network consisting entirely of 3-phase line segments.

represents the 3-phase connection structure between each remaining bus i and the line segments in $\mathcal{L}$. A numerical example illustrating the construction of $\bar{\boldsymbol{A}}$ for an unbalanced radial network is given in [15, App. C] .

The squared voltage magnitudes, real and reactive loads, and real and reactive power flows over line segments for the unbalanced radial distribution network are compactly denoted by the following column vectors:[8]

$$\begin{aligned}
\boldsymbol{v}(t) &= [\boldsymbol{v}_1(t)^T, \boldsymbol{v}_2(t)^T, ..., \boldsymbol{v}_N(t)^T]^T \\
\boldsymbol{p}(t) &= [\boldsymbol{p}_1(t)^T, \boldsymbol{p}_2(t)^T, ..., \boldsymbol{p}_N(t)^T]^T \\
\boldsymbol{q}(t) &= [\boldsymbol{q}_1(t)^T, \boldsymbol{q}_2(t)^T, ..., \boldsymbol{q}_N(t)^T]^T \\
\boldsymbol{P}(t) &= [\boldsymbol{P}_{BP(1)1}(t)^T, ..., \boldsymbol{P}_{BP(N)N}(t)^T]^T \\
\boldsymbol{Q}(t) &= [\boldsymbol{Q}_{BP(1)1}(t)^T, ..., \boldsymbol{Q}_{BP(N)N}(t)^T]^T
\end{aligned}$$

Resistances and reactances for the line segments in the edge-set $\mathcal{L}$ are compactly denoted by $3N \times 3N$ block diagonal matrices $\boldsymbol{D}_r$ and $\boldsymbol{D}_x$ such that the main-diagonal blocks are 3×3 square matrices and all off-diagonal blocks are zero matrices:

$$\begin{aligned}
\boldsymbol{D}_r &= \text{diag}(\bar{\boldsymbol{R}}_{BP(1)1}, ..., \bar{\boldsymbol{R}}_{BP(N)N}) \\
\boldsymbol{D}_x &= \text{diag}(\bar{\boldsymbol{X}}_{BP(1)1}, ..., \bar{\boldsymbol{X}}_{BP(N)N})
\end{aligned}$$

The j-th main-diagonal blocks of $\boldsymbol{D}_r$ and $\boldsymbol{D}_r$ are $\bar{\boldsymbol{R}}_{BP(j)j}$ and $\bar{\boldsymbol{X}}_{BP(j)j}$ corresponding to a particular line segment $\ell_j \in \mathcal{L}$. The squared voltage magnitudes for bus 0 in the unbalanced radial distribution network are represented by $\boldsymbol{v}_0 = [v_0^a, v_0^b, v_0^c]^T$.

Given these notational conventions, the LinDistFlow equatons (2.2a)-(2.2c) for an unbalanced radial distribution network can be compactly expressed as follows:

$$\boldsymbol{A}\boldsymbol{P}(t) = -\boldsymbol{p}(t) \tag{2.6a}$$

$$\boldsymbol{A}\boldsymbol{Q}(t) = -\boldsymbol{q}(t) \tag{2.6b}$$

$$\begin{bmatrix}\boldsymbol{A}_0 \ \boldsymbol{A}^T\end{bmatrix} \begin{bmatrix}\boldsymbol{v}_0(t) \\ \boldsymbol{v}(t)\end{bmatrix} = 2\Big(\boldsymbol{D}_r\boldsymbol{P}(t) + \boldsymbol{D}_x\boldsymbol{Q}(t)\Big) \tag{2.6c}$$

Since the matrix $\boldsymbol{M}^T$ is invertible, the matrix $\boldsymbol{A}^T$ is also invertible. Substituting (2.6a) and (2.6b)

[8] The squared voltage magnitudes and the real and reactive loads at buses i are sorted in accordance with the ordering of these buses from small to large values of i. The real and reactive power flows over line segments ℓ_j are sorted in accordance with the ordering of these line segments from small to large values of j.

into (2.6c), it is seen that the LinDistFLow formulation (2.6) can equivalently be expressed as

$$\boldsymbol{v}(t) = -[\boldsymbol{A}^T]^{-1}\boldsymbol{A}_0\boldsymbol{v}_0(t) - 2\boldsymbol{R}_D\boldsymbol{p}(t) - 2\boldsymbol{X}_D\boldsymbol{q}(t) \quad (2.7a)$$

$$\boldsymbol{R}_D = [\boldsymbol{A}^T]^{-1}\boldsymbol{D}_r\boldsymbol{A}^{-1} \quad (2.7b)$$

$$\boldsymbol{X}_D = [\boldsymbol{A}^T]^{-1}\boldsymbol{D}_x\boldsymbol{A}^{-1} \quad (2.7c)$$

2.6 TES Design Illustration: Household Model

For ease of notation, let $\psi = (u, \phi, i)$ denote a household with structural and preference attributes u located on an external 1-phase line with phase $\phi \in \Phi = \{a, b, c\}$, where this 1-phase line is connected to the distribution network at bus $i \in \mathcal{N}$; see Fig. 2.2. Recall from Section 2.3.2 that the operating period OP is assumed to be partitioned into a sequence $\mathcal{K} = (1, \ldots, NK)$ of NK successive sub-periods t.

To determine the optimal TCL power usage sequence for OP at the start of the look-ahead horizon LAH(OP), each household ψ needs to update its forecast for inside air temperature $T_\psi(0)$ (^oF) at the start of OP as well as its forecast for ambient outside air temperature $T_o(t)$ (^oF) at the start of each sub-period $t \in \mathcal{K}$. In addition, each household ψ also needs to forecast its real and reactive non-TCL power usage levels $p_\psi^{\mathsf{non}}(t)$ and $q_\psi^{\mathsf{non}}(t)$ (p.u.) for each sub-period $t \in \mathcal{K}$. The sequences of real and reactive non-TCL power usage levels for a household ψ during OP are denoted by the following $NK \times 1$ column vectors:

$$\mathcal{P}_\psi^{\mathsf{non}}(\mathcal{K}) = [p_\psi^{\mathsf{non}}(1), ..., p_\psi^{\mathsf{non}}(NK)]^T$$
$$\mathcal{Q}_\psi^{\mathsf{non}}(\mathcal{K}) = [q_\psi^{\mathsf{non}}(1), ..., q_\psi^{\mathsf{non}}(NK)]^T$$

The goal of each household ψ at the beginning of operating period OP is to maximize its net benefit attained during OP. This net benefit is assumed to take the general form:

$$\text{NetBen}_\psi = \text{Comfort}_\psi - \mu_\psi[\text{Electricity Cost}]_\psi \quad (2.8)$$

In (2.8), Comfort$_\psi$ (utils) denotes the benefit (thermal comfort) attained by household ψ from TCL power usage during OP, and Electricity Cost (cents) denotes the cost incurred by household ψ for TCL power usage during OP.[9] Finally, the benefit/cost trade-off parameter μ_ψ (utils/cent) denotes household ψ's *marginal utility of money* for OP, roughly defined to be the loss of benefit (utils) experienced by ψ for each cent increase in its electricity cost.[10] Here it is assumed that μ_ψ takes

[9] Recall that the non-TCL power usage of each household ψ during each operating period OP is assumed to be fixed, i.e., not price sensitive. Consequently, the inclusion in (2.8) of the benefit and cost of non-TCL power usage would not affect the solution to household ψ's net benefit maximization problem. The benefit and cost of non-TCL power usage is therefore omitted for ease of exposition.

[10] In economics, marginal utility of money valuations for customers are formally expressed as the dual variable solutions for budget constraints in customer utility maximization problems.

the explicit form

$$\mu_\psi \;=\; \frac{\gamma_\psi}{1-\gamma_\psi} \times \frac{1 \text{ util}}{1 \text{ cent}} \tag{2.9}$$

where $\gamma_\psi \in (0,1)$ denotes the benefit/cost slider-knob control setting communicated to the DSO by household ψ at the start of the negotiation process N(OP).[11]

Let $p_\psi(t)$ (p.u.) and $q_\psi(t)$ (p.u.) denote household ψ's real and reactive TCL power usage levels during any sub-period $t \in \mathcal{K}$. Also, let the sequences of real and reactive TCL power usage levels for a household ψ during OP be denoted by the following $NK \times 1$ column vectors:

$$\mathcal{P}_\psi(\mathcal{K}) = [p_\psi(1), \ldots, p_\psi(NK)]^T$$
$$\mathcal{Q}_\psi(\mathcal{K}) = [q_\psi(1), \ldots, q_\psi(NK)]^T$$

The *discomfort* (utils) experienced by ψ during any sub-period $t \in \mathcal{K}$ is measured by the discrepancy between ψ's inside air temperature $T_\psi(p_\psi(t))$ (^oF) at the end of sub-period t and the *bliss temperature* TB_ψ (^oF) at which ψ attains maximum thermal comfort, multiplied by a conversion factor c_ψ $\left(\text{utils}/(^oF)^2\right)$. The *comfort* $u_\psi(p_\psi(t))$ (utils) attained by ψ during t is then measured as the deviation between ψ's maximum attainable comfort u_ψ^{max} (utils) and ψ's discomfort:

$$u_\psi(p_\psi(t),t) = u_\psi^{\mathsf{max}} - c_\psi\left[T_\psi(p_\psi(t),t) - TB_\psi\right]^2 \tag{2.10}$$

The total comfort (utils) attained by ψ during $\mathcal{K}$ is then given by

$$U_\psi(\mathcal{P}_\psi(\mathcal{K})) = \sum_{t\in\mathcal{K}} u_\psi(p_\psi(t),t) \tag{2.11}$$

As explained in Section 2.3, the prices (cents/kWh) charged to ψ for its real TCL power usage $\mathcal{P}_\psi(\mathcal{K})$ during $\mathcal{K}$ are given by the price sequence $\boldsymbol{\pi}_\psi(\mathcal{K})$ determined by the negotiation process N(OP) between ψ and the DSO conducted during LAH(OP). Finally, let Δt denote the length of each sub-period t measured in hourly units; and let S_{base} denote the base power (kW) used to convert real power levels (kW) into per unit (p.u.) power levels by simple division.

Using the above notational conventions, the optimization problem of a household ψ for operating period OP can be expressed as follows:

$$\max_{\mathcal{P}_\psi(\mathcal{K})} \left[U_\psi(\mathcal{P}_\psi(\mathcal{K})) - \mu_\psi \boldsymbol{\pi}_\psi(\mathcal{K})\mathcal{P}_\psi(\mathcal{K}) S_{\mathsf{base}} \Delta t\right] \tag{2.12}$$

[11] See [15, App. D] for a constructive definition of γ_ψ and discussion regarding the determination of μ_ψ from γ_ψ.

subject to:

$$\begin{aligned}
T_\psi(p_\psi(1),1) &= \alpha_\psi^H T_\psi(0) \pm \alpha_\psi^P p_\psi(1) S_{\mathsf{base}} \Delta t \\
&\quad + (1-\alpha_\psi^H) T_o(1) \,; && \text{(2.13a)} \\
T_\psi(p_\psi(t),t) &= \alpha_\psi^H T_\psi(p_\psi(t-1),t-1) \\
&\quad \pm \alpha_\psi^P p_\psi(t) S_{\mathsf{base}} \Delta t \\
&\quad + (1-\alpha_\psi^H) T_o(t), \ \ \forall t \in \mathcal{K} \backslash \{1\} \,; && \text{(2.13b)} \\
0 \ \le \ p_\psi(t) &\le \ p_\psi^{\mathsf{max}}, \ \ \forall t \in \mathcal{K} && \text{(2.13c)}
\end{aligned}$$

Constraints (2.13a)-(2.13b) make use of a discrete linearized thermal model, adapted from [47]-[49], to model the fluctuation in household ψ's inside air temperature $T_\psi(t)$ during the successive sub-periods $t \in \mathcal{K}$.[12] For simplicity of exposition, the exogenously given ambient outside air temperature $T_o(t)$ for each sub-period t is assumed to be the same for each household ψ. The parameters α_ψ^H (unit-free) and α_ψ^P (^oF/kWh) are assumed to be positively valued. Constraint (2.13c) imposes an upper limit p_ψ^{max} (p.u.) on household ψ's real TCL power usage, assumed to represent the rated real power (p.u.) for household ψ's TCL devices.

Clearly, an optimal solution $\mathcal{P}_\psi(\mathcal{K})$ for household ψ's optimization problem (2.12) depends on the negotiated price-to-go sequence $\boldsymbol{\pi}_\psi(\mathcal{K})$. Let

$$\mathcal{X}_\psi(\mathcal{K}) = \{\mathcal{P}_\psi(\mathcal{K}) \in \mathbb{R}^{NK} | \mathcal{P}_\psi(\mathcal{K}) \text{ satisfies (2.13)}\} \tag{2.14}$$

An optimal solution for (2.12), given $\boldsymbol{\pi}_\psi(\mathcal{K})$, can then be expressed as follows:

$$\begin{aligned}
\mathcal{P}_\psi(\boldsymbol{\pi}_\psi(\mathcal{K})) \ \in \ \underset{\mathcal{P}_\psi(\mathcal{K}) \in \mathcal{X}_\psi(\mathcal{K})}{\operatorname{argmax}} \Big[& U_\psi(\mathcal{P}_\psi(\mathcal{K})) \\
& - \mu_\psi \boldsymbol{\pi}_\psi(\mathcal{K}) \mathcal{P}_\psi(\mathcal{K}) S_{\mathsf{base}} \Delta t \Big]
\end{aligned} \tag{2.15}$$

The TCL devices owned by each household ψ are assumed to operate at a constant positive power factor $\mathrm{PF}_\psi(t)$ (unit free) for each $t \in \mathcal{K}$.[13] Given this assumption, the TCL power-factor function f_ψ for each household ψ can be expressed as a collection $\{f_{\psi,t} | t \in \mathcal{K}\}$ of *TCL power-ratio functions* $f_{\psi,t}$ taking the linear form

$$q \ = \ f_{\psi,t}(p) \ = \ \eta_\psi(t) p \ , \ \forall t \in \mathcal{K} \tag{2.16}$$

[12] Temperature fluctuation, given by the terms preceded by the symbol $\pm$ in (2.13a) and (2.13b), takes a '+' sign for heating and a '-' sign for cooling.

[13] Given a TCL real power level $p(\tau) > 0$ and a TCL reactive power level $q(\tau)$ at a time-point τ, the TCL power factor pf(τ) at τ is defined to be the ratio $p(\tau)/\sqrt{p(\tau)^2 + q(\tau)^2}$ in (0,1]. See [15, App. E] for further discussion of the assumption of a constant TCL power factor PF(t) for each sub-period t; i.e, pf(τ) = PF(t) at all time points $\tau \in t$.

where

$$\eta_{\psi}(t) \ = \ \sqrt{\frac{1}{[\mathrm{PF}_{\psi}(t)]^2} - 1} \tag{2.17}$$

Note, by construction, that the unit-free coefficient $\eta_{\psi}(t)$ defined by (2.17) is non-negatively valued. Finally, let $\boldsymbol{H}_{\psi}(\mathcal{K})$ denote the *TCL power-ratio matrix* for household ψ for operating period OP; this $NK \times NK$ matrix is defined as follows:

$$\boldsymbol{H}_{\psi}(\mathcal{K}) = \mathrm{diag}\big(\eta_{\psi}(1), \eta_{\psi}(2), ..., \eta_{\psi}(NK)\big) \tag{2.18}$$

2.7 TES Design Illustration: DSO Modeling

2.7.1 DSO Modeling: Overview

Consider an unbalanced radial distribution network populated by households, as modeled in Sections 2.5 and 2.6. The independent DSO that is tasked with managing a consensus-based TES design for this distribution network operates at the linkage bus b^*, which is assumed to be the head bus 0 of the radial network.

As depicted in Fig. 2.1, each operating period OP during an operating day D is proceeded in time by a real-time market RTM(OP) followed by a look-ahead horizon LAH(OP). The negotiation process N(OP) between the DSO and the distribution system households takes place during LAH(OP).

The general goal of the DSO is to maximize household net benefit during OP, subject to network reliability constraints and the maintenance of household privacy. Since the distribution network has no distributed generation, the real and reactive power usage of the households must be serviced by wholesale power that is delivered at b^* in stepped-down voltage form. The price charged to the DSO for wholesale power is assumed to be LMP(b^*, OP) (cents/kWh), the locational marginal price determined in RTM(OP) for OP at b^*.

2.7.2 DSO Optimization Problem in Centralized Form

Recall that each household $\psi \in \Psi$ is characterized by a vector $\psi = (u, \phi, i)$, where u denotes the households structural and physical attributes, and (ϕ, i) indicates the household is located on an external phase-ϕ line connected to the distribution network at bus i. Let $\mathcal{U}_{i,\phi}$ denote the set of all household attributes u such that (u, ϕ, i) denotes a household $\psi \in \Psi$. For each $i \in \mathcal{N}$ and $\phi \in \Phi$, let $p_i^{\phi}(t)$ and $q_i^{\phi}(t)$ denote the real and reactive load for phase ϕ at bus i during sub-period t:

$$p_i^{\phi}(t) = \sum_{u \in \mathcal{U}_{i,\phi}} [p_{\psi}(t) + p_{\psi}^{\mathsf{non}}(t)], \ \forall i \in \mathcal{N}, \ \forall \phi \in \Phi \tag{2.19a}$$

$$q_i^{\phi}(t) = \sum_{u \in \mathcal{U}_{i,\phi}} [q_{\psi}(t) + q_{\psi}^{\mathsf{non}}(t)], \ \forall i \in \mathcal{N}, \ \forall \phi \in \Phi \tag{2.19b}$$

Using the column vector expressions $\boldsymbol{p}_i(t)$, $\boldsymbol{q}_i(t)$, $\boldsymbol{p}(t)$, and $\boldsymbol{q}(t)$ given in Sections 2.5.3 and 2.5.4, together with (2.16) and (2.19), it is seen that the power flow equation (2.7a) can equivalently be expressed as follows for any sub-period $t \in \mathcal{K}$:

$$\boldsymbol{v}(t, \boldsymbol{p}_\Psi(t)) = \boldsymbol{v}^{\mathsf{non}}(t) - 2\boldsymbol{s}(t, \boldsymbol{p}_\Psi(t)) \tag{2.20}$$

where

$$\begin{aligned}
&\boldsymbol{p}_\Psi(t) = \{p_\psi(t) \mid \psi \in \Psi\} \\
&\boldsymbol{s}(t, \boldsymbol{p}_\Psi(t)) = \sum_{\psi \in \Psi} \left[\boldsymbol{h}_\psi(t, p_\psi(t))\right] \\
&\boldsymbol{h}_\psi(t, p_\psi(t)) = \boldsymbol{r}_D(i, N_\psi^{\mathsf{ph}}) p_\psi(t) + \boldsymbol{x}_D(i, N_\psi^{\mathsf{ph}}) \eta_\psi(t) p_\psi(t) \\
&N_\psi^{\mathsf{ph}} = \begin{cases} 1 & \text{if household } \psi \text{ connects to phase a} \\ 2 & \text{if household } \psi \text{ connects to phase b} \\ 3 & \text{if household } \psi \text{ connects to phase c} \end{cases} \\
&\boldsymbol{v}^{\mathsf{non}}(t) = -[\boldsymbol{A}^T]^{-1} \boldsymbol{A}_0 \boldsymbol{v}_0(t) - 2\boldsymbol{s}^{\mathsf{non}}(t) \\
&\boldsymbol{s}^{\mathsf{non}}(t) = \sum_{\psi \in \Psi} \left[\boldsymbol{r}_D(i, N_\psi^{\mathsf{ph}}) p_\psi^{\mathsf{non}}(t) + \boldsymbol{x}_D(i, N_\psi^{\mathsf{ph}}) q_\psi^{\mathsf{non}}(t)\right]
\end{aligned}$$

In (2.20), the $3N \times 1$ column vector $\boldsymbol{v}^{\mathsf{non}}(t)$ consists of the 3-phase squared voltage magnitudes for t at all non-head buses, assuming zero TCL; and the $3N \times 1$ column vector $\boldsymbol{v}_0(t)$ consists of the 3-phase squared voltage magnitudes for t at the head bus 0. Also, $\psi = (u, \phi, i)$ is the generic term for a household in the household set Ψ, and $\boldsymbol{r}_D(i, N_\psi^{\mathsf{ph}})$ and $\boldsymbol{x}_D(i, N_\psi^{\mathsf{ph}})$ are $3N \times 1$ column vectors; specifically, they are the $\{3(i-1) + N_\psi^{\mathsf{ph}}\}$-th columns of the $3N \times 3N$ matrices $\boldsymbol{R}_D$ and $\boldsymbol{X}_D$ defined as in (2.7b) and (2.7c).

Let the sequence of LMPs (cents/kWh) determined in RTM(OP) at the linkage bus b^* for the sub-periods $t \in \mathcal{K}$ comprising operating period OP be denoted by the $1 \times NK$ row vector $\mathbf{LMP}(\mathcal{K})$ = $[\text{LMP}(b^*, 1), ..., \text{LMP}(b^*, NK)]$. Also, let $\bar{P}$ (p.u.) denote an upper limit imposed on total demand during each sub-period $t \in \mathcal{K}$ for distribution network reliability, and let $\bar{\boldsymbol{P}}(\mathcal{K})$ denote the $NK \times 1$ column vector $[\bar{P}, \ldots, \bar{P}]^T$. In addition, let the $3N \times 1$ column vectors $\boldsymbol{v}_{\mathsf{min}}(t)$ and $\boldsymbol{v}_{\mathsf{max}}(t)$ denote lower and upper bounds (p.u.) imposed on the 3-phase squared voltage magnitudes during each sub-period $t \in \mathcal{K}$ for network reliability.

The *centralized DSO optimization problem* at the start of N(OP) is then expressed as follows:

$$\begin{aligned}
\max_{\mathcal{P}(\mathcal{K}) \in \mathcal{X}(\mathcal{K})} \sum_{\psi \in \Psi} \Big[& U_\psi(\mathcal{P}_\psi(\mathcal{K})) \\
& - \mu_\psi \mathbf{LMP}(\mathcal{K}) \mathcal{P}_\psi(\mathcal{K}) S_{\mathsf{base}} \Delta t \Big]
\end{aligned} \tag{2.21}$$

subject to the following demand and voltage network reliability constraints for each $t \in \mathcal{K}$:

$$\sum_{\psi \in \Psi} [p_{\psi}(t) + p_{\psi}^{\mathsf{non}}(t)] \leq \bar{P} \tag{2.22a}$$

$$\boldsymbol{v}_{\mathsf{min}}(t) \leq \boldsymbol{v}(t, \boldsymbol{p}_{\Psi}(t)) \leq \boldsymbol{v}_{\mathsf{max}}(t) \tag{2.22b}$$

where

$$\begin{aligned}
\mathcal{P}(\mathcal{K}) &= \{\mathcal{P}_{\psi}(\mathcal{K}) \mid \psi \in \Psi\} = \{\boldsymbol{p}_{\Psi}(t)) \mid t \in \mathcal{K}\} \\
\mathcal{X}(\mathcal{K}) &= \prod_{\psi \in \Psi} \mathcal{X}_{\psi}(\mathcal{K})
\end{aligned}$$

Finally, let the $(3N \cdot NK) \times 1$ column vectors $\boldsymbol{v}(\mathcal{P}(\mathcal{K}))$, $\boldsymbol{v}_{\mathsf{max}}(\mathcal{K})$, and $\boldsymbol{v}_{\mathsf{min}}(\mathcal{K})$ be defined as follows:

$$\begin{aligned}
\boldsymbol{v}(\mathcal{P}(\mathcal{K})) &= [\boldsymbol{v}(1, \boldsymbol{p}_{\Psi}(1))^T, \ldots, \boldsymbol{v}(NK, \boldsymbol{p}_{\Psi}(NK))^T]^T \\
\boldsymbol{v}_{\mathsf{max}}(\mathcal{K}) &= [\boldsymbol{v}_{\mathsf{max}}(1)^T, \ldots, \boldsymbol{v}_{\mathsf{max}}(NK)^T]^T \\
\boldsymbol{v}_{\mathsf{min}}(\mathcal{K}) &= [\boldsymbol{v}_{\mathsf{min}}(1)^T, \ldots, \boldsymbol{v}_{\mathsf{min}}(NK)^T]^T
\end{aligned}$$

Definition: Primal Problem. The centralized DSO optimization problem (2.21) can be expressed in a standard *nonlinear programming (NP)* form as follows:

$$\max_{\boldsymbol{x} \in \mathcal{X}} F(\boldsymbol{x}) \text{ subject to } \boldsymbol{g}(\boldsymbol{x}) \leq \boldsymbol{c} \tag{2.23}$$

where

$$\mathcal{X} = \mathcal{X}(\mathcal{K}) = \prod_{\psi \in \Psi} \mathcal{X}_{\psi}(\mathcal{K}) \subseteq \mathbb{R}^d$$

$$x_{\psi}(t) = p_{\psi}(t) \in \mathbb{R}$$

$$\boldsymbol{x}_{\psi} = \{x_{\psi}(t) \mid t \in \mathcal{K}\} = \mathcal{P}_{\psi}(\mathcal{K}) \in \mathbb{R}^{NK}$$

$$\boldsymbol{x} = \{\boldsymbol{x}_{\psi} \mid \psi \in \Psi\} = \mathcal{P}(\mathcal{K}) \in \mathbb{R}^d$$

$$F(\boldsymbol{x}) = \sum_{\psi \in \Psi} F_{\psi}(\boldsymbol{x}_{\psi})$$

$$F_{\psi}(\boldsymbol{x}_{\psi}) = \left[U_{\psi}(\boldsymbol{x}_{\psi}) - \mu_{\psi} \mathbf{LMP}(\mathcal{K}) \boldsymbol{x}_{\psi} \cdot S_{\mathsf{base}} \Delta t\right]$$

$$
\boldsymbol{g}(\boldsymbol{x}) = \begin{bmatrix} \sum_{\psi\in\Psi}[\boldsymbol{x}_{\psi} + \mathcal{P}^{\mathsf{non}}_{\psi}(\mathcal{K})] \\ \boldsymbol{v}(\boldsymbol{x}) \\ -\boldsymbol{v}(\boldsymbol{x}) \end{bmatrix}_{m\times 1}
$$

$$
\boldsymbol{c} = \begin{bmatrix} \bar{\boldsymbol{P}}(\mathcal{K}) \\ \boldsymbol{v}_{\mathsf{max}}(\mathcal{K}) \\ -\boldsymbol{v}_{\mathsf{min}}(\mathcal{K}) \end{bmatrix}_{m\times 1}
$$

and: NH = number of households ψ; NK = number of sub-periods $t \in \mathcal{K}$; $d = NK \cdot NH$; N = number of non-head buses; and $m = ([1+6N]\cdot NK)$. Hereafter, problem (2.23) will be referred to as the *Primal Problem*. Depending on the context, a *solution* for this Primal Problem will variously be denoted by $\boldsymbol{x}^* = \{\boldsymbol{x}^*_{\psi} \mid \psi \in \Psi\} = \{\mathcal{P}^*_{\psi}(\mathcal{K}) \mid \psi \in \Psi\} = \mathcal{P}^*(\mathcal{K})$.

A critical point to note for later purposes is that the Primal Problem (2.23) does not directly depend on the retail prices the DSO signals to the households under the consensus-based TES design. What is sought below is a way to connect the optimal solution for the Primal Problem to the decentralized household optimal solutions determined as functions of the DSO's retail price signals.

2.7.3 DSO Optimization Problem in Hierarchical Control Form

The centralized DSO optimization problem (2.21) for operating period OP incorporates the local constraints $\mathcal{X}_{\psi}(\mathcal{K})$ for each household ψ as well as the network reliability constraints (2.22). Thus, to solve problem (2.21), the DSO would need a great deal of information about each household, a violation of household privacy.

Consequently, the DSO cannot directly solve the centralized optimization problem. Rather, as seen in Fig.2.2, the DSO resorts to indirect control. The DSO iteratively sets the price-to-go sequence $\boldsymbol{\pi}_{\psi}(\mathcal{K})$ for each household ψ's real TCL power usage to ensure that the resulting household real and reactive power usage levels for OP are consistent with the DSO's network reliability constraints for OP. As discussed in Section 2.4, each household ψ is required to continually submit its optimal real TCL power usage schedule $\mathcal{P}_{\psi}(\boldsymbol{\pi}_{\psi}(\mathcal{K}))$ for each possible price-to-go sequence $\boldsymbol{\pi}_{\psi}(\mathcal{K})$ sent by the DSO during period N(OP) until the negotiation process halts.[14]

The next section develops a specific analytical formulation for this hierarchical control method for the household TES design illustration.

[14] Note that this negotiation process replaces the use of bid functions in bid-based TES designs; it provides an alternative way for households to communicate their price-sensitive power-usage preferences to the DSO.

2.8 TES Design Illustration: Solution Method

2.8.1 Solution Overview

This section replaces the centralized DSO optimization problem (2.21) with a specific formulation of the consensus-based TES design proposed in Section 2.3. Thus, a centralized design requiring the DSO to exert direct control over household TCL power usage is replaced with a hierarchical control in which the DSO uses price signals to modify household TCL power usage decisions. A dual decomposition algorithm is developed to implement the negotiation process for this TES design, and the convergence and optimality properties of this algorithm are established analytically.

2.8.2 TES Equilibrium

From the formulation (2.15) for each household ψ's optimization problem for an operating period OP, it is seen that ψ's choice of a TCL power-usage sequence for $\mathcal{K}$ depends on the price-to-go sequence $\boldsymbol{\pi}_{\psi}(\mathcal{K})$ for $\mathcal{K}$. The DSO can take advantage of this price dependence during N(OP) to ensure that household power usage does not violate any network reliability constraints.

Let $\boldsymbol{\pi}(\mathcal{K}) = \{\boldsymbol{\pi}_{\psi}(\mathcal{K}) \mid \psi \in \Psi\}$ denote a collection of price-to-go sequences communicated by the DSO to households during some iteration of the negotiation process N(OP). The real TCL power-usage sequences that households communicate back to the DSO in response to these communicated price-to-go sequences will then be denoted by $\mathcal{P}(\boldsymbol{\pi}(\mathcal{K})) = \{\mathcal{P}_{\psi}(\boldsymbol{\pi}_{\psi}(\mathcal{K})) \mid \psi \in \Psi\}$.

Definition: TES Equilibrium. Suppose an optimal solution $\boldsymbol{x}^* = \mathcal{P}^*(\mathcal{K})$ for the Primal Problem (2.23) equals $\mathcal{P}(\boldsymbol{\pi}^*(\mathcal{K}))$ for some collection $\boldsymbol{\pi}^*(\mathcal{K})$ of retail price-to-go sequences for an operating period OP. Then the pairing $(\mathcal{P}^*(\mathcal{K}), \boldsymbol{\pi}^*(\mathcal{K}))$ will be called a *TES equilibrium for OP*.

For each sub-period $t \in \mathcal{K}$, let $\lambda_{\bar{P}}(t)$ denote the non-negative dual variable (utils/p.u.) associated with the peak demand constraint (2.22a). Also, let the $1 \times 3N$ row vectors $\boldsymbol{\lambda}_{v_{\mathsf{max}}}(t)$ and $\boldsymbol{\lambda}_{v_{\mathsf{min}}}(t)$ denote the non-negative dual variables (utils/p.u.) associated with the upper and lower 3-phase voltage inequality constraints (2.22b). The $1 \times m$ row vector $\boldsymbol{\lambda}$ whose components consist of all of these non-negative dual variables is then denoted by

$$\boldsymbol{\lambda} = [\boldsymbol{\lambda}_{\bar{P}}(\mathcal{K}), \boldsymbol{\lambda}_{v_{\mathsf{max}}}(\mathcal{K}), \boldsymbol{\lambda}_{v_{\mathsf{max}}}(\mathcal{K})] \tag{2.24}$$

where the component row vectors for $\boldsymbol{\lambda}$ are given by

$$\begin{aligned} \boldsymbol{\lambda}_{\bar{P}}(\mathcal{K}) &= [\lambda_{\bar{P}}(1), \ldots, \lambda_{\bar{P}}(NK)]_{1 \times NK} \\ \boldsymbol{\lambda}_{v_{\mathsf{max}}}(\mathcal{K}) &= [\boldsymbol{\lambda}_{v_{\mathsf{max}}}(1), \ldots, \boldsymbol{\lambda}_{v_{\mathsf{max}}}(NK)]_{1 \times (3N \cdot NK)} \\ \boldsymbol{\lambda}_{v_{\mathsf{min}}}(\mathcal{K}) &= [\boldsymbol{\lambda}_{v_{\mathsf{min}}}(1), \ldots, \boldsymbol{\lambda}_{v_{\mathsf{min}}}(NK)]_{1 \times (3N \cdot NK)} \end{aligned}$$

Finally, for later purposes, the dual variables corresponding to the upper and lower 3-phase voltage inequality constraints (2.22b) are also expressed in the following matrix form:

$$\boldsymbol{\Lambda}_{v_{\mathsf{max}}}(\mathcal{K}) = \begin{bmatrix} \boldsymbol{\lambda}_{v_{\mathsf{max}}}(1) \\ \vdots \\ \boldsymbol{\lambda}_{v_{\mathsf{max}}}(NK) \end{bmatrix}_{NK\times 3N}$$

$$\boldsymbol{\Lambda}_{v_{\mathsf{min}}}(\mathcal{K}) = \begin{bmatrix} \boldsymbol{\lambda}_{v_{\mathsf{min}}}(1) \\ \vdots \\ \boldsymbol{\lambda}_{v_{\mathsf{min}}}(NK) \end{bmatrix}_{NK\times 3N}$$

The *Lagrangian Function L*: $\mathcal{X} \times \mathbb{R}^m_+ \to \mathbb{R}$ for the centralized DSO optimization problem (2.21), equivalently represented in the Primal Problem form (2.23), is then given by

$$L(\boldsymbol{x},\boldsymbol{\lambda}) = F(\boldsymbol{x}) + \boldsymbol{\lambda}[\boldsymbol{c} - \boldsymbol{g}(\boldsymbol{x})] \tag{2.25}$$

where

$$\boldsymbol{x} = \{\boldsymbol{x}_\psi \mid \psi \in \Psi\} = \mathcal{P}(\mathcal{K}) \tag{2.26}$$

Finally, for each $t \in \mathcal{K}$, let $\boldsymbol{x}_\Psi(t) = \{x_\psi(t) \mid \psi \in \Psi\}$ where, as previously defined in Section 2.7.3,

$$\{x_\psi(t) \mid \psi \in \Psi\} = \{p_\psi(t) \mid \psi \in \Psi\} = \boldsymbol{p}_\Psi(t) \tag{2.27}$$

Then the Lagrangian Function (2.25) can equivalently be expressed as follows:

$$\begin{aligned} L(\boldsymbol{x},\boldsymbol{\lambda}) = F(\boldsymbol{x}) & \\ + \boldsymbol{\lambda}_{\bar{\boldsymbol{P}}}(\mathcal{K})\big[\bar{\boldsymbol{P}}(\mathcal{K}) - \sum_{\psi\in\Psi}[\boldsymbol{x}_\psi + \mathcal{P}^{\mathsf{non}}_\psi(\mathcal{K})]\big] & \\ + \sum_{t\in\mathcal{K}} \big[\boldsymbol{\lambda}_{v_{\mathsf{max}}}(t)[\boldsymbol{v}_{\mathsf{max}}(t) - \boldsymbol{v}(t,\boldsymbol{x}_\Psi(t))]\big] & \\ + \sum_{t\in\mathcal{K}} \big[\boldsymbol{\lambda}_{v_{\mathsf{min}}}(t)[-\boldsymbol{v}_{\mathsf{min}}(t) + \boldsymbol{v}(t,\boldsymbol{x}_\Psi(t))]\big] & \end{aligned} \tag{2.28}$$

Definition: Saddle Point. A point $(\boldsymbol{x}^*,\boldsymbol{\lambda}^*)$ in $\mathcal{X} \times \mathbb{R}^m_+$ is said to be a *saddle point* for the Lagrangian Function $L(\boldsymbol{x},\boldsymbol{\lambda})$ defined in (2.25) if the following condition holds:

$$L(\boldsymbol{x},\boldsymbol{\lambda}^*) \le L(\boldsymbol{x}^*,\boldsymbol{\lambda}^*) \le L(\boldsymbol{x}^*,\boldsymbol{\lambda}) \tag{2.29}$$

for all $\boldsymbol{\lambda} \in \mathbb{R}^m_+$ and $x \in \mathcal{X}$.

Definition: Dual Problem. Let the *dual function D*:$\mathbb{M} \to \mathbb{R}$ for the Primal Problem (2.23) be defined as follows:

$$D(\boldsymbol{\lambda}) = \max_{\boldsymbol{x}\in\mathcal{X}} L(\boldsymbol{x},\boldsymbol{\lambda}) \tag{2.30}$$

where

$$\mathbb{M} = \{\boldsymbol{\lambda} \in \mathbb{R}^m_+ \mid D(\boldsymbol{\lambda}) \text{ is a well-defined finite value}\} \tag{2.31}$$

Then the *Dual Problem* associated with the Primal Problem (2.23) is defined to be

$$\min_{\boldsymbol{\lambda} \in \mathbb{M}} D(\boldsymbol{\lambda}) \tag{2.32}$$

Proposition 1 (Classical): *A point $(\boldsymbol{x}^*, \boldsymbol{\lambda}^*)$ in $\mathcal{X} \times \mathbb{R}^m_+$ is a saddle point (2.29) for the Lagrangian Function $L(\boldsymbol{x}, \boldsymbol{\lambda})$ defined in (2.25) if and only if:*

- **[P1.A]** $\boldsymbol{x}^*$ *is a solution for the Primal Problem (2.23) ;*
- **[P1.B]** $\boldsymbol{\lambda}^*$ *is a solution for the Dual Problem (2.32) ;*
- **[P1.C]** $D(\boldsymbol{\lambda}^*) = F(\boldsymbol{x}^*)$ *(strong duality).*

Proof of Proposition 1: See [15, App. G].

Proposition 2: *Suppose $(\boldsymbol{x}^*, \boldsymbol{\lambda}^*)$ in $\mathcal{X} \times \mathbb{R}^m_+$ is a saddle point for the Lagrangian Function $L(\boldsymbol{x}, \boldsymbol{\lambda})$ defined in (2.25), where $\boldsymbol{x}^* = \mathcal{P}^*(\mathcal{K})$. Suppose, also, that $\boldsymbol{x}^*$ uniquely maximizes $L(\boldsymbol{x}, \boldsymbol{\lambda}^*)$ with respect to $\boldsymbol{x} \in \mathcal{X}$. Define $\boldsymbol{\pi}^*(\mathcal{K}) = \{\boldsymbol{\pi}^*_\psi(\mathcal{K}) \mid \psi \in \Psi\}$, where the price-to-go sequence $\boldsymbol{\pi}^*_\psi(\mathcal{K})$ for each household $\psi \in \Psi$ takes the following form:*

$$\begin{aligned} \boldsymbol{\pi}^*_\psi(\mathcal{K}) \;=\; & \boldsymbol{LMP}(\mathcal{K}) + \frac{1}{\mu_\psi S_{\mathsf{base}} \Delta t} \Big[\boldsymbol{\lambda}^*_{\bar{P}}(\mathcal{K}) \\ & - 2 \cdot \boldsymbol{r}_D(i, N^{\mathsf{ph}}_\psi)^T \left[\boldsymbol{\Lambda}^*_{v_{\mathsf{max}}}(\mathcal{K}) - \boldsymbol{\Lambda}^*_{v_{\mathsf{min}}}(\mathcal{K}) \right]^T \\ & - 2 \cdot \boldsymbol{x}_D(i, N^{\mathsf{ph}}_\psi)^T \left[\boldsymbol{\Lambda}^*_{v_{\mathsf{max}}}(\mathcal{K}) - \boldsymbol{\Lambda}^*_{v_{\mathsf{min}}}(\mathcal{K}) \right]^T \boldsymbol{H}_\psi(\mathcal{K}) \Big] \end{aligned} \tag{2.33}$$

The pairing $(\mathcal{P}^*(\mathcal{K}), \boldsymbol{\pi}^*(\mathcal{K}))$ then constitutes a TES equilibrium for OP.

Proof of Proposition 2: See [15, App. G].

For later purposes, note that the price-to-go sequence (2.33) depends on the attributes of household $\psi = (u, \phi, i)$. Specifically, the right-hand side of (2.33) depends on $\psi's$ preference and physical attributes u: namely, ψ's marginal utility of money μ_ψ; and ψ's TCL power-ratio function (2.16) as characterized by the $NK \times NK$ TCL power-ratio matrix $\boldsymbol{H}_\psi(\mathcal{K})$ defined in (2.18). In addition, the right-hand side of (2.33) depends on ψ's phase and bus location attributes ϕ and i through the $1 \times 3N$ row vectors $\boldsymbol{r}_D(i, N^{\mathsf{ph}}_\psi)^T$ and $\boldsymbol{x}_D(i, N^{\mathsf{ph}}_\psi)^T$.

Note, also, that the price-to-go sequence (2.33) depends on the extent to which network reliability constraints would be violated by household power usage choices if retail prices for OP were simply set equal to the elements of the $1 \times NK$ price vector $\mathbf{LMP}(\mathcal{K})$, i.e., to the LMP values determined for OP by RTM(OP). As seen in (2.33), the extent to which deviations from $\mathbf{LMP}(\mathcal{K})$ are needed to avoid network reliability constraint violations depends on the non-negative magnitudes of the dual variables (2.24) associated with the peak demand and voltage magnitude constraints for the Primal Problem (2.23).

2.8.3 TES Equilibrium Solution Strategy

Algorithm DDA: Dual Decomposition Method for Approximate Determination of a TES Equilibrium

---

S1: Initialization. At the initial iteration time $y = 0$, the DSO specifies positive scalar step-sizes β_1, β_2, and β_3. In addition, the DSO sets initial dual variable values as follows: $\boldsymbol{\lambda}^y_{\bar{P}}(\mathcal{K}) = \mathbf{0}$, $\boldsymbol{\lambda}^y_{v_{\mathsf{max}}}(\mathcal{K}) = \mathbf{0}$, and $\boldsymbol{\lambda}^y_{v_{\mathsf{min}}}(\mathcal{K}) = \mathbf{0}$.

S2: Set price-to-go sequences. The DSO sets the price-to-go sequence $\boldsymbol{\pi}^y_{\psi}(\mathcal{K})$ for each household $\psi \in \Psi$ as follows:

$$\boldsymbol{\pi}^y_{\psi}(\mathcal{K}) \; = \; \mathbf{LMP}(\mathcal{K}) + \frac{1}{\mu_{\psi} S_{\mathsf{base}} \Delta t} \Big[\boldsymbol{\lambda}^y_{\bar{P}}(\mathcal{K}) - 2 \cdot \boldsymbol{r}_D(i, N^{\mathsf{ph}}_{\psi})^T \big(\boldsymbol{\Lambda}^y_{v_{\mathsf{max}}}(\mathcal{K}) - \boldsymbol{\Lambda}^y_{v_{\mathsf{min}}}(\mathcal{K}) \big)^T$$
$$- 2 \cdot \boldsymbol{x}_D(i, N^{\mathsf{ph}}_{\psi})^T \big(\boldsymbol{\Lambda}^y_{v_{\mathsf{max}}}(\mathcal{K}) - \boldsymbol{\Lambda}^y_{v_{\mathsf{min}}}(\mathcal{K}) \big)^T \boldsymbol{H}_{\psi}(\mathcal{K}) \Big]$$

Note that $\boldsymbol{\pi}^y_{\psi}(\mathcal{K})$ reduces to $\mathbf{LMP}(\mathcal{K})$ if $y = 0$.

S3: Update primal variables by $\boldsymbol{x}^y = \mathrm{argmax}_{\boldsymbol{x} \in \mathcal{X}} L(\boldsymbol{x}, \boldsymbol{\lambda}^y)$. This updating of primal variable values is implemented as follows. The DSO communicates to each household $\psi \in \Psi$ the price-to-go sequence $\boldsymbol{\pi}^y_{\psi}(\mathcal{K})$. Each household $\psi \in \Psi$ then adjusts its TCL power usage schedule to $\boldsymbol{x}^y_{\psi} = \mathcal{P}_{\psi}(\boldsymbol{\pi}^y_{\psi}(\mathcal{K}))$. and communicates $\boldsymbol{x}^y_{\psi}$ back to the DSO. If this primal variable updating step triggers the *Stopping Rule* outlined in Section 2.4, the negotiation process stops. Otherwise, the process proceeds to step **S4**.

S4: Update dual variables. The DSO determines updated dual variable values as follows: For each $t \in \mathcal{K}$,

$$\lambda^{y+1}_{\bar{P}}(t) = \Big[\lambda^y_{\bar{P}}(t) + \beta_1 \big[\sum_{\psi \in \Psi} [x^y_{\psi}(t) + p^{\mathsf{non}}_{\psi}(t)] - \bar{P} \big] \Big]^+$$
$$\boldsymbol{\lambda}^{y+1}_{v_{\mathsf{max}}}(t) = \Big[\boldsymbol{\lambda}^y_{v_{\mathsf{max}}}(t) + \beta_2 \big[\boldsymbol{v}^{\mathsf{non}}(t) - 2\boldsymbol{s}(t, \boldsymbol{x}^y(t)) - \boldsymbol{v}_{\mathsf{max}}(t) \big]^T \Big]^+$$
$$\boldsymbol{\lambda}^{y+1}_{v_{\mathsf{min}}}(t) = \Big[\boldsymbol{\lambda}^y_{v_{\mathsf{min}}}(t) + \beta_3 \big[-\boldsymbol{v}^{\mathsf{non}}(t) + 2\boldsymbol{s}(t, \boldsymbol{x}^y(t)) + \boldsymbol{v}_{\mathsf{min}}(t) \big]^T \Big]^+$$

where $[\ \cdot\ ]^+$ denotes projection on R^k_+ for appropriate dimension k, and β_1, β_2, and β_3 are the positive scalar step-sizes specified by the DSO in step **S1**. Expressed in more compact form, $\boldsymbol{\lambda}^{y+1} = \big[\boldsymbol{\lambda}^y + [\boldsymbol{g}(\boldsymbol{x}^y) - \boldsymbol{c}]^T \boldsymbol{B} \big]^+$ where $\boldsymbol{B}$ is an $m \times m$ diagonal positive-definite matrix constructed as follows: the diagonal entries of $\boldsymbol{B}$ associated with $\boldsymbol{\lambda}_{\bar{P}}(\mathcal{K})$, $\boldsymbol{\lambda}_{v_{\mathsf{max}}}(\mathcal{K})$, and $\boldsymbol{\lambda}_{v_{\mathsf{min}}}(\mathcal{K})$ are repeated entries of β_1, β_2, and β_3, respectively.

S5: Update iteration time. The iteration time y is assigned the updated value $y + 1$ and the process loops back to step **S2**

A dual decomposition algorithm DDA is presented for practical implementation of the negotiation process N(OP) between the DSO and the households. As discussed more carefully in [15, App.F], dual decomposition is a classical decentralized method that alternates the updating of primal and dual variables until convergence to optimal primal and dual variable solutions takes place within a specified tolerance level.

A key issue is whether any limit point $(\boldsymbol{x}^*, \boldsymbol{\lambda}^*)$ resulting from the specific dual decomposition algorithm DDA is guaranteed to determine a TES equilibrium for OP. The following propositions 3-5 establish sufficient conditions for this to be the case.

Proposition 3: *Suppose the Primal Problem (2.23) and the dual decomposition algorithm DDA satisfy the following three conditions:*

- **[P3.A]** $\mathcal{X}$ *is compact, and the objective function* $F(\boldsymbol{x})$ *and constraint function* $\boldsymbol{g}(\boldsymbol{x})$ *are continuous over* $\mathcal{X}$.

- **[P3.B]** *For every* $\boldsymbol{\lambda} \in \mathbb{R}^m_+$, *the Lagrangian Function* $L(\boldsymbol{x}, \boldsymbol{\lambda})$ *defined in (2.25) achieves a finite maximum at a unique point* $\boldsymbol{x}(\boldsymbol{\lambda}) \in \mathcal{X}$, *implying the dual function domain in (2.31) satisfies* $\mathbb{M} = \mathbb{R}^m_+$.

- **[P3.C]** *The sequence* $(\boldsymbol{x}^y, \boldsymbol{\lambda}^y)$ *determined by the dual decomposition algorithm DDA converges to a limit point* $(\boldsymbol{x}^*, \boldsymbol{\lambda}^*)$ *as the iteration time y approaches* $+\infty$.

Then the limit point $(\boldsymbol{x}^*, \boldsymbol{\lambda}^*)$ *is a saddle point (2.29) for the Lagrangian Function (2.25), and this saddle point determines a TES equilibrium for OP.*

Proof of Proposition 3: See [15, App. H].

Proposition 4: *Suppose the the Primal Problem (2.23) and the Dual Function (2.30) satisfy the following four conditions:*

- **[P4.A]** *Conditions [P3.A] and [P3.B] both hold;*

- **[P4.B]** *The Lagrangian Function (2.25) has a saddle point* $(\boldsymbol{x}^*, \boldsymbol{\lambda}^*)$ *in* $\mathcal{X} \times \mathbb{R}^m_+$;

- **[P4.C]** ***Extended Lipschitz Continuity Condition:*** *There exists a real symmetric positive-definite* $m \times m$ *matrix* $\boldsymbol{J}$ *such that, for all* $\boldsymbol{\lambda}_1, \boldsymbol{\lambda}_2 \in \mathbb{R}^m_+$,

$$\left\langle \nabla D_+(\boldsymbol{\lambda}_1) - \nabla D_+(\boldsymbol{\lambda}_2), \boldsymbol{\lambda}_1 - \boldsymbol{\lambda}_2 \right\rangle \;\leq\; ||\boldsymbol{\lambda}_1 - \boldsymbol{\lambda}_2||^2_{\boldsymbol{J}}$$

  where: $\nabla D_+(\boldsymbol{\lambda})$ *denotes the gradient of the dual function* $D(\boldsymbol{\lambda})$ *in (2.30) for* $\boldsymbol{\lambda} \in \mathbb{R}^m_{++}$ *and the right-hand gradient of* $D(\boldsymbol{\lambda})$ *at boundary points of* $\mathbb{R}^m_+$; $\langle \, , \, \rangle$ *denotes vector inner product; and* $||\cdot||^2_{\boldsymbol{J}} = (\cdot)\boldsymbol{J}(\cdot)^T$

- **[P4.D]** The matrix $[\boldsymbol{I} - \boldsymbol{J}\boldsymbol{B}]$ *is positive semi-definite, where* $\boldsymbol{I}$ *denotes an* $m \times m$ *identity* *matrix, and where $\boldsymbol{B}$ is the $m \times m$ diagonal positive-definite matrix defined in step **S4** of the dual decomposition algorithm DDA.*

Then the primal-dual point $(\boldsymbol{x}^y, \boldsymbol{\lambda}^y)$ determined by the dual decomposition algorithm DDA at iteration time y converges to a saddle point as $y \to +\infty$.

Proof of Proposition 4: See [15, App. I].

The Extended Lipschitz Continuity Condition [P4.C] in Prop. 4 is expressed in a relatively complicated form. The following proposition provides sufficient conditions for [P4.C] that are easier to understand.

Proposition 5: *Suppose the Primal Problem (2.23) satisfies condition [P3.A] in Prop. 3 plus the following three additional conditions:*

- **[P5.A]** *$\mathcal{X}$ is a non-empty compact convex subset of $\mathbb{R}^d$.*
- **[P5.B]** *The objective function $F{:}\mathbb{R}^d \to \mathbb{R}$ restricted to $\mathcal{X} \subseteq \mathbb{R}^d$ has the quadratic form*

$$F(\boldsymbol{x}) \;=\; \frac{1}{2}\boldsymbol{x}^T\boldsymbol{W}\boldsymbol{x} + \boldsymbol{\rho}^T\boldsymbol{x} + \boldsymbol{\sigma} \tag{2.34}$$

  where $\boldsymbol{W}$ is any real symmetric negative-definite $d \times d$ matrix, $\boldsymbol{\rho}$ is any real $d \times 1$ column vector, and $\boldsymbol{\sigma}$ is any real positive scalar.

- **[P5.C]** *The constraint function $g{:}\mathbb{R}^d \to \mathbb{R}^m$ restricted to $\mathcal{X} \subseteq \mathbb{R}^d$ has the linear affine form*

$$g(\boldsymbol{x}) \;=\; \boldsymbol{C}\boldsymbol{x} + \boldsymbol{b} \tag{2.35}$$

  where $\boldsymbol{C}$ is any real $m \times d$ matrix, and $\boldsymbol{b}$ is any real $m \times 1$ column vector.

Then the Extended Lipschitz Continuity Condition [P4.C] in Prop. 4 holds for $\boldsymbol{J} = \boldsymbol{C}\boldsymbol{H}^{-1}\boldsymbol{C}^T$, where $\boldsymbol{H} = -\boldsymbol{W}$.

Proof of Proposition 5: See [15, App. J].

An important aspect of the negotiation process N(OP) implemented by means of the dual decomposition algorithm DDA is that the DSO does not directly communicate iterated dual variable solutions to the households. Rather, the DSO communicates iterated retail price sequences to the households, requesting only that these households communicate back to the DSO what power amounts they would be willing to procure at these retail prices.

Consequently, N(OP) is based on an empirically meaningful exchange of information that households should find readily understandable. Moreover, N(OP) does not require the DSO to solve an optimization problem in order to determine an approximate TES equilibrium for OP. This greatly reduces computational requirements for the DSO.

2.9 Case Study

2.9.1 Overview

This section explores the practical effectiveness of our proposed consensus-based TES design by means of a case study.

As detailed below, the distribution network for this case study is an unbalanced 123-bus radial network populated by 345 households. A DSO is tasked with managing the power usage requirements of these households. The DSO's centralized optimization problem is formulated as a concave programming problem with a strictly concave quadratic objective function $\boldsymbol{F}(\boldsymbol{x})$ and a linear affine constraint function $\boldsymbol{g}(\boldsymbol{x})$ defined over a non-empty compact convex subset $\mathcal{X} \subseteq \mathbb{R}^d$. The DSO decentralizes this optimization problem by implementing a consensus-based TES design.

The case study examines the performance of this consensus-based TES design for a single simulated 24-hour day D. The simulation is conducted using MATLAB R2019b, which integrates the YALMIP Toolbox [50] with the IBM ILOG CPLEX 12.9 solver [51]. For each simulated operating period OP, the negotiation process N(OP) converged in less than 500s (8.4m). Technical mathematical underpinnings for the case study are provided in [15, App. K] .

2.9.2 Unbalanced Radial Distribution Network

The standard IEEE 123-bus radial distribution network [52], shown in Fig.2.6, is modified in three ways. First, 345 households, each with non-TCL and TCL, are distributed across the 123 buses. Second, the distribution network is connected to a transmission network at bus 0. Third, power is supplied to the distribution network through this transmission-distribution interface. The parameters for the distribution network are set as follows: $S_{\mathsf{base}} = 100$ (kVA); $\boldsymbol{v}_{\mathsf{min}}(t) = [0.95, 0.95, 0.95]^T$; $\boldsymbol{v}_{\mathsf{max}}(t) = [1.05, 1.05, 1.05]^T$; $\boldsymbol{v}_0(t) = [1.04, 1.04, 1.04]^T$; $V_{\mathsf{base}} = 4.16$ (kV); and $\bar{P} = 32$.

2.9.3 Household Modeling

For simplicity, all households are assumed to have the same parameter values. The non-TCL profile of each household ψ during day D is shown in Fig. 2.7. The initial inside air temperature for each household ψ at the start of day D is $T_\psi(0) = 74$ (^oF). The ambient outside air temperature for each household ψ during day D is shown in Fig.2.8.

The specific thermal dynamic parameter values set for each household ψ are: $\alpha_\psi^H = 0.96$ (unit-free); $\alpha_\psi^P = 0.7$ $(^oF/\text{kWh})$; $p_\psi^{\mathsf{max}} = 0.05$; and $\text{PF}_\psi(t) = 0.9$ for each sub-period t, which implies $\eta_\psi(t) = 0.48$ for each sub-period t.

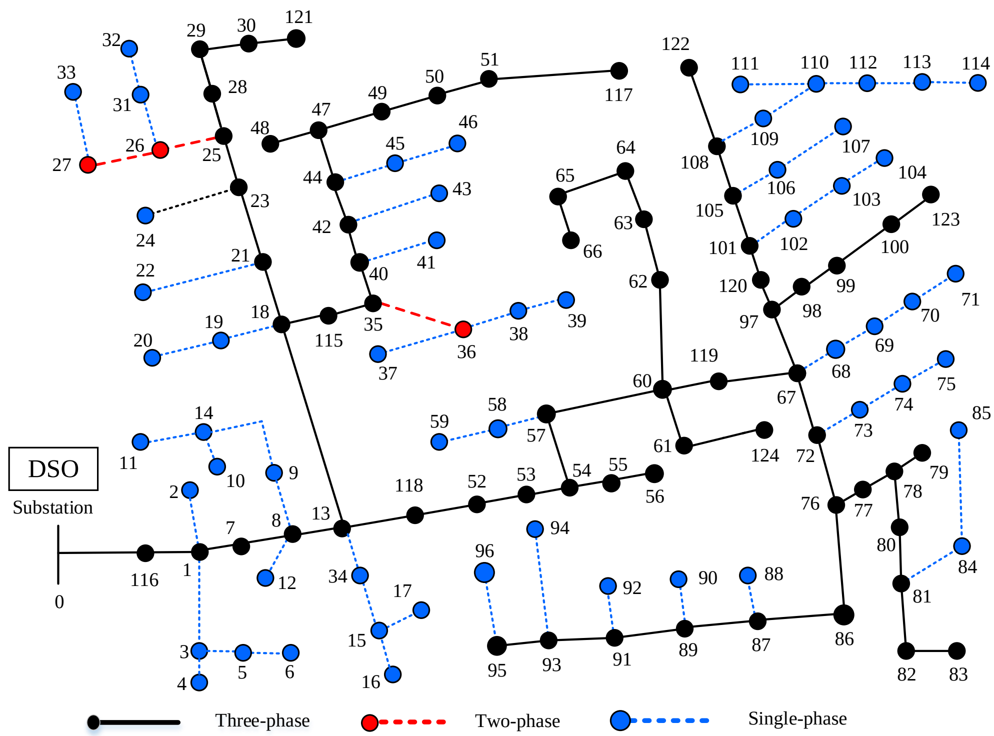

Figure 2.6: IEEE 123-bus radial distribution network.

As detailed in [15, App. K] , each household ψ has a strictly concave net-benefit objective function defined over a feasible choice set that is non-empty, compact, and convex. The specific preference parameter values set for each household ψ are: $c_\psi = 6.12$ $\left(\text{utils}/({}^oF)^2\right)$; $u_\psi^{\max} = 1.20 \times 10^4$ (utils); $TB_\psi = 72$ $({}^oF)$; and $\mu_\psi = 1$ (utils/cent).

2.9.4 DSO, RTM, and N(OP) Modeling

A DSO operates at the radial network head bus 0 as a linkage entity that participates in both transmission and distribution system operations. An RTM operates over the transmission grid, and the DSO purchases power from this RTM in order to meet the power usage needs of distribution system households.

The simulated day D is partitioned into 24 operating hours OP. The duration of RTM(OP) and LAH(OP) for each operating hour OP are set to 1min and 59min; cf. Fig. 2.1. The number of sub-periods t partitioning each operating hour OP is set to $NK = 1$, and the length of this single sub-period t is set to Δt = 1h. The profile of RTM LMPs at the radial network head bus 0 determined in RTM(OP) for each operating hour OP of day D is depicted in Fig.2.8.

The objective of the DSO is to align local household goals and constraints with distribution network reliability constraints in a manner that respects household privacy. As detailed in [15, App. K] , in

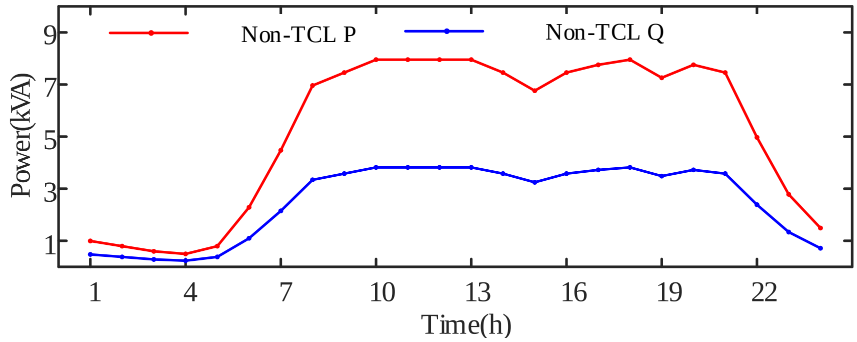

Figure 2.7: Non-TCL real and reactive power profiles during day D.

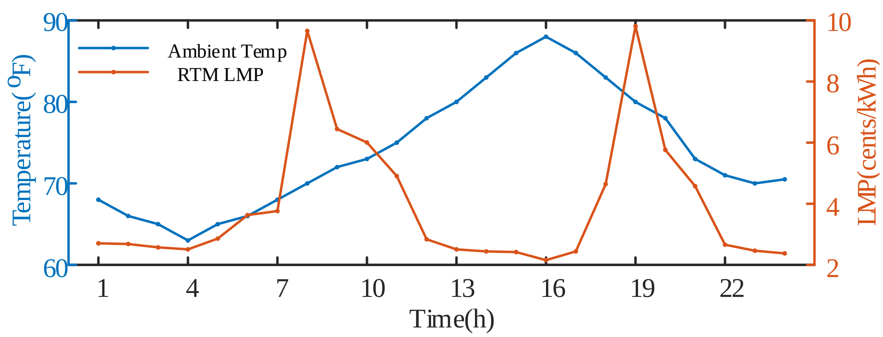

Figure 2.8: Ambient outside air temperature and RTM LMPs during day D.

the absence of household privacy constraints the DSO's centralized optimization problem for each operating period OP can be expressed as a concave programming problem with a strictly concave objective function and linear affine constraint function defined over a domain that is non-empty, compact, and convex. To avoid violation of household privacy, the DSO instead implements a consensus-based TES design that permits approximate implementation of the centralized optimal solution for each OP.

For each operating period OP during day D, the parameter values for the dual decomposition algorithm DDA used to implement the negotiation process N(OP) are set as follows: β_1 = 15; $\beta_2 = \beta_3$ = 50,000; and I_{max} = 200.

2.9.5 Simulation Results

As detailed in Section 2.7.2, the DSO imposes two distinct types of network reliability constraints for each operating hour OP during day D: (i) an upper limit on the peak demand (kW) realized during OP; and (ii) lower and upper bounds imposed on the 3-phase squared voltage magnitudes (p.u.) realized during OP.

Consider, first, the case in which the DSO does not manage the power usage of its household customers. Rather, the DSO simply sets retail prices for all non-TCL and TCL household loads during day D equal to the RTM LMPs depicted in Fig. 2.8.

As shown in Fig.2.9, the peak demand is 2962kW. Thus, as long as the upper limit on peak demand is set higher than this level, say at $\bar{P}$ = 3200kW, no peak demand limit violation occurs. On the other hand, lower and upper bounds on 3-phase squared voltage magnitudes (p.u.) are commonly set at 0.95 (p.u.) and 1.05 (p.u.). Given these bounds, it is seen in Fig. 2.9 that a voltage violation occurs at hour 17; specifically, the phase-a voltage magnitude drops to 0.9485 (p.u.).

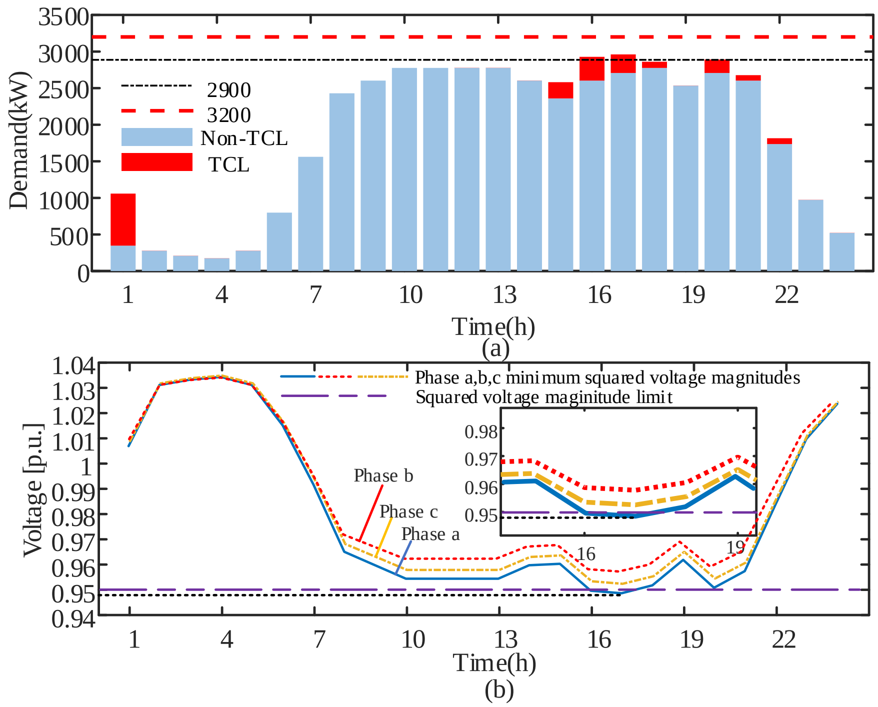

Figure 2.9: Unmanaged System Case (Peak Demand Limit 3200kW): (a) Total household power demand (kW) and (b) 3-phase minimum squared voltage magnitudes (p.u.) across the distribution network during each hour of day D. The peak demand limit 3200kW is satisfied; but a phase-a violation of the lower voltage bound 0.95 (p.u.) occurs at hour 17.

Next, suppose one change is made to the Unmanaged System Case specifications: namely, the DSO now uses the consensus-based TES to manage household power usage. In particular, the DSO conducts a negotiation process N(OP) with households in advance of each operating hour OP during day D, implemented by means of the dual decomposition algorithm DDA. As explained in Section 2.3.4, the negotiation process N(OP) continues until either there are no network reliability constraint violations or the number of negotiation rounds reaches the maximum permitted limit $I_{\max} = 200$.

Fig.2.10 reports the total household power demand and 3-phase minimum squared voltage magnitudes that result for each hour of day D, given this change from no system management to TES management. As seen in Fig.2.10, all network reliability constraints are now satisfied. In partic-

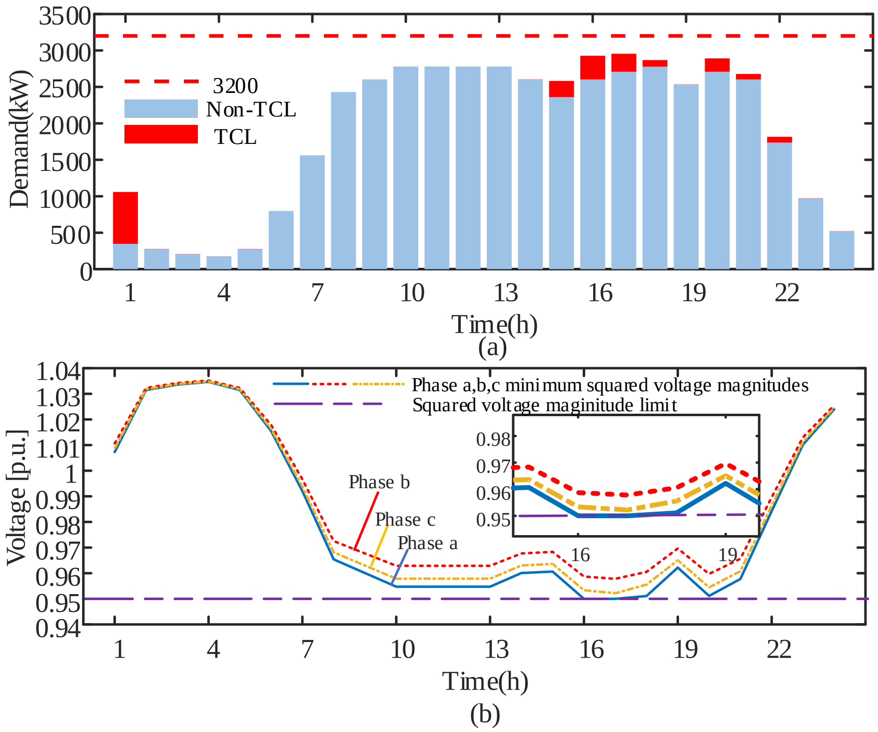

Figure 2.10: TES Management Case 1 (Peak Demand Limit 3200kW): (a) Total household power demand (kW) and (b) 3-phase minimum squared voltage magnitudes (p.u.) across the distribution network during each hour of day D. The DSO-managed negotiation process ensures that no violations of the peak demand limit 3200kW or voltage magnitude bounds [0.95, 1.05] (p.u.) occur.

ular, the switch to the use of the consensus-based TES design enables the DSO to eliminate the previously realized phase-a voltage constraint violation at hour 17 while still satisfying all other network reliability constraints.

Finally, suppose the peak demand limit is reduced from 3200kW to 2900kW, i.e., $\bar{P}$ = 2900kW. For the Unmanaged System Case, this change in peak demand limit has no effect on system operations. Consequently, as shown in Fig. 2.9, the peak demand 2962kW resulting for this case is now in violation of the reduced peak demand limit 2900kW; and the voltage magnitude violation for hour 17 continues to occur.

In contrast, given TES management, this reduction in peak demand limit from 3200kW to 2900kW results in a change in the DSO-conducted negotiation process with households. As seen in Fig. 2.10, the peak demand resulting for TES Management Case 1 (Peak Demand Limit 3200kW) does not satisfy the reduced peak demand limit 2900kW during some hours. Consequently, the DSO must now iteratively set retail prices for households in a different manner to ensure their power usage satisfies this reduced peak demand limit as well as the lower and upper voltage magnitude bounds.

The resulting demand outcomes for this TES Management Case 2 (Peak Demand 2900kW) are reported in Fig. 2.11. As seen, peak demand is maintained at or below the reduced peak demand limit 2900kW during all hours of day D. At the same time (not shown), the 3-phase minimum squared voltage magnitudes across the distribution network are maintained within their allowable limits [0.95, 1.05] (p.u.) during all hours of day D. For example, the smallest squared voltage magnitude across the distribution network during day D is 0.951 (p.u.).

As illustrated by these test cases, the core feature of the consensus-based TES design – namely, the DSO-managed negotiation process with distribution system customers – permits the DSO to protect against network reliability constraint violations, whatever form these constraints might take.

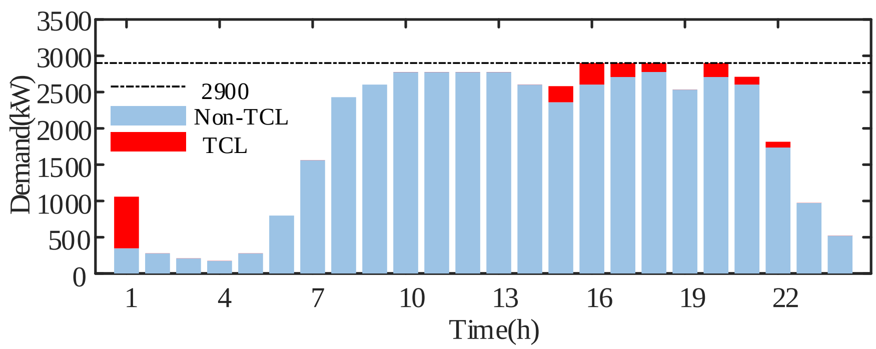

Figure 2.11: TES Management Case 2 (Peak Demand Limit 2900kW): Total household power demand (kW) during each hour of day D. The DSO-managed negotiation process ensures that no peak demand limit violations occur.

2.9.6 Relationship Between Prices and Constraints

The retail price-to-go sequence for a household ψ in a TES equilibrium for an operating period OP, partitioned into sub-periods $t \in \mathcal{K}$, is shown in Section 2.8.2 to take form $\boldsymbol{\pi}^*_\psi(\mathcal{K})$ in (2.33). This form is the summation of an initial price sequence, set by the DSO, that the DSO then modifies as necessary during the negotiation process N(OP) to ensure all network reliability constraints for OP are met.

As noted in Section 2.8.2, the price-to-go sequence (2.33) for household ψ depends on $\psi's$ preference and physical attributes as well as ψ's network location. Specifically, the right-hand side of (2.33) depends on: (i) ψ's marginal utility of money μ_ψ; (ii) ψ's TCL power-ratio function (2.16) as characterized by the TCL power-ratio matrix $\boldsymbol{H}_\psi(\mathcal{K})$ defined in (2.18); and (iii) ψ's phase and bus location attributes ϕ and i through the terms $\boldsymbol{r}_D(i, N^{\text{ph}}_\psi)^T$ and $\boldsymbol{x}_D(i, N^{\text{ph}}_\psi)^T$.

For simplicity, this study assumes that the initial price-to-go sequence set by the DSO at the beginning of the negotiation process N(OP) is the sequence $\mathbf{LMP}(\mathcal{K})$ of LMPs determined in the real-time market RTM(OP) at the linkage bus b^*. This linkage bus, which connects the distribution network to a relatively large transmission network, is also the head bus 0 for the radial distribution network.

Any subsequent deviations from this initial price-to-go sequence that result from the negotiation process N(OP) are expressed in terms of dual variables for the network reliability constraints for OP. Specifically, these deviations are functions of the non-negative dual variables $\boldsymbol{\lambda}^*_{\bar{P}}(\mathcal{K})$, $\boldsymbol{\Lambda}^*_{v_{\min}}(\mathcal{K})$, and $\boldsymbol{\Lambda}^*_{v_{\max}}(\mathcal{K})$ corresponding to the peak demand constraint and the lower and upper voltage magnitude constraints for each $t \in \mathcal{K}$, where each of these constraints is expressed as an inequality constraint.

In a TES equilibrium for OP, the values of these dual variables must coincide, by definition, with the dual variable solutions for the Primal Problem (2.23). If strict inequality holds for a network reliability constraint in this Primal Problem solution, i.e., the constraint is *inactive*, then the corresponding dual variable solution must be zero. Thus, if strict inequality holds for all network reliability constraints in this Primal Problem solution, the retail price-to-go sequences communicated to households will simply coincide with the DSO's initially set RTM LMPs. The remainder of this section analyzes how TES equilibrium retail price outcomes deviate from RTM LMPs during the simulated day D for cases in which at least one network reliability constraint is active in the Primal Problem solution.

Consider, first, the TES equilibrium retail price outcomes for hour 17 that are reported in Fig. 2.12 for TES Management Case 1 with peak demand limit $\bar{P} = 3200$kW. These retail price outcomes are seen to vary with respect to both bus location and phase. What explains this variation?

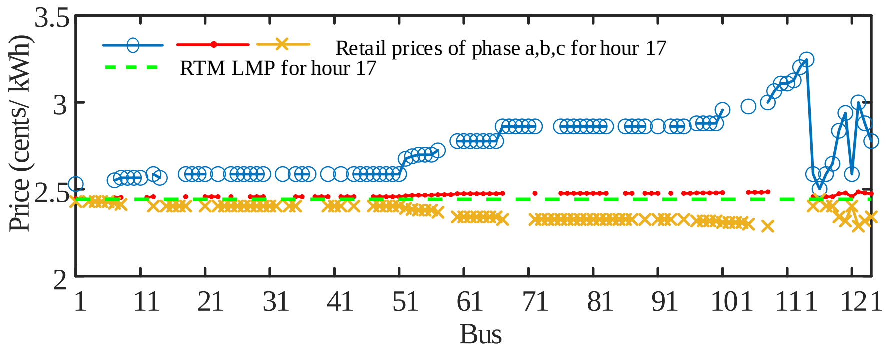

Figure 2.12: TES Management Case 1 (Peak Demand Limit 3200kW): TES equilibrium retail prices for hour 17 of day D across the distribution network (buses 1-123), compared with the RTM LMP at bus 0 for hour 17 of day D.

As seen in Fig.2.10, during hour 17 the peak demand remains strictly below the peak demand limit 3200kW. Thus, the peak demand constraint is inactive, implying that the dual variable solution associated with this inactive peak demand constraint must be zero, i.e., $\boldsymbol{\lambda}^*_{\bar{P}}(\mathcal{K}) = \mathbf{0}$.

On the other hand, during hour 17 the minimum squared voltage magnitude across phases and buses reaches the lower bound 0.95 (p.u.), i.e., the lower-bound voltage constraint is active. Typically,[15] the dual variable solution $\boldsymbol{\Lambda}^*_{v_{\min}}(\mathcal{K})$ associated with this active voltage constraint will then

[15] By Lemma 1 in [15, App. G] , a non-negative dual variable solution for an inactive constraint must be 0, but the

be strictly positive. In this case, the TES equilibrium price-to-go sequence (2.33) determined for each household ψ for hour 17 will deviate from the RTM LMP at bus 0 for hour 17, i.e., the initial retail price commonly set by the DSO for each household ψ in the negotiation process for hour 17.

These findings have the following important implication. Even if all households populating a distribution network have identical benefit (comfort) functions and identical structural house attributes, this does *not* imply they should be charged the same retail power price. Rather, in the presence of active voltage reliability constraints, optimal pricing will typically require households associated with different marginal utility of money parameters, different power factors, different phases, and/or different bus locations to be charged different retail prices. This differential retail pricing reflects the roles played by *household preference attributes, power factors and network locations* in ensuring the satisfaction of these voltage reliability constraints.

Consider, next, the relationship between TES equilibrium retail price outcomes and network reliability constraints for the TES Management Case 2 with peak demand limit $\bar{P}$ = 2900kW. As discussed in Section 2.9.5, for this case the voltage reliability constraints are inactive; hence, all dual variable solutions associated with these voltage constraints are zero. It follows that the TES equilibrium price-to-go sequence (2.33) for each household ψ has the following reduced form:

$$\boldsymbol{\pi}^*_{\psi}(\mathcal{K}) = \mathbf{LMP}(\mathcal{K}) + \frac{1}{\mu_{\psi} S_{\mathsf{base}} \Delta t} \boldsymbol{\lambda}^*_{\bar{P}}(\mathcal{K}) \tag{2.36}$$

On the other hand, as shown in Fig.2.11, the peak demand constraint is active for hours 16-18 and 20 during day D. The TES equilibrium retail price outcomes for these hours are reported in Fig.2.13. The retail price is strictly higher than the RTM LMP for each of these hours, indicating that the dual variable solution vector $\boldsymbol{\lambda}^*_{\bar{P}}(\mathcal{K})$ for the peak demand constraints during day D, appearing in (2.36) includes strictly positive values for these four hours.

The form of household ψ's TES equilibrium price-to-go sequence $\boldsymbol{\pi}^*_{\psi}(\mathcal{K})$ in (2.36) has the following important implication. Note that household ψ's marginal utility of money parameter μ_{ψ} appears in the denominator of the far-right term in (2.36). Consequently, even if voltage network constraints are inactive during day D, households with different marginal utility of money assessments will typically be charged different prices during each hour of day D for which the peak demand limit constraint is active.

As noted in 2.9.3, for the case study at hand the marginal utility of money parameter μ_{ψ} is commonly set to μ_{ψ} = 1 (utils/cent) for each household $\psi \in \Psi$. Consequently, as seen in Fig. 2.13, for this special case the TES equilibrium retail prices for TES Management Case 2 are the same for

converse does not necessarily hold. That is, the dual variable solution corresponding to an active constraint is not necessarily strictly positive.

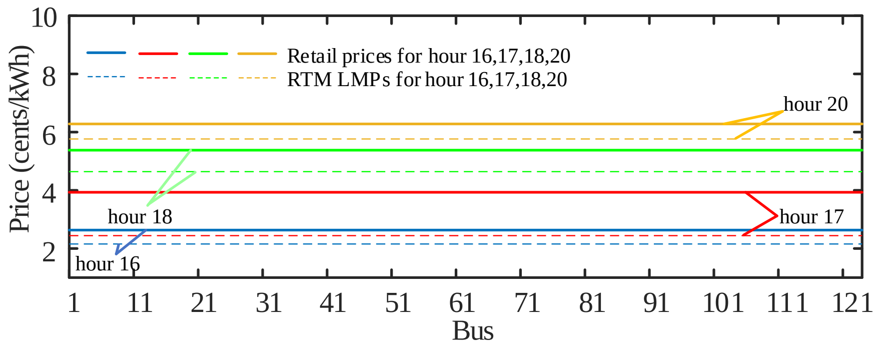

Figure 2.13: TES Management Case 2 (Peak Demand Limit 2900kW): TES equilibrium retail prices for hours 16-18 and 20 of day D across the distribution network (buses 1-123), compared with the RTM LMP outcomes at bus 0 for these same hours.

each household ψ during the operating hours 16-18 and 20 even though the peak demand limit is active for these hours.

2.9.7 Optimality Verification and Comparison

This subsection explores the following important question: Does the TES equilibrium determined by the consensus-based TES design closely approximate the optimal solution for the centralized DSO optimization problem (2.21)? An affirmative answer is provided for the case study developed in previous subsections. Illustrative results are presented below for TES Management Case 1 (Peak Demand Limit 3200kW).

Fig. 2.14 compares the solutions obtained for total household TCL during each hour of day D using these two different methods. Fig. 2.15 provides a finer-grained comparison for total phase-a household TCL during hour 17 across the 123 buses comprising the entire distribution network. In each case, the resulting solutions are seen to be virtually indistinguishable.

This finding has two important implications. First, the consensus-based TES design achieves optimality while protecting the privacy of participating customers. In contrast, the centralized DSO optimization method requires extensive knowledge of customer attributes, including benefit (utility) functions and local feasibility constraints. Second, the consensus-based TES design is a decentralized solution method, which results in reduced computational requirements and improved scalability properties.[16] In contrast, the centralized DSO optimization method requires the DSO to solve a multiperiod optimization problem whose computational requirements dramatically increase with the number of participating customers.

[16] As will be discussed in Section 2.10, the consensus-based TES design can be extended to incorporate aggregators as intermediaries between the DSO and various subsets of customers, thus further enhancing its scalability.

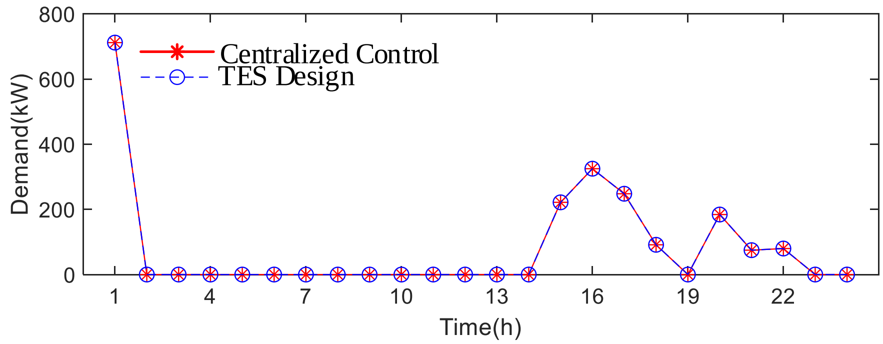

Figure 2.14: Comparison of TES equilibrium and centralized DSO optimal solutions for total household TCL during day D.

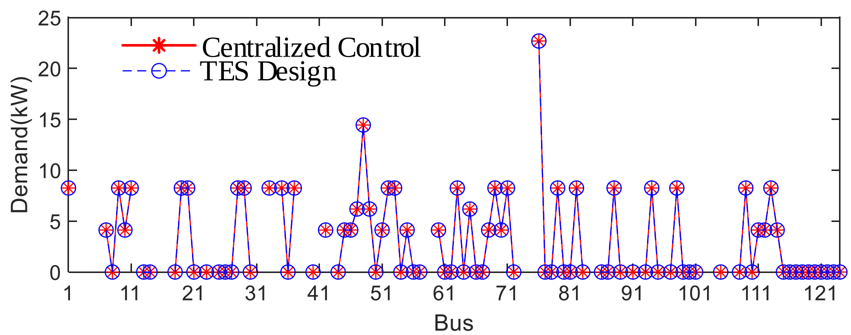

Figure 2.15: Comparison of TES equilibrium and centralized DSO optimal solutions for total phase-a household TCL across the distribution network (123 buses) during operating hour 17.

2.10 Conclusion and Future Research

This study develops a new consensus-based TES design for unbalanced distribution networks populated by customers with both fixed and price-sensitive power usage demands. The design is managed by a DSO. However, it is implemented as a distributed optimization problem, thus permitting alignment of system goals and network reliability constraints with local customer goals and constraints in a manner that respects customer privacy.

The core feature of this consensus-based TES design is a multi-round negotiation process N(OP) between the DSO and participant customers, to be held in advance of each operating period OP. At the start of N(OP), the DSO sets initial prices based on RTM LMPs. During each successive negotiation round, the DSO communicates updated price-to-go sequences to customers for OP; and the customers respond by communicating back to the DSO their optimal price-sensitive power usage levels for OP conditional on these prices and on private local constraints. The negotiation process terminates either when all network reliability constraints are satisfied by these customer power usage responses or when a stopping rule is activated.

A complete analytical formulation of the consensus-based TES design is developed for an unbalanced radial distribution network populated by welfare-maximizing households. Each operating day D is partitioned into operating periods OP of arbitrary duration, with look-ahead horizons LAH(OP). The negotiation process N(OP) for each operating period OP is then implemented during LAH(OP) by means of a newly developed dual decomposition algorithm DDA.

Making use of both classical and newly established results, sufficient conditions are established for the DDA to converge to a TES equilibrium whose power usage levels coincide with the optimal power usage solutions for a centralized full-information optimization problem that incorporates all network reliability constraints. Moreover, the TES equilibrium price-to-go sequences determined by the DDA are shown to have an informative additive structure that expresses deviations from initial prices in terms of the dual variable solutions associated with network reliability constraints.

A case study for an unbalanced 123-bus radial distribution network is presented to illustrate the capabilities of the consensus-based TES design and its DDA implementation. Numerical results are presented that demonstrate the convergence of the DDA to a TES equilibrium that closely approximates a centralized full-information optimal solution.

Future studies will seek to extend the capabilities of the consensus-based TES design in three main directions. First, the TES design will be generalized to permit consideration of customer-owned distributed generation as well as customer power usage levels. Particular attention will be focused on the inclusion of inverter-based distributed generation such as wind and solar power facilities. This extension will permit a more careful consideration of reactive power as an ancillary service product, supplied in return for appropriate compensation.

Second, the consensus-based TES design will be extended to permit the inclusion of aggregators operating as intermediaries between the DSO and its managed customers. The communication network would still take a radial form; however, the ability of aggregators to perform intermediate aggregation of customer responses could reduce communication times. For example, it could permit an efficient bundling of customers into distinct aggregator-managed subsets on the basis of their observable attributes or their historically observed behaviors. This bundling could enhance the ability of the DSO to ensure all network reliability constraints are met through the negotiation process in a practically reasonable amount of time.

Third, the negotiation process for the consensus-based TES design will be modified to permit more sophisticated specifications for the initial price-to-go sequences set by the DSO. In the current study, these initial prices are simply set equal to RTM LMPs. Noted in Section 2.3.4, this specification could expose customers to undesirable price volatility. Hence, a better alternative might be to set these initial prices equal to time and/or spatially averaged RTM LMPs.

However, an additional issue must also be considered. In order for the DSO to ensure its independent status, any net revenues or net costs that the DSO incurs through its operations must be allocated back to its managed customers. Consequently, the DSO's initial price-to-go sequences for customer price-sensitive demands should be set to ensure the DSO breaks even on average over time; that is, its operational revenues should match its operational costs on average over time. This break-even requirement could force a DSO to set initial prices at levels that deviate from RTM LMPs, even if setting initial prices equal to RTM LMPs would not result in any network reliability constraint violations.

References

[1] FERC, "Participation of Distributed Energy Resource Aggregations in Markets Operated by Regional Transmission Organizations and Independent System Operators,", U.S. Federal Energy Regulatory Commission (FERC), Docket No. RM18-9-000, Order No. 2222, Final Rule, September 17, 2020.

[2] L. Tesfatsion, *A New Swing-Contract Design for Wholesale Power Markets*, 20 chapters, 288pp., John Wiley & Sons, Inc. (IEEE Press Series on Power Engineering), Hoboken, NJ, USA, 2021.

[3] S. Battula, L. Tesfatsion, and Z. Wang, "A customer-centric approach to bid-based transactive energy system design," *IEEE Trans. Smart Grid*, vol. 11, no. 6, pp. 4996-5008, 2020.

[4] S. Battula, L. Tesfatsion, and T.E. McDermott, "An ERCOT test system for market design studies," *Appl. Energy*, vol. 275, October. 2020.

[5] H.T. Nguyen, S. Battula, R.R. Takkala, Z. Wang, and L. Tesfatsion, "An integrated transmission and distribution test system for evaluation of transactive energy designs," *Appl. Energy*, vol. 240, pp. 666-679, 2019.

[6] S. Ma, Z. Wang, and L. Tesfatsion, "Swing contracts with dynamic reserves for flexible service management," *IEEE Trans. on Power Syst*., vol. 34, no. 5, pp. 4024-4037, 2019.

[7] Swathi Battula, "Transactive Energy System Design for Integrated Transmission and Distribution Systems," PhD Thesis, Department of Electrical and Computer Engineering, Iowa State University, February 2021.

[8] S. Battula and L. Tesfatsion, *AMES V5.0: GitHub Code/Data Repository*, 2020: https://github.com/ames-market/AMES-V5.0

[9] S. Battula, L. Tesfatsion, and T.E. McDermott, *ERCOT Test System: GitHub Code/Data Repository*, 2020: https://github.com/ITDProject/ERCOTTestSystem

[10] S. Battula and L. Tesfatsion, *ITD Project/Household Formulation: GitHub Code/Data Repository*, 2020: https://github.com/ITDProject/HouseholdFormulationRepository

[11] S. Battula and L. Tesfatsion, *ITD TES Platform V2.0: GitHub Code/Data Repository, 2021:* https://github.com/ITDProject/ITDTESPlatform

[12] L. Tesfatsion and S. Battula, "Analytical SCUC/SCED optimization formulation for AMES V5.0," AMES V5.0 Documentation, Economics Working Paper #20014, ISU Digital Repository, August 2020.

[13] L. Tesfatsion and S. Battula, "Notes on the GridLAB-D household equivalent thermal parameter model," ITD TES Platform V2.0 Documentation, Economics Working Paper #19001, ISU Digital Rep., July 2020.

[14] A.B. Birchfield, T. Xu, K.M. Gegner, K.S. Shetye, and T.J. Overbye, "Grid structural characteristics as validation criteria for synthetic networks", *IEEE Transactions on Power Systems*, vol. 32, no. 4, pp. 3258-3265, 2017.

[15] R. Cheng, L. Tesfatsion, and Z. Wang, "A multiperiod consensus-based transactive energy system for unbalanced distribution networks," ISU Digital Repository, Iowa State Univ., Ames, IA, USA, 2021. [Online]. Available: https://lib.dr.iastate.edu_workingpapers/127.

[16] GridWise Architectural Council, *GridWise Transactive Energy Framework Version 1.0*, January, 2015.

[17] K. Kok, *The PowerMatcher: Smart Coordination for the Smart Electricity Grid*, SIKS Dissertation Series No. 2013-17, Dutch Research School for Information and Knowledge Systems, TNO, The Netherlands, 2013. http://dare.ubvu.vu.nl/handle/1871/43567

[18] L. Hurwicz, "The design of mechanisms for resource allocation," *The American Economic Review*, vol. 63, no. 2, pp.1-30, 1973.

[19] Royal Swedish Academy of Sciences, *Mechanism Design Theory: Scientific Background on the Sveriges Riksbank Prize in Economic Sciences in Memory of Alfred Nobel*, compiled by the Prize Committee, 2007.

[20] K. Kok, and S. Widergren, "A society of devices: Integrating intelligent distributed resources with transactive energy," *IEEE Power and Energy Mag*., vol. 14, no. 3, pp. 34-45, 2016.

[21] R. Deng, Z. Yang, M.Y. Chow, and J. Chen, "A survey on demand response in smart grids: Mathematical models and approaches," *IEEE Trans. Ind. Informat.*, vol. 11, no. 3, pp. 570-582, June 2015.

[22] E. Koch and M.A. Piette, "Direct versus facility centric load control for automated demand," presented at the Grid-Interop Forum, Denver, CO, USA, 2009.

[23] S. Chen, Q. Chen, Y. Xu, "Strategic bidding and compensation mechanism for a load aggregator with direct thermostat control capabilities," *IEEE Trans. Smart Grid*, vol. 9, no. 3, pp. 2327-2336, May 2018.

[24] YN. O'Connell, P. Pinson, H. Madsen, and M. O'Malley, "Benefits and challenges of electrical demand response: A critical review," *Renew. Sust. Energ. Rev*., vol. 39, pp. 686-699, 2014.

[25] L. Gan and S.H. Low, "Convex relaxations and linear approximation for optimal power flow in multiphase radial network," in *18th Power Systems Computation Conference (PSCC)*, 2014.

[26] E. Celebi and J.D. Fuller, "Time-of-use pricing in electricity markets under different market structures," IEEE Trans. Power. Syst., vol. 27, no. 3, pp. 1170-1181, Aug. 2012.

[27] K. Herter, "Residential implementation of critical-peak pricing of electricity," *Energy Policy*, vo. 35, pp. 2121-2130, Apr. 2007.

[28] A.G. Thomas and L. Tesfatsion, "Braided cobwebs: cautionary tales for dynamic pricing in retail electric power markets," *IEEE Trans. Power Syst.*, vol. 33, no. 6, pp. 6870-6882, 2018.

[29] H. Hao, C.D. Corbin, K. Kalsi, and R.G. Pratt, "Transactive control of commercial buildings for demand response," *IEEE Trans. Power Syst.*, vol. 32, no. 1, pp. 774-783, Jan. 2017.

[30] F. Rahimi and A. Ipakchi, "Using a transactive energy framework: providing grid services from smart buildings," *IEEE Electrification Mag*., vol. 4, pp. 23-29, 2016.

[31] S. Chen and C.C. Liu, "From demand response to transactive energy: State of the art," *J. Mod. Power Syst. Clean Energy,* vol. 5, no. 1, pp. 10-19, 2017.

[32] E. Mengelkamp, J. Gärttner, K. Rock, S. Kessler, L. Orsini, and C. Weinhardt, "Designing microgrid energy markets: A case study: The Brooklyn microgrid," *Appl. Energy*, vol. 210, pp. 870-880, Jan. 2018.

[33] N. Atamturk and M. Zafar, "Transactive energy: A surreal vision or a necessary and feasible solution to grid problems," California Public Utilities Commission, Policy Planning Division, San Francisco, CA, USA, Tech. Rep., 2014.

[34] D.J. Hammerstrom, R. Ambrosio, T.A. Carlon *et al*., "Pacific northwest gridwise test bed demonstration projects," Pacific Northwest Nat. Lab., Richard, WA, USA, Tech. Rep. PNNL-17167, 2007.

[35] S.E. Widergren, K. Subbarao, J.C. Fuller *et al*., "AEP Ohio grid smart demonstration project real-time pricing demonstration analysis," Pacific Northwest Nat. Lab., Richland, WA, USA, Tech. Rep. PNNL-23192, 2014.

[36] S. Li, W. Zhang, J. Lian, and K. Kalsi, "Market-based coordination of thermostatically controlled loads-Part I: A mechanism design formulation," *IEEE Trans. Power Syst*., vol. 31, no. 2, pp. 1170-1178, Mar. 2016.

[37] Z. Liu, Q. Wu, K. Ma, M. Shahidehpour, Y. Xue, and S. Huang, "Two stage optimal scheduling of electric vehicle charging based on transactive control," IEEE Trans. Smart Grid, vol. 10, no. 3, pp. 2948-2958, May 2019.

[38] S. Vandael, B. Claessens, M. Hommelberg, T. Holvoet, and G. Deconinck, "A scalable three-step approach for demand side management of plug-in hybrid vehicles," *IEEE Trans. Smart Grid*, vol. 4, no. 2, pp. 720-728, Jun. 2013.

[39] S. Weckx, R. D'Hulst, B. Claessens, and J. Driesensam, "Multiagent charging of electric vehicles respecting distribution transformer loading and voltage limits," *IEEE Trans. Smart Grid*, vol. 5, no. 6, pp. 2857-2867, Nov. 2014.

[40] J. Hu, G. Yang, H.W. Bindner, and Y. Xue, "Application of network-constrained transactive control to electric vehicle charging for secure grid operation," *IEEE Trans. Sustain. Energy,* vol. 8, no. 2, pp. 505-515, Apr. 2017.

[41] ERCOT. Nodal Protocols – Section 6: Adjustment Period and Real-time Operations. Electric Reliability Council of Texas; 2020.

[42] M.E. Baran and F.F. Wu, "Optimal capacitor placement on radial distribution systems," *IEEE Trans. Power Del.,* vol. 4, no. 1, pp 725-734, Jan. 1989.

[43] M.E. Baran and F.F. Wu, "Network reconfiguration in distribution system for loss reduction and load balancing," *IEEE Trans. Power Del*., vol. 4, no. 2, pp. 1401-1407, Apr. 1989.

[44] B.A. Robbins and A.D. Domínguez-García, “Optimal reactive power dispatch for voltage regulation in unbalanced distribution systems,” *IEEE Trans. Power Syst.*, vol. 31, no, 4, pp. 2903-2913, Jul. 2016.

[45] Q. Zhang, K. Dehghanpour and Z. Wang, “Distributed CVR in unbalanced distribution networks with PV penetration,” *IEEE Trans. SmartGrid*., vol. 10, no. 5, pp. 5308-5319, Sep. 2019.

[46] H. Zhu and H.J. Liu, “Fast local voltage control under limited reactive power: optimality and stability analysis,” *IEEE Trans. Power Syst.*, vol. 31, no. 5, pp. 3794-3803, Sep. 2016.

[47] M. Ilic, J.W. Black and J.L. Watz, “Potential benefits of implementing load control,” in *Proc. IEEE Power Eng. Soc. Winter Meeting*, New York, NY, USA, 2002, pp. 177-182.

[48] Z. Chen, L. Wu and Y. Fu, “Real-time price-based demand response management for residential appliances via stochastic optimization and robust optimization,” IEEE Trans. Smart Grid, vol. 3, no. 4, pp. 1822-1831, Dec. 2012.

[49] Y. Hong, J. Lin, C. Wu, and C. Chuang, “Multi-objective air-conditioning control considering fuzzy parameters using immune clonal selection programming.” *IEEE Trans. Smart Grid*, vol. 3, pp. 1603-1610, Dec. 2012.

[50] J. Löfberg, “YALMIP: A toolbox for modeling and optimization in MATLAB,” in *Proc. CACSD Conf*., Taipei, Taiwan, 2004.

[51] C. Bliek, P. Bonami, and A. Lodi, “Solving mixed-integer quadratic programming problems with IBM-CPLEX: a progress report,” in *Proc. 26th RAMP Symposium*, Tokyo, Japan, Oct. 2014.

[52] W.H. Kersting, “Radial distribution test feeders,” in *Proc. IEEE Power Eng. Soc. Win. Meeting*, pp. 908-912, 2001.

[53] D.P. Bertsekas, *Nonlinear Programming*, Second Edition, Athena Scientific, Belmont, MA, USA, 1999.

[54] D.P. Bertsekas, *Convex Analysis and Optimization: Chapter 8 Solutions*, Athena Scientific, Belmont, MA, USA, 2003. http://www.athenasc.com

[55] S. Boyd and L. Vandenberghe, *Convex Optimization*, Seventh Printing, Cambridge University Press, Cambridge, UK, 2009.

[56] P. Giselsson, “Improving Fast Dual Ascent for MPC – Part I: The Distributed Case,” *arXiv: 1312.3012*, 2013.

[57] D.P. Bertsekas, *Convex Optimization Theory*, Athena Scientific, Belmont, MA, USA, 2009.

Part II

Analysis of Market Structures to Harness Flexibilities of Distributed Energy Resources (DERs)

Subhonmesh Bose
Khaled Alshehri, Graduate Student
Mariola Ndrio, Graduate Student
Anna Winnicki, Graduate Student

University of Illinois at Urbana-Champaign

For information about this project, contact

Subhonmesh Bose
4058 ECE Building
306 N. Wright St.,
Urbana, Illinois 91081
Phone: 217-244-2101
Email: boses@illnois.edu

Power Systems Engineering Research Center

The Power Systems Engineering Research Center (PSERC) is a multi-university Center conducting research on challenges facing the electric power industry and educating the next generation of power engineers. More information about PSERC can be found at the Center's website: http://www.pserc.org.

For additional information, contact:

Power Systems Engineering Research Center
Arizona State University
527 Engineering Research Center
Tempe, Arizona 85287-5706
Phone: 480-965-1643
Fax: 480-727-2052

Notice Concerning Copyright Material

Table of Contents

List of Figures

List of Tables

1. Introduction

Part II of this final report collects our works on the design and analysis of coordination mechanisms for harnessing the flexibility offered by distributed energy resources (DERs) connected to the grid-edge. Residential DERs in isolation are typically too small to offer meaningful grid services to the distribution or transmission grid. Coordinated control of these resources can provide such services. This part of the report is dedicated to the analysis of two possible designs. The first among these considers third-party profit-maximizing retail aggregators who act as coordinating intermediaries between prosumers and the wholesale market. By prosumers, we mean the consumers who have the ability to supply power sometimes, owing to the presence of DERs such as rooftop solar. The focus of this research is on quantifying the impact of strategic incentives of the aggregator. The second design considers a wholesale market-style retail market that utilizes a distribution grid-constrained dispatch of DERs over the distribution network. Here, our key goal is to analyze market-relevant properties of distribution locational marginal prices.

- Chapter 2 presents a game-theoretic framework to study the interaction between an aggregator and a collection of prosumers with DERs. In our framework, the aggregator offers a price to the prosumers, who in return, supplies power at that offered price. The aggregator then offers the collective supply from all DERs to the wholesale market. The aggregator is assumed to be profit-motivated. That is, the aggregator seeks to maximize its profit from arbitrage between the price it faces in the wholesale market and the price it offers to the DER owner-operators. The key insight from the analysis is that profit-motivation of the aggregators can reduce the overall market efficiency from the impractical but ideal benchmark where prosumers can directly participate in the wholesale market.

- Chapter 3 seeks to characterize properties of a pricing mechanism that accounts for the non-convex nature of the constraints imposed by the power flow equations in the distribution grid within a retail market environment. We define and analyze properties of real and reactive power prices that are derived from a second-order cone programming-based relaxation of these equations. For these prices, we study conditions under which the market mechanism supports an efficient market equilibrium and is revenue adequate. Efficient market equilibrium ensures that all market participants follow the dispatch signal, given the announced prices. Revenue adequacy ensures that a distribution system operator does not run cash negative after settling the payments of the market participants.

2. Quantifying Market Efficiency Impacts of Aggregated Distributed Energy Resources

2.1 Introduction

Widespread adoption of distributed energy resources (DERs) coupled with advances in communication and information technology, are pushing electricity markets to a more decentralized consumer-centric model. DERs typically include rooftop solar, small-scale wind turbines, electric vehicles as well as demand-response schedules. More generally, a DER is "any resource on the distribution system that produces electricity and is not otherwise included in the formal NERC definition of the Bulk Electric System (BES)" [2]. The low-voltage side of the grid, traditionally comprising mostly of passive small-scale consumers, is rapidly transforming into an active component of the grid where prosumers respond to price signals for managing their consumption and production of energy [3].

Transmission system operators lack visibility into the low and medium voltage distribution grid where DERs are connected. Furthermore, DERs have relatively small capacities that together with the high costs and complexities involved in their integration, render it impractical for such resources to directly offer their services in wholesale electricity markets. Despite significant research on effective means to harness such resources, a unifying framework for integration and compensation of DERs remains under debate.[1] See [4–7] for insightful discussions.

One line of work suggests the implementation of distribution electricity markets operated by an independent distribution system operator (DSO), that acts as a market manager and dispatcher of DERs [8–10]. In this model, the DSO is responsible for collecting the offers and bids from market participants and determine the appropriate prices to compensate DER asset owner-operators [11–13]. Another approach advocates fully distributed market structures, where prosumers trade DER services with each other as members of a coordinated and purely transactive community [14, 15].

In this chapter, we focus on a third DER participation model through an aggregator $\mathscr{A}$ – "a company that acts as an intermediary between electricity end-users and DER owners, and the power system participants who wish to serve these end-users or exploit the services provided by these DERs", according to [16]. California Independent System Operator (CAISO) allows such aggregators with capacities north of 0.5MW to participate in its wholesale markets for energy and ancillary services. See [17] for an analysis of CAISO's model. Our focus is on efficiency impacts of a profit-motivated retail aggregator – a topic that has not yet received much attention.

[1] FERC has issued Order 841 on energy storage and a Notice of Proposed Rulemaking on DERs, but is yet to define a binding framework for general DER participation in US wholesale markets.

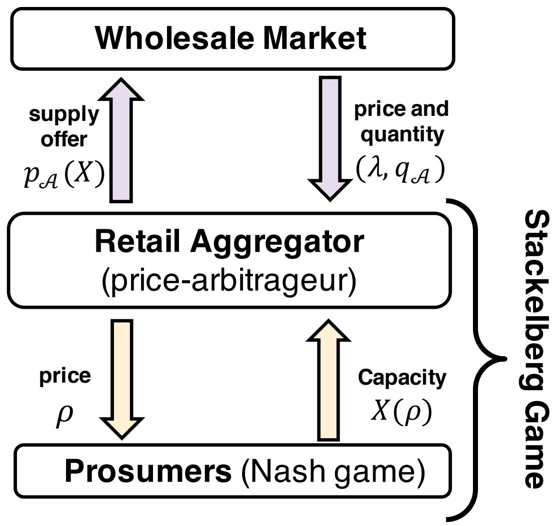

Figure 2.1: Interactions between prosumers, the DER aggregator, and the wholesale market.

We model the interaction between an aggregator $\mathscr{A}$ and prosumers with DERs as a Stackelberg game in Section 2.2. $\mathscr{A}$ procures DER capacities from prosumers upon offering them a uniform price, and sells the aggregated capacity at the wholesale market price, profiting from arbitrage. DER capacities are uncertain. $\mathscr{A}$ faces penalties for defaulting on its promised offer to the wholesale market that she allocates among the prosumers. We analyze the resulting interaction, depicted in Figure 2.1 via game theory and characterize its equilibria that explicitly models uncertainties in DER supply. In Section 2.3, we introduce a new metric we call *Price of Aggregation* (PoAg) that compares power procurement costs in the wholesale market from two different DER participation models. In the first model, prosumers participate through $\mathscr{A}$. In the second one, they participate directly and offer their capacities in the wholesale market. The second model serves as the ideal yet impractical benchmark for efficient DER participation. PoAg computes the efficiency loss due to the strategic nature of the aggregator. We analyze the game between $\mathscr{A}$ and the prosumers with various uncertainty models in DER capacities in Section 2.4 and leverage these insights to study price of aggregation for illustrative example markets in Section 2.5. The results demonstrate how uncertainty and the amount of DER integration affect the PoAg metric. We conclude the chapter in Section 2.6 with remarks and future research directions. This chapter has been published in [18]; proofs are omitted here for brevity.

2.2 The game between the prosumers and the DER aggregator

Consider a retail aggregator $\mathscr{A}$ who procures energy from a collection of prosumers $\mathbb{N} := \{1, \ldots, N\}$ with DERs and offers the aggregate supply into the wholesale electricity market. $\mathscr{A}$ does not own any generation or consumption asset. She purely acts as an intermediary. To procure DER supply, she announces a uniform price ρ for all prosumers at which she aims to buy energy from them. The latter respond by choosing how much energy each of the prosumers wishes to sell from their DERs such as rooftop photovoltaic panels, plug-in electric vehicles, wall-mounted batteries, thermostatically controlled loads, etc. DER supply is uncertain, owing to random variations in temperature, solar insolation, electric vehicle usage, etc. As a result, the realized aggregate supply from all prosumers may fall short of $\mathscr{A}$'s promised offer in the day-ahead (DA) market.[2] In that event, $\mathscr{A}$ faces a penalty for defaulting on its promise and allocates this penalty to the prosumers. In this section, we mathematize this interaction between $\mathscr{A}$ and the prosumers in $\mathbb{N}$ as a Stackelberg game (see Figure 2.1). [3] Later in this chapter, we explore how the outcomes of this game impact wholesale market efficiency.

Given a wholesale day-ahead market price λ_{DA}, $\mathscr{A}$ sets ρ, the price to procure energy from the prosumers. Then, prosumer $i \in \mathbb{N}$ responds by offering to sell x_i to $\mathscr{A}$, who then offers the aggregate procured DER supply[4]

$$X := \mathbf{1}^\intercal (x_1, \ldots, x_N)^\intercal := \mathbf{1}^\intercal \boldsymbol{x}$$

to the DA market at price λ_{DA}. Here, $\mathbf{1}$ is a vector of all ones of appropriate size. We assume that $\mathscr{A}$ is a price-taker in the wholesale market. That is, she believes that her wholesale offer will not influence the wholesale market prices. This assumption is natural as aggregators today typically do not command enough DER supply to exercise significant market power. In order to compute the DA offer, let $\mathscr{A}$ believe that its entire offer will be cleared in the DA market. Thus, $\mathscr{A}$ hopes to earn $(\lambda_{\text{DA}} - \rho)X$ from DA transactions. The revenue from DA sales stems from price arbitrage. $\mathscr{A}$ buys X from prosumers at price ρ and sells it to the wholesale market at price λ_{DA}, bagging the difference. Setting a higher ρ reduces the price difference from the DA market price, but generally incentivizes the prosumers to sell more of their DER supply, in turn, increasing the energy that $\mathscr{A}$ can offer in the DA market.

Assume that prosumers in $\mathbb{N}$ are homogenous, each of whom can supply power from a collection of DERs with installed capacity $\overline{C}$. Let $C_i \in [0, \overline{C}]$ denote the sum-total of capacities from all DERs with prosumer i. When offering to sell energy to $\mathscr{A}$, this capacity remains unknown. Denote by F, the joint cumulative distribution function (cdf) of

$$\boldsymbol{C} := (C_1, \ldots, C_N) \in [0, \overline{C}]^N.$$

DER supply being uncertain, $\mathscr{A}$ may not be able to supply X in real-time that is promised in the DA market. Assume that $\mathscr{A}$ buys back the deficit $(X - \mathbf{1}^\intercal \boldsymbol{C})^+$ at the real-time price λ_{RT}, where we use the notation $z^+ := \max\{z, 0\}$ for a scalar z. $\mathscr{A}$ then proceeds to allocate this penalty to the prosumers. We adopt the cost-sharing mechanism studied in [20] to design said penalties. Specifically, prosumer i pays the penalty

$$\phi(x_i, \boldsymbol{x}_{-i}; \boldsymbol{C}) := \lambda_{\text{RT}} \left(X - \mathbf{1}^\intercal \boldsymbol{C} \right)^+ \frac{(x_i - C_i)^+}{\sum_{j=1}^N (x_j - C_j)^+}. \tag{2.1}$$

[2] For ease of exposition, in this chapter, we do not consider spatial variations in prices. However, our conclusions remain applicable to such considerations.
[3] For a comprehensive discussion on Stackelberg games, see to [19].
[4] We do not consider economic witholding or strategic capacity reporting.

- Nonnegativity: $\phi(x_i, \boldsymbol{x}_{-i}; \boldsymbol{C}) \geq 0$.
- Budget balance: $\sum_{i=1}^{N} \phi(x_i, \boldsymbol{x}_{-i}; \boldsymbol{C}) = \lambda_{\mathrm{RT}}(X - \mathbf{1}^\intercal \boldsymbol{C})^+$.
- No exploitation: $x_i - C_i \leq 0 \implies \phi(x_i, \boldsymbol{x}_{-i}; \boldsymbol{C}) = 0$.
- Symmetry: $x_i - C_i = x_j - C_j \implies \phi(x_i, \boldsymbol{x}_{-i}; \boldsymbol{C}) = \phi(x_j, \boldsymbol{x}_{-j}; \boldsymbol{C})$.
- Monotonicity: $x_i - C_i \geq x_j - C_j \implies \phi(x_i, \boldsymbol{x}_{-i}; \boldsymbol{C}) \geq \phi(x_j, \boldsymbol{x}_{-j}; \boldsymbol{C})$.

Figure 2.2: Properties of the penalty sharing mechanism

The penalty depends on her own offer x_i, the collective offers $\boldsymbol{x}_{-i}$ of other prosumers and the realized supply $\boldsymbol{C}$. [5]

Such a penalty or cost sharing mechanism enjoys several desirable "fairness" axioms, thanks to the analysis in [20]. Each prosumer pays a fraction of the penalty that $\mathscr{A}$ pays for supply shortfall. A prosumer who is able to meet its promised supply does not pay any penalty. And, the penalty grows with the size of the shortfall. Finally, two prosumers with equal shortfalls face the same penalties. These properties are summarized mathematically in Figure 2.2.

Real-time transactions do not affect $\mathscr{A}$'s revenue as all shortfall penalties are passed on to the prosumers. $\mathscr{A}$ therefore seeks a price ρ that optimizes her profit from arbitrage in the day-ahead market and solves

$$\underset{\rho \geq 0}{\text{maximize}} \;\; \pi_{\mathscr{A}}(\rho, \boldsymbol{x}(\rho)) := (\lambda_{\mathrm{DA}} - \rho) X(\rho). \tag{2.2}$$

In the above problem, we make explicit the dependency of $\boldsymbol{x}$ and X on ρ. Wholesale markets often only allow aggregations of a minimum size to participate, e.g., CAISO requires a minimum capacity of 0.5 MW for a DER aggregator to participate [21]. Such restrictions can be included in (2.2); we ignore them for ease of exposition. In fact, our previous analysis in [22] showed that if one imposes a minimum capacity for the aggregator to participate, she might increase its offer price ρ to prosumers, attracting them to offer a sufficiently large aggregate capacity.

Prosumer i offers to sell x_i amount of energy to $\mathscr{A}$. In doing so, he trades off between supplying to $\mathscr{A}$ and consuming it locally. Denoting his utility of power consumption by u, prosumer i solves

$$\underset{0 \leq x_i \leq \overline{C}}{\text{maximize}} \;\; \pi_i(x_i, \boldsymbol{x}_{-i}, \rho) := \rho x_i + \mathbb{E}\left[u\left(d^0 + C_i - x_i\right) - \phi(x_i, \boldsymbol{x}_{-i}; \boldsymbol{C})\right], \tag{2.3}$$

[5] Our analysis of the prosumer's game remains unaffected if the price for the shortfall is different from the real-time market price λ_{RT}. If it is considered different, it may affect $\mathscr{A}$'s revenue, however.

given $\mathscr{A}$'s offer price ρ. By selling x_i to $\mathscr{A}$, she receives a compensation ρx_i at $\mathscr{A}$'s offer price ρ. Here, $d^0 \geq 0$ denotes the nominal energy consumption that prosumer i purchases at a fixed retail rate either from a distribution utility or $\mathscr{A}$. We ignore the cost considerations of nominal demand as it does not affect our analysis. Assume throughout that u is nonnegative, concave, and increasing. Also, we let $d^0 > \overline{C}$, i.e., DER supply is not large enough to cover the nominal demand.

Recall that prosumer i offers x_i before observing C_i and therefore, the aggregate real-time supply from all N prosumers can fall short of the promised supply. In that event, $\mathscr{A}$ faces a penalty that she allocates among the N prosumers, i's share being $\phi(x_i, \boldsymbol{x}_{-i}; \boldsymbol{C})$. Prosumers do not believe their energy sales will affect real-time prices. Hence, the expected penalty for prosumer i in (2.3) is given by

$$\mathbb{E}[\phi(x_i, \boldsymbol{x}_{-i}; \boldsymbol{C})] = \mathbb{E}[\lambda_{\mathrm{RT}}] \cdot \mathbb{E}\left[\left(X - \mathbf{1}^\intercal \boldsymbol{C}\right)^+ \frac{(x_i - C_i)^+}{\sum_{j=1}^N (x_j - C_j)^+}\right].$$

In the sequel, we abuse notation and write λ_{RT} in place of $\mathbb{E}[\lambda_{\mathrm{RT}}]$ throughout.

Given DA price λ_{DA} and expected real-time price λ_{RT}, the prosumer-aggregator interaction can be summarized as a Stackelberg game $\mathfrak{G}(\lambda_{\mathrm{DA}}, \lambda_{\mathrm{RT}})$. $\mathscr{A}$ acts as a Stackelberg leader who decides price ρ. Prosumers in $\mathbb{N}$ follow by responding simultaneously with energy offers $\boldsymbol{x}$. $\mathscr{A}$'s payoff is given by $\pi_{\mathscr{A}}$, while prosumer i's payoff is π_i. The pair $(\boldsymbol{x}^*(\rho^*), \rho^*)$ constitutes a Stackelberg equilibrium of $\mathfrak{G}(\lambda_{\mathrm{DA}}, \lambda_{\mathrm{RT}})$, if

$$\pi_i(x_i^*(\rho), \boldsymbol{x}_{-i}^*(\rho), \rho) \geq \pi_i(x_i, \boldsymbol{x}_{-i}^*(\rho), \rho)$$

for all $x_i \in [0, \overline{C}], \rho \geq 0, i \in \mathbb{N}$, and

$$\pi_{\mathscr{A}}(\rho^*, \boldsymbol{x}^*(\rho^*)) \geq \pi_{\mathscr{A}}(\rho, \boldsymbol{x}^*(\rho))$$

for all $\rho \geq 0$. We establish in Theorem 1 when such an equilibrium exists and is unique in the prosumer-aggregator game. The following assumption proves useful in the proof.

Assumption 1 (Random DER capacities)**.** *F is smooth, fully supported on $[0, \overline{C}]^N$, and invariant under permutations.*

Smoothness and full support imply that DER capacities do not have any probability mass, and F is strictly increasing in each argument over $[0, \overline{C}]^N$. Invariance under permutations is natural for geographically co-located DERs, implying that prosumers' supplies are exchangeable. Given this assumption, $\mathfrak{G}(\lambda_{\mathrm{DA}}, \lambda_{\mathrm{RT}})$ becomes a symmetric game among the prosumers. We establish the existence of a Stackelberg equilibrium with symmetric reactions from prosumers. Later in this chapter, we explicitly compute such equilibria and study their nature.

Theorem 1 (Existence and Uniqueness)**.** *Suppose Assumption 1 holds. Then, a Stackelberg equilibrium $(\boldsymbol{x}^*(\rho^*), \rho^*)$ always exists for $\mathfrak{G}(\lambda_{DA}, \lambda_{RT})$ with a unique symmetric response from prosumers,* *i.e.,* $x_i^*(\rho) = x^*(\rho)$ *for each* $\rho \geq 0$ *and* i *in* $\mathbb{N}$. *Furthermore, if for all* $\rho > 0$,

$$\frac{1}{2}(\lambda_{DA} - \rho)\frac{\partial^2 X^*(\rho)}{\partial \rho^2} < \frac{\partial X^*(\rho)}{\partial \rho} \tag{2.4}$$

the Stackelberg equilibrium with symmetric prosumer response is unique with $X^*(\rho) = \mathbf{1}^\intercal \boldsymbol{x}^*(\rho)$.

Our proof leverages a result from [23] that guarantees the existence of a symmetric Nash equilibrium of the game among prosumers, given $\mathscr{A}$'s price.[6] Exploiting the properties of the penalty sharing mechanism, we further establish that there exists a unique symmetric Nash equilibrium $\boldsymbol{x}^*(\rho)$ that varies smoothly with ρ. $\mathscr{A}$ will never opt for a price higher than λ_{DA} and her profit varies smoothly in $\rho \in [0, \lambda_{\text{DA}}]$. The smooth profit attains a maximum over that interval, leading to existence of a Stackelberg equilibrium. The relation in (2.4) implies that $\mathscr{A}$'s profit becomes strictly concave and hence, the maximum and the equilibrium become unique.

Next, we quantify the impact of DERs on wholesale market efficiency along the equilibrium path in the prosumer-aggregator game.

2.3 Price of aggregation

Prosumers with available supply capacity can supplant conventional generation. Our goal is to characterize the impact of prosumer supply on the efficiency of the wholesale market. With a stylized wholesale market model, we compute the total energy procurement cost under two different models of prosumer participation. In the first model, aggregator $\mathscr{A}$ offers the aggregated procured supply capacity from individual prosumers to the wholesale market. The second model describes the ideal benchmark, where prosumers offer their supply capacity directly to the wholesale market. The comparison of the energy procurement costs in these two frameworks for prosumer participation leads to what we call the price of aggregation.

Consider a day-ahead wholesale market with dispatchable conventional generators and prosumers (participating directly or through an aggregator) competing to supply a point forecast of an inelastic demand D. Consider G dispatchable generators, labelled $1, \ldots, G$. Let producer j supply Q_j amount of energy within its production capability set as $\left[\underline{Q}_j, \overline{Q}_j\right]$. Let its dispatch cost for producing Q_j be given by $c_j(Q_j)$, where c_j is a convex, nondecreasing and nonnegative function. We assume that c_j truly reflects the production costs of the generator. In other words, we neglect possible market power of dispatchable power producers [25–27], leaving a study of effects of strategic interactions of conventional generators and aggregated prosumer supply to future endeavors. The economic dispatch problems in these two participation models that the system operator solves in day-ahead to clear the wholesale market are as follows.[7]

---

[6] We remark that when prosumers are not homogenous and F is not permutation invariant, Rosen's result in [24] still guarantees the existence of a Nash equilibrium in the game among prosumers.

[7] We have ignored transmission network constraints in the wholesale market description for ease of exposition. Intro-

When prosumers participate in the wholesale market through $\mathscr{A}$, the system operator clears the DA market by solving

$$\begin{aligned}
\mathscr{C}^*_{\mathscr{A}} := \quad & \underset{q_{\mathscr{A}}, \boldsymbol{Q}}{\text{minimum}} && \sum_{j=1}^{G} c_j(Q_j) + \int_0^{q_{\mathscr{A}}} p_{\mathscr{A}}(y)dy, \\
& \text{subject to} && \underline{Q}_j \leq Q_j \leq \overline{Q}_j, \;\; 0 \leq q_{\mathscr{A}} \leq X, \\
& && \sum_{j=1}^{G} Q_j + q_{\mathscr{A}} = D.
\end{aligned} \tag{2.5}$$

The inverse supply offer $p_{\mathscr{A}}(y)$ indicates the minimum price at which $\mathscr{A}$ is willing to sell y amount of energy. The aggregated supply capacity for a wholesale market price $p_{\mathscr{A}}$ is given by $X[\rho^*(p_{\mathscr{A}})]$, where $X = \mathbf{1}^T \boldsymbol{x}(\rho)$, and $(\boldsymbol{x}(\rho^*), \rho^*)$ is the Stackelberg equilibrium of the game $\mathfrak{G}(p_{\mathscr{A}}, \lambda_{\text{RT}})$. By utilizing the equilibrium price path $\rho^*(p_{\mathscr{A}})$ and taking the inverse of $X[\rho^*(p_{\mathscr{A}})]$, one can compute the inverse supply offer $p_{\mathscr{A}}(X)$. Once (2.5) is solved, the day-ahead price λ_{DA} is given by the optimal Lagrange multiplier of the supply-demand balance constraint.

When prosumers directly participate in the wholesale market, the system operator clears the DA market by solving

$$\begin{aligned}
\mathscr{C}^*_{\mathscr{P}} := \quad & \underset{\boldsymbol{q}, \boldsymbol{Q}}{\text{minimum}} && \sum_{j=1}^{G} c_j(Q_j) + \sum_{i=1}^{N} \int_0^{q_i} p_i(y_i)dy_i, \\
& \text{subject to} && \underline{Q}_j \leq Q_j \leq \overline{Q}_j, \;\; 0 \leq q_i \leq \overline{C}, \\
& && \sum_{j=1}^{G} Q_j + \sum_{i=1}^{N} q_i = D.
\end{aligned} \tag{2.6}$$

Here, $p_i(y_i)$ is the inverse supply offer for each prosumer. Given a wholesale market price p_i faced by prosumer i, his response $y_i(p_i)$ is computed by solving

$$\underset{y_i \in [0, \overline{C}]}{\text{argmax}} \left\{ p_i y_i + \mathbb{E}\left[u\left(d^0 + C_i - y_i\right) - \lambda_{\text{RT}}(y_i - C_i)^+ \right] \right\}. \tag{2.7}$$

Taking the inverse of $y_i(p_i)$, one can compute $p_i(y_i)$. The day-ahead price λ_{DA} is the optimal Lagrange multiplier of the supply-demand balance constraint. Note that here, there is no cost sharing game among prosumers, as they are directly penalized for their corresponding shortfalls. Alternatively, one can take $y_i(p_i)$ to be the symmetric equilibrium response by prosumers $y(p)$, taking into account their cost shares, and then finding its inverse $p(y)$. In that case, the benchmark model is one in which DER supplies are concatenated via a purely social aggregator, who does not make profits from price arbitrage. Our analysis and insights in this paper are largely unaffected by such a variant of the benchmark model.

ducing these constraints causes no conceptual difficulty.

The supply capacity of a prosumer is typically too small for consideration in a wholesale market, and computing the dispatch and settlement for a large number of prosumers places an untenable computational burden on the system operator. To complicate matters, a transmission system operator typically does not have visibility into a distribution network. Hence, neither can they ensure that the DER dispatch will induce feasible flows in the distribution network, nor can they audit the actual supply. It is imperative that DER supply capacities are aggregated for participation in the wholesale market. The idealized direct prosumer participation model serves as a benchmark for the performance of any aggregation mechanism. Our other model for prosumer participation analyzes the case of a single profit-maximizing DER aggregator who chooses to represent the supplies from all prosumers in a system operator's footprint. In reality, such an entity will either be regulated or several aggregators will compete for prosumer representation, e.g., in [28]. The loss in efficiency due to the strategic incentives of this single aggregator represents the maximum such loss the market will endure. Extending the model to incorporate competition for aggregation remains an interesting direction for future research. Without DER participation, the market does not harness possible resources, and hence, is inefficient. However, the presence of $\mathscr{A}$ brings an efficiency loss due to the strategic incentives of $\mathscr{A}$, compared to the benchmark case in which prosumers participate directly in the wholesale market. We introduce the following metric of efficiency loss.

Definition 1. *The Price of Aggregation (*PoAg*) is given by* $\frac{\mathscr{C}^*_{\mathscr{A}}}{\mathscr{C}^*_{\mathscr{P}}}$*, where* $\mathscr{C}^*_{\mathscr{A}}$ *is computed using the Stackelberg equilibrium supply offer and* $\mathscr{C}^*_{\mathscr{P}}$ *is computed using* (2.6).

$\mathsf{PoAg} \geq 1$ measures the efficiency loss of prosumer participation through an aggregator compared to direct prosumer participation. A larger PoAg indicates a higher efficiency loss due to aggregation. We will now analyze PoAg in various settings. To do so, one needs to construct the supply offers, that in turn, depends on the equilibrium in $\mathfrak{G}(\lambda_{\text{DA}}, \lambda_{\text{RT}})$. We construct these supply offers under two extreme cases for the stochasticity of DER supply.

2.4 Studying the equilibrium of $\mathfrak{G}(\lambda_{\mathbf{DA}}, \lambda_{\mathbf{RT}})$.

While Theorem 1 guarantees the existence of a Stackelberg equilibrium, it does not offer insights into the structure of said equilibrium. For general probability distributions on DER capacities in $\boldsymbol{C}$, characterization of such equilibrium remains challenging. Here, we study two settings for which such computation is easy–one where the capacities are completely dependent with identical components in $\boldsymbol{C}$, and the other where the capacities are independent but identically distributed (iid). One expects the capacities in practice to follow a distribution that is somewhere between these two extremes.

To motivate these two regimes, imagine that prosumers are supplying energy from rooftop solar. For geographically co-located prosumers, one expects high correlation among C_i's. If two prosumers are geographically separated, independence among C_i's might arise. A more realistic model is one with a collection of prosumer clusters that have highly correlated supply capacities within clusters, but independent between clusters. We relegate such considerations to future efforts and examine the two simpler settings here.

We study the iid case through the lens of mean-field (MF) games in the large prosumer limit $N \to \infty$. Such games have gained popularity following the seminal works in [29, 30] and are particularly useful to analyze interactions among a large number of players, where players respond to the population as a whole. Taking $N \to \infty$ in $\mathfrak{G}(\lambda_{\mathrm{DA}}, \lambda_{\mathrm{RT}})$ yields

$$\frac{\left(\sum_{j=1}^{N}(x_j - C_j)\right)^{+}/N}{\sum_{j=1}^{N}(x_j - C_j)^{+}/N} \to \beta \text{ almost surely,} \tag{2.8}$$

following the law of large numbers, where β is a constant. Then, the penalty of shortfall for prosumer i becomes $\beta \lambda_{\mathrm{RT}}(x_i - C_i)^{+}$ and he maximizes

$$\mathbb{E}\left[u\left(d^0 + C_i - x_i\right) + \rho x_i - \beta \lambda_{\mathrm{RT}}(x_i - C_i)^{+}\right], \tag{2.9}$$

given β. Further, β is such that the solution of the above maximization satisfies (2.8). Jensen's inequality on $f(z) = z^{+}$ yields $0 \le \beta \le 1$. Call this game $\mathfrak{G}^{\infty}(\lambda_{\mathrm{DA}}, \lambda_{\mathrm{RT}})$.

Theorem 2 (Prosumer Offer Characterization)**.** *Suppose Assumption 1 holds. If $\boldsymbol{C}$ has identical components, i.e., $C_i = C$ for $i \in \mathcal{N}$, then the prosumer offers for any $\rho \ge 0$ in $\mathfrak{G}(\lambda_{DA}, \lambda_{RT})$ satisfy*

$$F(x^*(\rho)) = \frac{1}{\lambda_{RT}}\left(-\mathbb{E}\left[u'(d^0 + C - x^*(\rho))\right] + \rho\right). \tag{2.10}$$

If C_i's are iid, then in the limit $N \to \infty$, the prosumer offers $x^*(\rho)$ for any $\rho \ge 0$ in $\mathfrak{G}^{\infty}(\lambda_{DA}, \lambda_{RT})$ satisfy

$$\beta F_i(x^*(\rho)) = \frac{1}{\lambda_{RT}}\left(-\mathbb{E}\left[u'(d^0 + C_i - x^*(\rho))\right] + \rho\right), \tag{2.11}$$

where $\beta \in [0,1]$ is defined as

$$\beta = \frac{x^*(\rho) - \mathbb{E}[C_i]}{\mathbb{E}\left[(x^*(\rho) - C_i)^{+}\right]}. \tag{2.12}$$

The expressions in (2.10) and (2.11) are quite similar, implying that equilibrium offers of prosumers in $\mathfrak{G}(\lambda_{\mathrm{DA}}, \lambda_{\mathrm{RT}})$ behave similarly between the two extreme settings with completely dependent and independent DER capacities. These two settings provide the best and the worst-case PoAg. The case with correlated but not fully dependent capacities in practice lies between these two extremes.

As the capacities become independent, the solution to the mean-field game satisfies $x^*(\rho) \ge \mathbb{E}[C_i]$ owing to $\beta \ge 0$. That is, a prosumer may offer more than his mean anticipated capacity. This optimism stems from independence in supply capacities; a prosumer hopes that other prosumers will likely cover any shortfall on his part, leading to zero penalty. In contrast, prosumers with completely dependent capacities may choose $x^*(\rho) < \mathbb{E}[C_i]$ for small enough ρ. The room for optimism disappears as all prosumers face the same uncertainty. Equipped with these insights into the equilibrium in $\mathfrak{G}(\lambda_{\mathrm{DA}}, \lambda_{\mathrm{RT}})$, we study the impact of DER aggregation on wholesale market efficiency through illustrative examples next.

2.5 Illustrative examples

We now study equilibrium offers of an example collection of prosumers, the same for an aggregator who participates in a wholesale market, and the resulting price of aggregation. Assume throughout that N prosumers have linear utilities defined by $u(z) = \gamma z$ with $\gamma > 0$. Accurately modeling the preferences $u(\cdot)$ of end-use customers in electricity consumption remains a challenging task (see [31] for a discussion) and it is beyond the scope of this chapter. While we adopt linear utilities here, we remark that logarithmic utilities are commonly used in the economics literature [32] for various commodities, and has recently found applications in the electricity market literature as well, e.g., in [28, 33, 34]. Using logarithmic utilities, along with deterministic DER supply, our previous analysis in [22] reveals similar insights for price of aggregation. In this work, we adopt linear utilities for ease of exposition and offer insights into the impact of uncertainty.

First, we examine the special case in which DER supply is deterministically $\overline{C}$, i.e., $C_i = \overline{C}$. Then, $\phi = 0$ and the payoffs of each prosumer is decoupled, given ρ. Each prosumer responds to ρ by solving

$$\underset{0\leq x\leq \overline{C}}{\text{maximize}} \;\; u(d^0 + \overline{C} - x) + \rho x.$$

If $\rho > \gamma$, each prosumer picks $x^* = \overline{C}$. As we show next, $\rho > \gamma$ is not sufficient for prosumers to sell their entire capacities when $\boldsymbol{C}$'s are stochastic in nature.

Proposition 1. *If $C_i = C,\; i \in \mathbb{N}$ is uniformly distributed in $[\mu - \sqrt{3}\sigma, \mu + \sqrt{3}\sigma]$, then the unique Stackelberg equilibrium $(\boldsymbol{x}^*(\rho^*), \rho^*)$ of $\mathfrak{G}(\lambda_{DA}, \lambda_{RT})$ satisfies*

$$x^*(\rho) = \mu - \sqrt{3}\sigma + \frac{2}{\lambda_{RT}}(\rho - \gamma)\sqrt{3}\sigma, \textit{ for } \rho \geq \gamma,$$

$$\rho^* = \frac{1}{2}(\lambda_{DA} + \gamma) - \frac{\lambda_{RT}(\mu - \sqrt{3}\sigma)}{4\sqrt{3}\sigma},$$

where

$$\sigma \in \left[\frac{\lambda_{RT}\mu}{2\sqrt{3}(\lambda_{DA} - \gamma + \lambda_{RT}/2)}, \frac{\mu}{\sqrt{3}}\right].$$

In the presence of uncertainty, prosumers' response increases linearly in ρ, leading to the uniqueness of the Stackelberg equilibrium, similar to what we obtained in Theorem 1. Larger the average random capacity μ, higher is the amount prosumers agree to sell. Higher the randomness, as captured by σ, lesser is the amount prosumers offer, owing to possible penalties they might face. Also, penalties are proportional to λ_{RT}. Consequently, increasing λ_{RT} decreases their offers. Higher the possible penalty, either due to higher σ or higher λ_{RT}, aggregator needs to increase its price offer ρ^* to attract DER supply. The bounds on σ are the ones for which the equilibrium path is well-defined.

Figure 2.3 visualizes the effect of varying σ. The plot corroborates our discussion above. For σ in the above range, we have $x^*(\rho) < \mu/2$. Contrast this result with iid capacities. Theorem 2

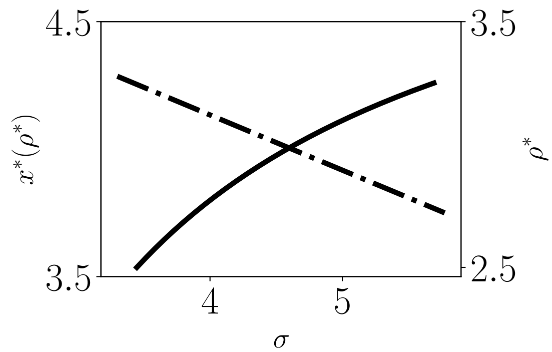

Figure 2.3: Variation of equilibrium offer $x^*(\rho)$ and $\mathscr{A}$'s offer price ρ^* with linear utilities. We choose $\gamma = 2.5, \mu = 10, \lambda_{\text{DA}} = 4, \lambda_{\text{RT}} = 4$.

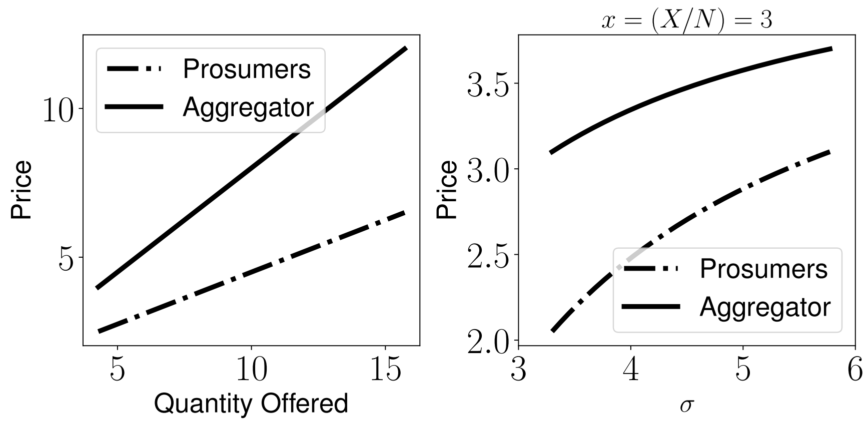

Figure 2.4: Left: Equilibrium supply offers. Here, $\gamma = 2.5, \mu = 10, \sigma = 3.3$, and $\lambda_{\text{RT}} = 4$. Right: The influence of varying σ on supply offers, for a fixed supply quantity.

reveals that the mean-field solution satisfies $x^*(\rho) \geq \mu$. In fact for this problem, we have $\beta = 0$ and $x^*(\rho) = \mu$ for $\rho \geq \gamma$ and $\rho^* = \gamma$. The offer with iid capacities can be significantly higher than with identical capacities.

2.5.1 Inverse supply functions

The equilibrium of $\mathfrak{G}(p_{\mathscr{A}}, \lambda_{\text{RT}})$ characterized in Proposition 1 implies the following aggregated supply as a function of $\mathscr{A}$'s price offer $p_{\mathscr{A}}$:

$$X[\rho^*(p_{\mathscr{A}})] = \frac{N}{2}\left[\mu - \sqrt{3}\sigma + \frac{2}{\lambda_{\text{RT}}}(p_{\mathscr{A}} - \gamma)\sqrt{3}\sigma\right] \tag{2.13}$$

The aggregator's inverse supply offer is then described by its inverse

$$p_{\mathscr{A}}(X) = \lambda_{\text{RT}}(2X/N - \mu + \sqrt{3}\sigma)/(2\sqrt{3}\sigma) + \gamma. \tag{2.14}$$

The best response provided by Proposition 1 analogously solves (2.7), since capacities are completely dependent and prosumers are identical. The optimal supply offer by each prosumer is then

$$x(p) = \mu - \sqrt{3}\sigma + \frac{2}{\lambda_{\mathrm{RT}}}(p-\gamma)\sqrt{3}\sigma. \tag{2.15}$$

Each prosumer's offer enters the objective function in problem (2.6) via its induced cost given by

$$p(x) = \lambda_{\mathrm{RT}}(x - \mu + \sqrt{3}\sigma)/(2\sqrt{3}\sigma) + \gamma. \tag{2.16}$$

It is of importance to contrast how the aggregate supply capacity of the prosumers get offered in the wholesale market under two different prosumer participation models, using (2.14) when $\mathscr{A}$ is present, and using (2.16) for the prosumers-only case. Aggregator $\mathscr{A}$ offers the same supply capacity at a higher price than the collection of prosumers in aggregate. This price inflation is a consequence of the aggregator's aim to maximize her profits from arbitrage between the wholesale market prices and the prices she offers the prosumers (see Figure 2.4). To elaborate on the effects of uncertainty, we fix a quantity X/N, and then vary σ. We observe that as the variance increases, DER owners require higher prices that are also closer to $\mathscr{A}$'s offer price. This is a consequence of the risks of paying a penalty for the shortfall.

2.5.2 The price of aggregation

We now exploit the results in the previous subsection to analytically characterize the PoAg in the next proposition.

Proposition 2. *In a wholesale market with N DER suppliers, and one conventional generator with cost*

$$c(Q) = \kappa Q, \qquad \kappa > \gamma, \qquad Q \in [0, \infty],$$

the PoAg *is given by* $\mathscr{C}^*_{\mathscr{A}}/\mathscr{C}^*_{\mathscr{P}}$, *where*

$$\begin{aligned}
\mathscr{C}^*_{\mathscr{A}} &= \kappa D - \frac{Nq^*}{2}\left(\kappa - \gamma + \frac{\lambda_{RT}(\mu - \sqrt{3}\sigma)}{2\sqrt{3}\sigma} - \frac{q^*\lambda_{RT}}{4\sqrt{3}\sigma}\right),\\
\mathscr{C}^*_{\mathscr{P}} &= \kappa D - Nq^*\left(\kappa - \gamma + \frac{\lambda_{RT}(\mu - \sqrt{3}\sigma)}{2\sqrt{3}\sigma} - \frac{q^*\lambda_{RT}}{4\sqrt{3}\sigma}\right),\\
q^* &= \mu - \sqrt{3}\sigma + \frac{2}{\lambda_{RT}}(\kappa - \gamma)\sqrt{3}\sigma,\\
\sigma &\in \left[\frac{\lambda_{RT}\mu}{2\sqrt{3}(\lambda_{DA} - \gamma + \lambda_{RT}/2)}, \frac{\mu}{\sqrt{3}}\right].
\end{aligned}$$

Furthermore, in the absence of DER supply, the optimal procurement cost is κD.

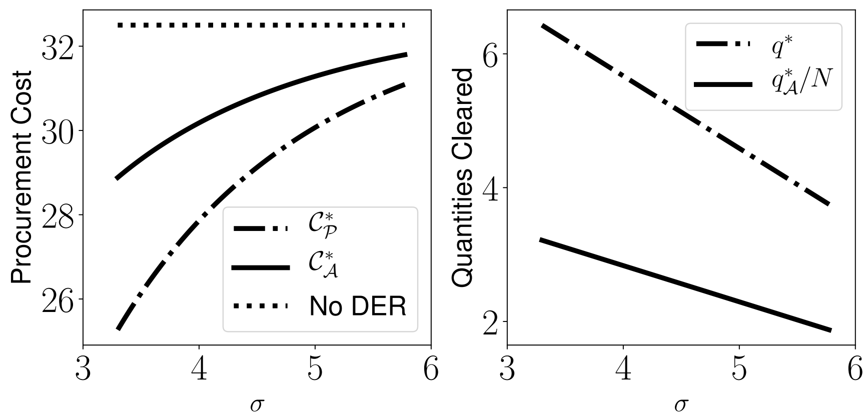

Figure 2.5: Left: Procurement costs as σ increases for 3 cases: without DER supply (maximum cost), with DER supply and the existence of the aggregator (partial savings), and when prosumers offer their DER supply directly to the system operator (minimum cost). Increasing uncertainty makes DER participation unattractive to participants. Right: DER quantities cleared as σ increases. More utilization of resources when DER owners directly participate. We use $\mu = 10, \lambda_{\mathrm{RT}} = 4, \gamma = 2.5, \kappa = 3.25, D/N = 10$.

One can readily observe by the above proposition that

$$\kappa D > \mathscr{C}^*_{\mathscr{A}} > \mathscr{C}^*_{\mathscr{P}}.$$

Figure 2.5 plots the optimal procurement costs and quantities cleared as σ varies. As one expects, procurement costs are minimized when prosumers offer their supply directly to the wholesale market, and savings diminish as uncertainty increases. Aggregation via profit-maximizing $\mathscr{A}$ strikes a balance between two extreme possibilities; no DER supply, and direct DER participation to the wholesale market. This is also consistent with the supply curves in Figure 2.4. We note that intermediaries are inevitable, given the current wholesale market structures.

As the uncertainty increases, PoAg gets smaller as prosumers choose to sell less energy to the wholesale market, leaving $\mathscr{A}$ with smaller profits. As the DER integration increases, more prosumers sell energy, leading to increased profits for the aggregator. The worst-case PoAg is attained at 100% integration and σ being near its lowest possible value at which the equilibrium path is well-defined. Such a $\mathsf{PoAg} \approx 1.15$ here, which implies that the cost with the aggregator is at most 15% higher than the benchmark case. Both costs are still smaller than having no DER participation at all. Figure 2.6 illustrates these tradeoffs.

2.6 Conclusions and future directions

Our analysis points to debates surrounding the right design choice for incorporation of DERs in wholesale electricity markets. Should they be aggregated by third-party for-profit aggregators, perhaps where they vie to represent prosumers' supplies in the wholesale electricity market? Or, should a not-for-profit entity such as an independent distribution system operator be established to

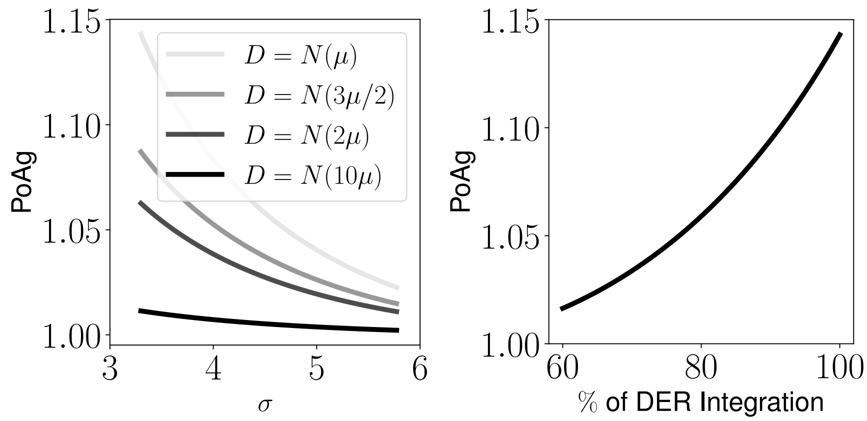

Figure 2.6: Left: The price of aggregation as σ increases. The PoAg is monotonically decreasing with σ. PoAg improves as DER contributes less towards the overall demand. Right: The Price of Aggregation vs. % of DER supply. The PoAg is monotonically increasing with DER integration. We use $\lambda_{\text{RT}} = 4, \gamma = 2.5$, and $\kappa = 3.25$. For the curve on the right, $D/N = 10, \sigma = 3.3$, and μ varies from 6 to 10, reflecting percentage of integration.

harness supply capacities of resources at the grid-edge? While the debates themselves are beyond the scope of this chapter, we have provided a framework to quantify the benefits of different design choices.

In this chapter, we considered and compared two different models of DER participation in wholesale electricity markets. In the first model, DERs directly offer their capacities in the wholesale market, while in the second one DERs participate in aggregate via a third-party for-profit aggregator. We modeled the strategic interactions between prosumers and the aggregator as a stochastic Stackelberg game. We characterized equilibria and explored two extreme cases: DER capacities are completely dependent or independent and identically distributed. At the equilibrium, we quantified the effects of aggregation through a metric we called Price of Aggregation (PoAg).

There are several directions for future work. We assumed the DER aggregator to be a price-taker in the wholesale market. However, under high penetration of DERs, it may be possible that aggregators can influence the wholesale market price and engage in strategic bidding, especially if they are located in transmission "load pockets" formed due to congestion in the transmission network. Furthermore, wholesale electricity markets typically have multiple settlements for energy procured in each hour. Analysis of DER participation with and without an aggregator with stochastic supply and multi-settlement wholesale market structure is another important direction for future work.

In our current work, we have only considered the efficiency impacts of a single for-profit DER aggregator. Competition among several competing DER aggregators will likely shrink the efficiency losses that result from the profit motivation of these aggregators. We aim to analytically and empirically characterize how this competition will impact the overall market efficiency. Only then, can we provide a more complete answer to the question whether DER coordination must occur via competing for-profit aggregators or it necessitates a neutral/independent distribution system operator.

3. On Convex Relaxation-Based Distribution Locational Marginal Prices

3.1 Introduction

The deepening penetration of distributed energy resources (DERs) coupled with the need to harness demand flexibility of end-use consumers has led to a rapidly increasing interest in defining appropriate price signals for distribution networks [1, 9, 11, 35, 36]. The proposals have tried to emulate the experience from wholesale electricity markets and locational marginal prices (LMPs). These prices have been commonly referred to as distribution LMPs or DLMPs. Ideally, such prices will encode grid requirements that DERs will respond to.

The core theoretical framework for spot pricing of electricity [37] is ideally suited to a lossless linearized network model, often utilizing the so-called DC approximations[1]. Prices defined using market clearing problems with linearized power flow models exhibit a number of desirable qualities. These properties are typically a consequence of the convexity of the market clearing problem. Such linearizations, however, often ignore considerations of losses, voltage magnitudes and reactive power in the network–considerations that cannot be ignored in distribution grids. Specifically, distribution grids have relatively high resistance to reactance ratios and reactive power injections play an important role in maintaining voltage magnitudes within specified limits. Thus, a direct extension of LMPs with DC approximations of power flow equations to the distribution grids is not appropriate.

In order to take into account the necessary characteristics of distribution networks, we derive our prices for real and reactive power from a second-order cone programming (SOCP) based convex relaxation of the dispatch problem with nonlinear AC power flow equations. Popularized by [39, 40], these relaxations seek to optimize grid assets over a convex set that contains the feasible set described by the power flow equations. The SOCP based convex relaxation with branch flow model has been extensively analyzed in [41–43] and is particularly suitable for radial distribution networks. Under certain conditions, these relaxations often yield an optimal solution that satisfies the power flow equations, e.g., see [43, 44]. Authors of [1, 45] have utilized duality theory of this SOCP relaxation to define DLMPs. However, they do not accompany their proposals with an analysis that justifies their design from an economic standpoint—the precise focus of our current effort.

In this chapter, we restrict our attention to the mathematical foundations of DLMPs and sidestep issues surrounding the adoption of such pricing schemes to harness DERs. See [46] for insightful discussions on the same. We align with the view in [36] to consider a retail market operated by an independent distribution system operator (DSO) responsible for dispatch and pricing of resources

[1] See [38] for the perils of ad hoc measures to include losses.

in the distribution network.

In Section 3.2, we describe the branch flow model for radial distribution networks that we utilize to formulate the dispatch and the pricing problems in Section 3.3. In Section 3.4, we identify conditions under which the DLMPs—derived from the SOCP relaxation of the dispatch problem—support an efficient market equilibrium and are revenue adequate. These properties provide the economic rationale behind adopting DLMPs derived from SOCP-based relaxations in a retail market environment. We illustrate our theoretical results via illustrative examples in Section 3.5, and conclude the chapter in Section 3.6. This chapter is based on our published work in [47]; we remove mathematical proofs in this chapter for brevity.

3.2 Modeling the radial distribution network

Distribution grids are often multi-phase unbalanced networks with components such as capacitor banks and tap-changing transformers that play a vital role in maintaining voltage magnitudes within specified limits. In this work, we ignore these special characteristics and model the distribution grid as a single-phase equivalent of a three-phase network, where controllable and uncontrollable assets operated by asset-owners connect at the various buses of the network.

Throughout, let $\mathbb{R}$ and $\mathbb{C}$ denote the sets of real and complex numbers, respectively. For $y \in \mathbb{C}$, denote its real and imaginary parts by $\mathrm{Re}(y)$ and $\mathrm{Im}(y)$, respectively, and $\mathbf{i} := \sqrt{-1}$. Vectors and matrices are distinguished with boldfaced letters.

Consider a radial electric distribution network on n buses, the collection of which is defined by $\mathbb{N}$. By radial, we mean that the network does not contain any cycles. Represent the network by a directed graph with $\mathbb{E}$ as the collection of m directed edges. For k and ℓ in $\mathbb{N}$, the edge $k \to \ell \in \mathbb{E}$ represents a line joining k and ℓ. The directions of the edges are chosen arbitrarily.

Let $V_k \in \mathbb{C}$ be the voltage phasor at each bus $k \in \mathbb{N}$. For each $k \to \ell \in \mathbb{E}$, Ohm's law dictates

$$V_k - V_\ell = z_{k\ell} I_{k\ell}, \tag{3.1}$$

where $z_{k\ell} := r_{k\ell} + \mathbf{i} x_{k\ell}$ is the complex impedance of the line and $I_{k\ell}$ is the current phasor from bus k to bus ℓ. Then, the sending-end apparent power flow on $k \to \ell$ is given by

$$S_{k\ell} := P_{k\ell} + \mathbf{i} Q_{k\ell} = V_k I_{k\ell}^{\mathsf{H}}, \tag{3.2}$$

where we use the notation y^{H} to denote the complex conjugate of y. The apparent power received at bus ℓ from bus k is then given by

$$V_\ell I_{k\ell}^{\mathsf{H}} = (V_\ell - V_k) I_{k\ell}^{\mathsf{H}} + V_k I_{k\ell}^{\mathsf{H}} = -z_{k\ell} J_{k\ell} + S_{k\ell}, \tag{3.3}$$

where $J_{k\ell} := |I_{k\ell}|^2$ denotes the squared current magnitude on line $k \to \ell$. Enforcing power balance at each bus utilizing (3.2) and (3.3), we get[2]

$$\begin{aligned} p_k^G - p_k^D &= \sum_{\ell':k\to\ell'} P_{k\ell'} - \sum_{\ell':\ell'\to k} \left(P_{\ell' k} - r_{\ell' k} J_{\ell' k}\right), \\ q_k^G - q_k^D &= \sum_{\ell':k\to\ell'} Q_{k\ell'} - \sum_{\ell':\ell'\to k} \left(Q_{\ell' k} - x_{k\ell'} J_{\ell' k}\right). \end{aligned} \tag{3.4}$$

Here we assume that each bus has a controllable generation resource injecting an apparent power of $p_k^G + \mathbf{i} q_k^G$ at bus k and an uncontrollable demand drawing $p_k^D + \mathbf{i} q_k^D$ at bus k. The demands are assumed known and the generation resources can produce power within known capacity limits, satisfying

$$\underline{p}_k^G \le p_k^G \le \overline{p}_k^G, \qquad \underline{q}_k^G \le q_k^G \le \overline{q}_k^G. \tag{3.5}$$

An uncontrollable generation resource is modeled as a negative demand in our formulation and a controllable load as negative generation. Associate with the injection of $p_k^G + \mathbf{i} q_k^G$ the cost $c_k(p_k^G, q_k^G)$ that is linear in its arguments. Such costs can encode both production costs and disutility of deferred demand. In a retail market environment, such costs will be inferred from supply offers and demand bids. Our results largely continue to hold with general convex costs.

Thermal considerations dictate an upper bound on the amount of current flowing over a line. We include these constraints as limits on both sending-end and receiving-end real powers on $k \to \ell$ in[3]

$$P_{k\ell} \le f_{k\ell}, \qquad r_{k\ell} J_{k\ell} - P_{k\ell} \le f_{k\ell}, \tag{3.6}$$

where $f_{k\ell} > 0$ denotes the line capacity. Let $w_k := |V_k|^2$ be the squared voltage magnitude at bus k that is constrained as

$$\underline{v}_k^2 \le w_k \le \overline{v}_k^2 \tag{3.7}$$

with known limits $\underline{v}_k^2$, $\overline{v}_k^2$. From (3.2), we obtain

$$P_{k\ell}^2 + Q_{k\ell}^2 = |S_{k\ell}|^2 = |V_k|^2 \, |I_{k\ell}|^2 = w_k J_{k\ell} \tag{3.8}$$

and the definition of w's yield

$$w_k - w_\ell = V_k V_k^{\mathsf{H}} - V_\ell V_\ell^{\mathsf{H}} = V_k z_{k\ell}^{\mathsf{H}} I_{k\ell}^{\mathsf{H}} + z_{k\ell} I_{k\ell} V_\ell^{\mathsf{H}}.$$

Leveraging (3.2) and (3.3) in the above equation becomes

$$\begin{aligned} w_k - w_\ell &= z_{k\ell}^{\mathsf{H}} S_{k\ell} + z_{k\ell} \left(S_{k\ell} - z_{k\ell} J_{k\ell}\right)^{\mathsf{H}} \\ &= 2\mathrm{Re}\left(z_{k\ell}^{\mathsf{H}} S_{k\ell}\right) - |z_{k\ell}|^2 J_{k\ell} \\ &= 2(P_{k\ell} r_{k\ell} + Q_{k\ell} x_{k\ell}) - (r_{k\ell}^2 + x_{k\ell}^2) J_{k\ell}. \end{aligned} \tag{3.9}$$

[2] We ignore shunt admittances and associated currents for simplicity.
[3] See [1, 43] for alternate definitions of line capacity limits.

The branch flow model represents Kirchhoff's laws in terms of $\boldsymbol{w}$ and $\boldsymbol{P},\boldsymbol{Q},\boldsymbol{J}$, where the vectors collect the corresponding variables over $\mathbb{N}$ and $\mathbb{E}$. If $\boldsymbol{w},\boldsymbol{P},\boldsymbol{Q},\boldsymbol{J}$ satisfy (3.8), (3.9), then one can recover voltage phasors $\boldsymbol{V} \in \mathbb{C}^n$ that satisfy (3.1), (3.2). See [42] for details.

3.3 The market clearing procedure

With the branch flow model of the power flow equations written in terms of $\boldsymbol{w},\boldsymbol{P},\boldsymbol{Q},\boldsymbol{J}$, we now define the dispatch and the pricing problem that a DSO solves.

3.3.1 The dispatch problem

The DSO solves the following dispatch problem that seeks to minimize (real and reactive) power procurement costs from controllable assets to meet the needs of the uncontrollable assets over the distribution grid.

$$
\begin{aligned}
&\text{minimize} \quad \sum_{k=1}^{n} c_k(p_k^G, q_k^G), \\
&\text{subject to} \\
&\quad p_k^G - p_k^D = \sum_{\ell':k\to\ell'} P_{k\ell'} - \sum_{\ell':\ell'\to k} \left(P_{\ell'k} - r_{\ell'k}J_{\ell'k}\right), && \text{(3.10a)}\\
&\quad q_k^G - q_k^D = \sum_{\ell':k\to\ell'} Q_{k\ell'} - \sum_{\ell':\ell'\to k} \left(Q_{\ell'k} - x_{k\ell'}J_{\ell'k}\right), && \text{(3.10b)}\\
&\quad P_{k\ell} \le f_{k\ell},\ r_{k\ell}J_{k\ell} - P_{k\ell} \le f_{k\ell}, && \text{(3.10c)}\\
&\quad \underline{p}_k^G \le p_k^G \le \overline{p}_k^G,\ \underline{q}_k^G \le q_k^G \le \overline{q}_k^G, && \text{(3.10d)}\\
&\quad \underline{v}_k^2 \le w_k \le \overline{v}_k^2, && \text{(3.10e)}\\
&\quad w_\ell = w_k - 2(P_{k\ell}r_{k\ell} + Q_{k\ell}x_{k\ell}) + (r_{k\ell}^2 + x_{k\ell}^2)J_{k\ell}, && \text{(3.10f)}\\
&\quad P_{k\ell}^2 + Q_{k\ell}^2 = J_{k\ell}w_k && \text{(3.10g)}\\
&\quad \text{for } k \in \mathbb{N},\ k\to\ell \in \mathbb{E}
\end{aligned}
$$

over the variables $\boldsymbol{p}^G,\boldsymbol{q}^G,\boldsymbol{w},\boldsymbol{P},\boldsymbol{Q},\boldsymbol{J}$. Problem (3.10) is nonconvex, owing to the quadratic equality constraint in (3.10g). As will be clear in Section 3.3.2, the pricing problem is a convex relaxation of (3.10).

3.3.2 DLMPs from the pricing problem

We relax the nonconvex quadratic equality in the dispatch problem to arrive at the following pricing problem. In what follows, we derive the DLMPs from the optimal Lagrange multipliers of the pricing problem.

$$
\begin{aligned}
\text{minimize} \quad & \sum_{k=1}^{n} c_k(p_k^G, q_k^G), \\
\text{subject to} \quad & P_{k\ell}^2 + Q_{k\ell}^2 \leq J_{k\ell} w_k, \text{(3.10a)} - \text{(3.10f)} \\
& \text{for } k \in \mathbb{N},\ k \to \ell \in \mathbb{E}
\end{aligned}
\tag{3.11}
$$

over the variables $\boldsymbol{p}^G, \boldsymbol{q}^G, \boldsymbol{w}, \boldsymbol{P}, \boldsymbol{Q}, \boldsymbol{J}$. The inequality constraint in (3.11) is a relaxation of (3.10g) in the dispatch problem. Furthermore, it is a second-order cone constraint. The cost and the rest of the constraints being linear in the optimization variables, the pricing problem in (3.11) can be solved as a second-order cone program (SOCP).

Associate Lagrange multipliers λ_k^p and λ_k^q with the real and reactive power balance constraints (3.10a)-(3.10b), respectively for the pricing problem.

Definition 2 (Distribution LMPs)**.** *The relaxation-based DLMPs for real and reactive powers at each bus $k \in \mathbb{N}$ are defined as the optimal Lagrange multipliers $\lambda_k^{p,*}$ and $\lambda_k^{q,*}$ from the SOCP-based pricing problem* (3.11).

We emphasize that our dispatch is derived from the non-convex dispatch problem in (3.10), while the electricity prices are obtained from its SOCP relaxation in (3.11). These prices reflect losses, congestion, and account for reactive power flow in the network as these considerations are explicit in the pricing problem. DLMPs $\lambda_k^{p,*}$ and $\lambda_k^{q,*}$ retain an economic interpretation analogous to transmission LMPs–they represent the short-run marginal cost to the system to supply an additional unit of real and reactive power demand at bus k. A more detailed discussion on the economic interpretation of such DLPMs is given in [1].

If the dispatch decision of the controllable asset is given by $p_k^{G,*}, q_k^{G,*}$, then the DSO pays $\lambda_k^{p,*} p_k^{G,*} + \lambda_k^{q,*} q_k^{G,*}$ to the asset owner-operator. The uncontrollable asset at bus k pays $\lambda_k^{p,*} p_k^D + \lambda_k^{q,*} q_k^D$ to the DSO.

3.4 Properties of relaxation-based DLMPs

We now investigate the properties entrenched in relaxation-based DLMPs. We begin by describing desirable qualities of prices that we seek to establish.

Definition 3 (Efficient Market Equilibrium)**.** *The prescribed dispatch $(\boldsymbol{p}^G, \boldsymbol{q}^G)$ and prices $(\boldsymbol{\lambda}^p, \boldsymbol{\lambda}^q)$ constitute an efficient market equilibrium, if they satisfy the following conditions.*

- *Individual rationality for all controllable assets: Given the prices λ_k^p, λ_k^q, the controllable asset at each bus $k \in \mathbb{N}$ will produce $p_k^G + \mathbf{i} q_k^G$ in an effort to maximize its own profit, i.e., (p_k^G, q_k^G) is* *an optimizer of*

$$\begin{aligned} \underset{\tilde{p}^G,\tilde{q}^G}{\textit{maximize}} \quad & \lambda_k^p \tilde{p}^G + \lambda_k^q \tilde{q}^G - c_k(\tilde{p}^G, \tilde{q}^G), \\ \textit{subject to} \quad & \underline{p}_k^G \le \tilde{p}^G \le \overline{p}_k^G,\ \underline{q}_k^G \le \tilde{q}_k^G \le \overline{q}_k^G. \end{aligned} \tag{3.12}$$

- *Market clearing condition: The dispatch meets the power demands* $\boldsymbol{p}^D + \mathbf{i}\boldsymbol{q}^D$ *over the network and induce feasible power flows, i.e., there exists* $\boldsymbol{w}, \boldsymbol{P}, \boldsymbol{Q}, \boldsymbol{J}$ *such that* $(\boldsymbol{p}^G, \boldsymbol{q}^G, \boldsymbol{w}, \boldsymbol{P}, \boldsymbol{Q}, \boldsymbol{J})$ *satisfy* (3.10a) - (3.10g).

- *Efficiency of dispatch: There exists* $\boldsymbol{w}, \boldsymbol{P}, \boldsymbol{Q}, \boldsymbol{J}$ *such that* $(\boldsymbol{p}^G, \boldsymbol{q}^G, \boldsymbol{w}, \boldsymbol{P}, \boldsymbol{Q}, \boldsymbol{J})$ *optimizes* (3.10).

Individual rationality ensures that a controllable asset has no incentive to deviate from the DSO's prescribed dispatch, given the prices. Market clearing condition ensures that the dispatch meets the demand requirements over the network and an efficient dispatch ensures that it indeed optimizes the aggregate power procurement costs.

Definition 4 (Revenue Adequacy)**.** *The prescribed dispatch* $(\boldsymbol{p}^G, \boldsymbol{q}^G)$ *and prices* $(\boldsymbol{\lambda}^p, \boldsymbol{\lambda}^q)$ *define a revenue adequate market mechanism if the merchandizing surplus given by*

$$MS := \sum_{k=1}^{n} \left[\lambda_k^p \left(p_k^D - p_k^G \right) + \lambda_k^q \left(q_k^D - q_k^G \right) \right] \tag{3.13}$$

is nonnegative.

Nonnegativity of MS implies that the DSO remains solvent after settling payments with market participants.

3.4.1 Main result

We now present our result that identifies sufficient conditions under which our market mechanism with relaxation-based DLMPs exhibits desirable properties mentioned above. Proofs are omitted from this report; see [47] for details.

Theorem 3. *Suppose the dispatch problem* (3.10) *is strictly feasible. Consider a dispatch* $(\boldsymbol{p}^{G,*}, \boldsymbol{q}^{G,*})$ *computed from* (3.10) *and DLMPs* $\boldsymbol{\lambda}^{p,*}, \boldsymbol{\lambda}^{q,*}$ *computed from* (3.11)*. If the inequality in* (3.11) *is tight at an optimum, then this dispatch and DLMPs support an efficient market equilibrium. Moreover, if the lower bound on voltage magnitudes is non-binding at every bus, then they define a revenue adequate market mechanism.*

Theorem 3 establishes the properties of relaxation-based DLMPs under the premise that the SOCP relaxation is exact. In other words, an optimal solution of the convex relaxation of the nonconvex dispatch problem produces an optimal dispatch. There are several sufficient conditions under which

Table 3.1: Parameter choices and outcomes of the pricing problem for our experiments on the 2-bus network.

#	f_{12}	r_{12}	x_{12}	k	p_k^D	q_k^D	$\overline{p}_k^G$	$\overline{q}_k^G$	$\underline{v}_k^2$	$\overline{v}_k^2$	c_k	w_k^*	MS
1	0.5	.10	.10	1	1.6	0	2.0	2.0	.81	1.20	10	1.20	+0.27
				2	2.0	.2	2.0	2.0	.81	1.20	20	1.12	
2	1.0	.10	.10	1	1.0	.5	2.0	1.0	.95	1.10	8	1.10	+0.71
				2	2.8	.5	2.0	1.5	.95	1.10	5	0.95	
3	1.0	.01	.01	1	0.8	.5	2.0	0.9	.86	0.95	10	0.95	-0.10
				2	0	0	1.2	0.2	.97	1.10	10	0.97	

this convex relaxation is exact, e.g., see [41, 43, 44]. Even when such conditions do not hold, relaxations over radial distribution networks are often exact.

We establish revenue adequacy under an additional condition on the lower bounds on voltage magnitudes. Our numerical experiments in Section 3.5 reveal that this extra condition is sufficient but not necessary for MS ≥ 0. We expect from the long literature on volt-VAR control problems that adequate reactive power support will likely lead to voltage magnitudes higher than their lower limits.

3.5 Numerical experiments

The pricing problem (3.11) for all experiments was solved in CVX in MATLAB. Power is reported in per units.

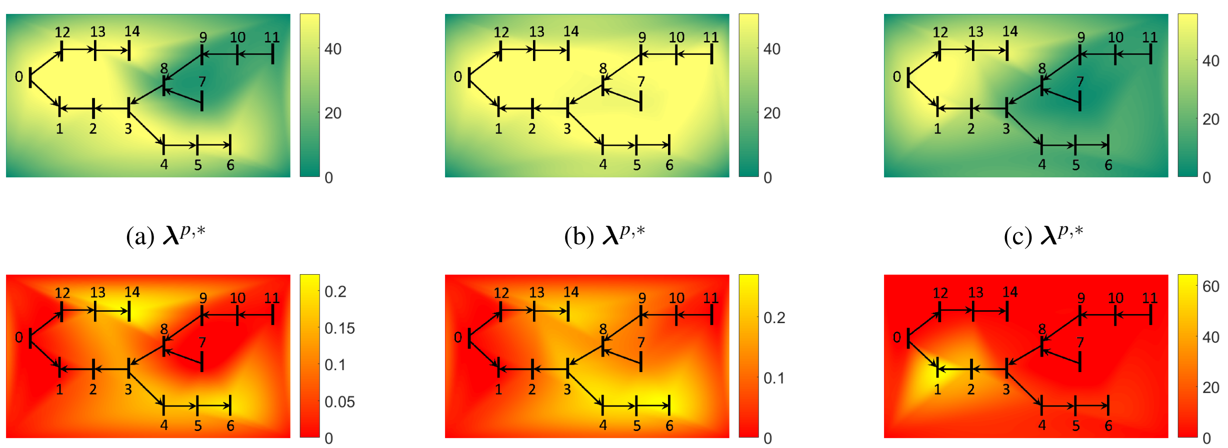

(a) $\boldsymbol{\lambda}^{p,*}$ (b) $\boldsymbol{\lambda}^{p,*}$ (c) $\boldsymbol{\lambda}^{p,*}$

(d) $\boldsymbol{\lambda}^{q,*}$ (e) $\boldsymbol{\lambda}^{q,*}$ (f) $\boldsymbol{\lambda}^{q,*}$

Figure 3.1: Plots (a), (d) show heatmaps of DLMPs on the 15-bus radial network adopted from [1]. Plots (b), (e) are derived with $p_{11}^D = 0.350$, and (c), (f) with $\overline{v}_i^2 = 1.05, i = 0, \ldots, 10$, $\underline{v}_1^2 = 1$.

3.5.1 On a 2-bus network example

We conduct three experiments on a 2-bus network with linear dispatch cost of the form $c_1 p_1^G + c_2 p_2^G$. Parameters for and outcomes of our experiments are given in Table 3.1. We set the lower limits $\underline{p}_k^G = 0$, $\underline{q}_k^G = 0$ for all buses in all experiments, except for $\underline{q}_2^G = 0.01$ in the third experiment. All relaxations were verified to be exact. In the first experiment, the voltage magnitude at each bus is strictly greater than the lower limit and we obtain MS ≥ 0, as Theorem 3 dictates. In the second experiment, voltage magnitude at bus 2 equals its lower limit, but we still obtain MS ≥ 0, revealing that Theorem 3 identifies a sufficient but not a necessary condition for nonnegative MS. Our third experiment violates the sufficient condition and yields a negative MS.

3.5.2 On a 15-bus network example

Figure 3.1 portrays DLMPs on a 15-bus radial network from [1] with the modification $p_{11}^D = 0.250$ and $q_{11}^D = 0.073$. Figures 3.1b, 3.1e reveal that increasing power demands at bus 11 increases real power prices around bus 11, illustrating the locational nature of these prices. Figures 3.1c,3.1f demonstrate that voltage limits significantly affect reactive power prices. Our experiments with various parameters always yielded MS ≥ 0.

3.6 Conclusions and future directions

In this chapter, we identify sufficient conditions under which DLMPs for real and reactive power derived from an SOCP-based market clearing problem support an efficient market equilibrium and satisfy revenue adequacy. We illustrate our results through numerical examples. Our proof techniques do not easily extend to cases where the relaxation is not exact – a case that requires further study. Extension of our work to consider multi-phase unbalanced distribution grid models with capacitor banks and tap-changing transformers is another interesting direction for future research.

In this chapter, we only investigated a pricing mechanism that is derived from a convex relaxation of the market clearing problem. We neither specified the formats of the bids and offers, nor did we delineate how these bids/offers are incorporated within market clearing. In future work, we aim to combine our work on scalar parameterized bids and offers (without a network) in [48] with the DLMP design studied here to propose a complete retail market mechanism. We also want to investigate how such a mechanism differentially affects prosumers with different economic backgrounds.

References

[1] A. Papavasiliou, “Analysis of distribution locational marginal prices,” *IEEE Transactions on Smart Grid*, vol. 9, no. 5, pp. 4872-4882, Sep. 2018.

[2] “Distributed Energy Resources: Connection Modeling and Reliability Considerations,” North American Electric Reliability Corporation, Tech. Rep., 2017.

[3] T. Morstyn, A. Teytelboym, and M.D. McCulloch, “Bilateral contract networks for peer-to-peer energy trading,” IEEE Transactions on Smart Grid, pp. 1-1, 2018.

[4] R. Tabors, G. Parker, P. Centolella, and M. Caramanis, “White paper on developing competitive electricity markets and pricing structures.” Tabors Caramanis Rudkevich, Inc. Prepared under contract for the New York State Energy Research and Development Authority., Tech. Rep., 2016.

[5] G.E. Asimakopoulou and N.D. Hatziargyriou, “Evaluation of economic benefits of der aggregation,” *IEEE Transactions on Sustainable Energy*, vol. 9, no. 2, pp. 499-510, 2018.

[6] “IEEE 1547-2018 – IEEE standard for interconnection and interoperability of distributed energy resources with associated electric power system interfaces,” IEEE, Tech. Rep., 2018.

[7] “Utility of the future study,” NextGrid Illinois, Tech. Rep., 2018.

[8] J. Lian, D. Wu, K. Kalsi, and H. Chen, “Theoretical framework for integrating distributed energy resources into distribution systems,” in *2017 IEEE Power Energy Society General Meeting*, July 2017, pp. 1-5.

[9] E. Ntakou and M. Caramanis, “Price discovery in dynamic power markets with low-voltage distribution-network participants,” in *2014 IEEE PES T&D Conference and Exposition*, April 2014, pp. 1-5.

[10] S.D. Manshadi and M.E. Khodayar, “A hierarchical electricity market structure for the smart grid paradigm,” IEEE Transactions on Smart Grid, vol. 7, no. 4, pp. 1866-1875, July 2016.

[11] P.M. Sotkiewicz and J.M. Vignolo, “Nodal pricing for distribution networks: efficient pricing for efficiency enhancing DG,” *IEEE Transactions on Power Systems*, vol. 21, no. 2, pp. 1013-1014, May 2006.

[12] J. Terra, R. Ferreira, C. Borges, and M. Carvalho, “Using distribution-level locational marginal pricing to value distributed generation: Impacts on revenues captured by generation agents,” in *2017 IEEE PES Innovative Smart Grid Technologies Conference – Latin America (ISGT Latin America)*, Sep. 2017, pp. 1-6.

[13] S. Huang, Q. Wu, S.S. Oren, R. Li, and Z. Liu, “Distribution locational marginal pricing through quadratic programming for congestion management in distribution networks,” *IEEE Transactions on Power Systems*, vol. 30, no. 4, pp. 2170-2178, July 2015.

[14] F. Moret and P. Pinson, “Energy collectives: a community and fairness based approach to future electricity markets,” *IEEE Transactions on Power Systems*, pp. 1-1, 2018.

[15] F.A. Rahimi and A. Ipakchi, "Transactive energy techniques: Closing the gap between wholesale and retail markets," *The Electricity Journal*, vol. 25, no. 8, pp. 29-35, 2012.

[16] S. Burger, J.P. Chaves-Ávila, C. Batlle, and I.J. Pérez-Arriaga, "A review of the value of aggregators in electricity systems," *Renewable and Sustainable Energy Reviews*, vol. 77, pp. 395-405, 2017.

[17] J. Gundlach and R. Webb, "Distributed energy resource participation in wholesale markets: Lessons from the California ISO," *Energy Law Journal*, vol. 39, no. 1, pp. 47-77, 2018.

[18] K. Alshehri, M. Ndrio, S. Bose, and T. Başar, "Quantifying market efficiency impacts of aggregated distributed energy resources," *IEEE Transactions on Power Systems*, vol. 35, no. 5, pp. 4067-4077, 2020.

[19] T. Başar and G.J. Olsder, *Dynamic Noncooperative Game Theory*. SIAM, 1999.

[20] W. Lin and E. Bitar, "Forward electricity markets with uncertain supply: cost sharing and efficiency loss," *53rd IEEE Conference on Decision and Control*, pp. 1707-1713, 2014.

[21] "Distributed energy resource provider participation guide with checklist," California ISO, Tech. Rep., 2016.

[22] K. Alshehri, M. Ndrio, S. Bose, and T. Başar, "The impact of aggregating distributed energy resources on electricity market efficiency," *Proc. 53rd Annual Conference on Information Systems and Sciences, Johns Hopkins University, Baltimore, Maryland*, March 20-22, 2019.

[23] S.-F. Chen, D.M. Reeves, Y. Vorobeychik, and M.P. Wellman, "Notes on equilibria in symmetric games," *Proceedings of Workshop on Game Theory and Decision Theory*, August 2004.

[24] J.B. Rosen, "Existence and uniqueness of equilibrium points for concave n-person games," *Econometrica*, vol. 33, no. 3, pp. 520-534, 1965.

[25] R. Baldick, R. Grant, and E. Kahn, "Theory and application of linear supply function equilibrium in electricity markets," *Journal of Regulatory Economics*, pp. 143-167, 2004.

[26] R.J. Green and D.M. Newbery, "Competition in the British electricity spot markets," *Journal of Political Economy*, vol. 100, no. 5, pp. 929-953, 1992.

[27] S. Bose, C. Wu, Y. Xu, A. Wierman, and H. Mohsenian-Rad, "A unifying market power measure for deregulated transmission-constrained electricity markets," *IEEE Transactions on Power Systems*, vol. 30, no. 5, pp. 2338-2348, 2014.

[28] K. Alshehri, J. Liu, X. Chen, and T. Başar, "A Stackelberg game for multi-period demand response management in the smart grid," *Proceedings of the 54th IEEE Conference on Decision and Control*, pp. 5889-5894, 2015.

[29] M. Huang, P. Caines, and R. Malhame, "Large-population cost-coupled LQG problems with non-uniform agents: individual-mass behavior and decentralized ε-Nash equilibria," *IEEE Trans. Automatic Control*, vol. 52, no. 9, pp. 1560-1571, 2007.

[30] J.-M. Lasry and P.-L. Lions, "Mean field games," *Japan J. Math.*, vol. 2, no. 1, pp. 229-260, 2007.

[31] F. Zhao, T. Zheng, and E. Litvinov, "Constructing demand curves in forward capacity market," *IEEE Trans. Power Systems*, vol. 33, no. 1, pp. 525-535, 2018.

[32] F. Kelly, A. Maulloo, and D. Tan, "Rate control for communication networks: shadow prices, proportional fairness and stability," *Journal of the Operational Research Society*, vol. 49, no. 3, pp. 237-252, 1998.

[33] B. Gao, W. Zhang, Y. Tang, M. Hu, M. Zhu, and H. Zhan, "Game-theoretic energy management for residential users with dischargeable plug-in electric vehicles," *Energies*, vol. 7, no. 11, pp. 7499-7518, 2014.

[34] S. Maharjan, Q. Zhu, Y. Zhang, S. Gjessing, and T. Başar, "Dependable demand response management in the smart grid: a Stackelberg game approach," *IEEE Trans. Smart Grid*, vol. 4, no. 1, pp. 120-132, 2013.

[35] Z. Yuan, M.R. Hesamzadeh, and D.R. Biggar, "Distribution locational marginal pricing by convexifies acopf and hierarchical dispatch," *IEEE Transactions on Smart Grid*, vol. 9, no. 4, pp. 3133-3142, July 2018.

[36] M. Caramanis, E. Ntakou, W.W. Hogan, A. Chakrabortty, and J. Schoene, "Co-optimization of power and reserves in dynamic T&D power markets with non-dispatchable renewable generation and distributed energy resources," *Proceedings of the IEEE*, vol. 104, no. 4, pp. 807-836, 2016.

[37] R.E. Bohn, M.C. Caramanis, and F.C. Schweppe, "Optimal pricing in electrical networks over space and time," *The RAND Journal of Economics*, vol. 15, no. 3, pp. 360-376, 1984.

[38] E. Litvinov, "Design and operation of the locational marginal prices-based electricity markets," *IET generation, transmission & distribution*, vol. 4, no. 2, pp. 315-323, 2010.

[39] J. Lavaei and S.H. Low, "Zero duality gap in optimal power flow problem," *IEEE Transactions on Power Systems*, vol. 27, no. 1, pp. 92-107, 2012.

[40] X. Bai, H. Wei, K. Fujisawa, and Y. Wang, "Semidefinite programming for optimal power flow problems," *International Journal of Electrical Power & Energy Systems*, vol. 30, no. 6, pp. 383-392, 2008.

[41] L. Gan, N. Li, U. Topcu, and S.H. Low, "Exact convex relaxation of optimal power flow in radial networks," *IEEE Transactions on Automatic Control*, vol. 60, no. 1, pp. 72-87, Jan. 2015.

[42] S. Bose, S.H. Low, T. Teeraratkul, and B. Hassibi, "Equivalent relaxations of optimal power flow," *IEEE Transactions on Automatic Control*, vol. 60, no. 3, pp. 729-742, 2015.

[43] M. Farivar and S.H. Low, "Branch flow model: Relaxations and convexification – part I," *IEEE Transactions on Power Systems*, vol. 28, no. 3, pp. 2554-2564, Aug. 2013.

[44] N. Li, L. Chen, and S.H. Low, "Exact convex relaxation of OPF for radial networks using branch flow model," in *2012 IEEE Third International Conference on Smart Grid Communications (SmartGridComm)*, Nov. 2012, pp. 7-12.

[45] Z. Yuan, M.R. Hesamzadeh, and D.R. Biggar, "Distribution locational marginal pricing by convexified ACOPF and hierarchical dispatch," *IEEE Transactions on Smart Grid*, vol. 9, no. 4, pp. 3133-3142, 2016.

[46] S. Bose and S.H. Low, "Some emerging challenges in electricity markets," in *Power Electronics and Power Systems.* Springer, 2018.

[47] A. Winnicki, M. Ndrio, and S. Bose, "On convex relaxation-based distribution locational marginal prices," in *2020 IEEE Power & Energy Society Innovative Smart Grid Technologies Conference (ISGT).* IEEE, 2020, pp. 1-5.

[48] M. Ndrio, K. Alshehri, and S. Bose, "A scalar-parameterized mechanism for two-sided markets," *IFAC-PapersOnLine*, vol. 53, no. 2, pp. 16952-16957, 2020.